

2013

The Study of Alternate, Solid-Phase Fluorinating Agents for Use in Reactive Gas Recycle of Used Nuclear Fuel

Dillon Inabinett
University of South Carolina

Follow this and additional works at: <https://scholarcommons.sc.edu/etd>



Part of the [Nuclear Engineering Commons](#)

Recommended Citation

Inabinett, D.(2013). *The Study of Alternate, Solid-Phase Fluorinating Agents for Use in Reactive Gas Recycle of Used Nuclear Fuel*. (Master's thesis). Retrieved from <https://scholarcommons.sc.edu/etd/3587>

This Open Access Thesis is brought to you by Scholar Commons. It has been accepted for inclusion in Theses and Dissertations by an authorized administrator of Scholar Commons. For more information, please contact dillarda@mailbox.sc.edu.

THE STUDY OF ALTERNATE, SOLID-PHASE FLUORINATING AGENTS FOR USE IN
REACTIVE GAS RECYCLE OF USED NUCLEAR FUEL

by

Dillon Inabinett

Bachelor of Science
University of South Carolina, 2012

Submitted in Partial Fulfillment of the Requirements

For the Degree of Master of Science in

Nuclear Engineering

College of Engineering and Computing

University of South Carolina

2013

Accepted by:

Travis W. Knight, Major Professor

Joshua Gray, Second Reader

Lacy Ford, Vice Provost and Dean of Graduate Studies

© Copyright by Dillon Inabinett, 2013
All Rights Reserved.

DEDICATION

I would like to dedicate this work to my mother, for her endless support throughout all of my endeavors. Though life may not have always been perfect, the one thing that remains true is her love and affection.

ACKNOWLEDGEMENTS

I would like to thank my two advisors, Dr. Travis Knight and Dr. Joshua Gray for giving me the opportunity to work on this project. I could not have completed this research without their guidance and mentoring. Also, I would like to thank Dr. Brenda Garcia-Diaz, or “Momma Brenda,” for her support during my internship at SRNL. To my colleagues, I would like to thank you for your assistance in both classes and research. In particular, I thank Seung Min Lee for allowing me to use his TGA at USC for my experiments, Kyle Hrutkay who doubled as my gym buddy and listened to countless hours of venting not only about research, but life in general, and Kallie Metzger, who accompanied me on my first real plane ride to San Diego, CA to present my research at Winter ANS 2012. Finally, I would like to extend my thanks and deep appreciation to the NANT (National Academy for Nuclear Training) Fellowship for funding me throughout this research.

ABSTRACT

Surrogate oxides of the Used Nuclear Fuel (UNF) matrix were fluorinated using alternate, solid-phase fluorinating agents XeF_2 and NH_4HF_2 to form volatile and non-volatile compounds and demonstrate the possibility of a chemical and thermal separations. A matrix of experiments was conducted at the milligram quantity scale using a Shimadzu DTG-60 TG/DTA installed at SRNL (Savannah River National Laboratory) for testing of all non-radioactive samples and a Netzsch STA 409 TGA installed in the laboratory at USC (University of South Carolina) for testing of all radioactive samples. The fluorination and subsequent volatilization potentials were analyzed by mixing excess fluorinating agent with a surrogate oxide at roughly a 2:1 ratio and then heated to elevated temperatures for analysis. Thermogravimetric and differential thermal analysis allowed for reaction pathways to be analyzed and suggest windows both thermally and chemically for separations of these various components. The differences in thermophysical properties of these products can be utilized as a starting point to effectively separate, isolate, and collect product streams with different product composition for further processing. The study of these chemistries could be incorporated into advanced separations methods to provide another possible solution for the long-term sustainability of nuclear power as the issue of reuse and disposal of commercial fuel continues to grow.

TABLE OF CONTENTS

DEDICATION	iii
ACKNOWLEDGEMENTS.....	iv
ABSTRACT	v
LIST OF TABLES	viii
LIST OF FIGURES	ix
LIST OF ABBREVIATIONS.....	xii
CHAPTER 1: MOTIVATION.....	1
CHAPTER 2: LITERATURE REVIEW	4
2.1 UNITED STATES CURRENT USED NUCLEAR FUEL POLICIES	4
2.2 OVERVIEW OF THE PUREX PROCESS	9
2.3 OVERVIEW OF FLUORIDE VOLATILITY.....	12
2.4 INVESTIGATION OF ALTERNATE FLUORINATING AGENTS	15
CHAPTER 3: METHODOLOGY	23
3.1 EXPERIMENTAL SETUP – NON RADIOACTIVE (SRNL).....	23
3.2 TG/DTA CALIBRATION (SRNL)	26
3.3 SAMPLE PREPARATION (SRNL).....	31
3.4 EXPERIMENTAL SETUP – RADIOACTIVE (SRNL)	32
3.5 EXPERIMENTAL SETUP (USC)	33
3.6 SAMPLE PREPARATION (USC)	38
CHAPTER 4: RESULTS AND DISCUSSION	41

4.1 THERMAL DECOMPOSITION OF XeF_2	41
4.2 THERMAL DECOMPOSITION OF NH_4HF_2	42
4.3 STRONTIUM OXIDE (SrO)	44
4.4 MOLYBDENUM TRIOXIDE (MoO_3).....	54
4.5 NIOBIUM PENTOXIDE (Nb_2O_5).....	60
4.6 RHODIUM (III) OXIDE (Rh_2O_3).....	63
4.7 RUTHENIUM (IV) OXIDE (RuO_2)	66
4.8 ZIRCONIUM DIOXIDE (ZrO_2)	69
4.9 URANIUM DIOXIDE (UO_2) - SRNL	71
4.10 TRIURANIUM OCTOXIDE (U_3O_8) - USC	74
CHAPTER 5: CONCLUSION AND FUTURE WORK	82
REFERENCES	85

LIST OF TABLES

Table 2.1 Composition of UNF	5
Table 2.2 Current Reprocessing Strategies	6
Table 2.3 Results from Chandler Study	7
Table 2.4 Volatility of Various UNF Components	14
Table 2.5 Expected Fluorination Reactions with NF_3	17
Table 2.6 Reaction Onset and Volatilization Temperatures using NF_3	19
Table 3.1 XRD Instrument Parameters	26

LIST OF FIGURES

Figure 2.1 Reaction Equations for PUREX Process	10
Figure 2.2 Secondary Waste Alternatives for PUREX Process.....	11
Figure 2.3 Flow Sheet for Fluoride Volatility Method	13
Figure 2.4 Basic Concept for HRS	15
Figure 2.5 Reaction of UO_2 with NH_4HF_2 to Produce UN_2	20
Figure 2.6 Observations Using XeF_2 as Fluorinating Agent	22
Figure 3.1 Installation of DTG-60	24
Figure 3.2 XRD Slide Preparation	25
Figure 3.3 Baseline Heating Results Prior to Adjustment	27
Figure 3.4 Baseline Heating Results Post Adjustment	28
Figure 3.5 TG/DTA Data for Melting of Tin.....	29
Figure 3.6 TG/DTA Data for Calcium Oxalate Monohydrate ($\text{CaC}_2\text{O}_4 \cdot \text{H}_2\text{O}$).....	30
Figure 3.7 Modified Dupont 951 TGA.....	33
Figure 3.8 CM 1730-12 HTF Tube Furnace.....	34
Figure 3.9 Close-up of Cooling Water Jacket and End Caps	35
Figure 3.10 Netzsch STA 409 TGA	36
Figure 3.11 Baseline 2 TGA Results	38
Figure 3.12 Metal Chunks of Uranium Prior to Oxidation in Furnace.....	39
Figure 3.13 Verification of U_3O_8 Material	40
Figure 4.1 Thermal Decomposition of XeF_2	41

Figure 4.2 Thermal Decomposition of NH_4HF_2	44
Figure 4.3 TG/DTA Data for SrO	46
Figure 4.4 TG/DTA Data for SrO/XeF_2	48
Figure 4.5 XRD Analysis for SrO/XeF_2	49
Figure 4.6 XRD Analysis for SrO/XeF_2 No TG/DTA.....	50
Figure 4.7 TG/DTA Data for $\text{SrO}/\text{NH}_4\text{HF}_2$ No Lid	52
Figure 4.8 TG/DTA Data for $\text{SrO}/\text{NH}_4\text{HF}_2$ Lid On	53
Figure 4.9 TG/DTA Data for MoO_3	55
Figure 4.10 TG/DTA Data for $\text{MoO}_3/\text{XeF}_2$	56
Figure 4.11 TG/DTA Data for $\text{MoO}_3/\text{NH}_4\text{HF}_2$ No Lid.....	58
Figure 4.12 TG/DTA Data for $\text{MoO}_3/\text{NH}_4\text{HF}_2$ Lid On.....	59
Figure 4.13 TG/DTA Data for Nb_2O_5	61
Figure 4.14 TG/DTA Data for $\text{Nb}_2\text{O}_5/\text{XeF}_2$	62
Figure 4.15 TG/DTA Data for Rh_2O_3	64
Figure 4.16 TG/DTA Data for $\text{Rh}_2\text{O}_3/\text{XeF}_2$	65
Figure 4.17 TG/DTA Data for RuO_2	67
Figure 4.18 TG/DTA Data for $\text{RuO}_2/\text{XeF}_2$	68
Figure 4.19 TG/DTA Data for ZrO_2	69
Figure 4.20 TG/DTA Data for $\text{ZrO}_2/\text{XeF}_2$	71
Figure 4.21 TGA Data for UO_2/XeF_2	72
Figure 4.22 TGA Data for $\text{UO}_2/\text{NH}_4\text{HF}_2$	74
Figure 4.23 Sealed Swagelok Volume after Heating in Tube Furnace.....	75
Figure 4.24 Sample as Removed from Swagelok Tube.....	76

Figure 4.25 Comparison of Materials from Runs 1 and 2 in the Tube Furnace	77
Figure 4.26 Resulting Residue from $\text{U}_3\text{O}_8/\text{XeF}_2$ after Tube Furnace	79
Figure 4.27 TGA analysis of $\text{U}_3\text{O}_8/\text{XeF}_2$ Sample Residue	80
Figure 4.28 Al_2O_3 Crucible after TGA Experiment.....	81

LIST OF ABBREVIATIONS

Al_2O_3	Alumina
BRC.....	Blue Ribbon Commission
$\text{CaC}_2\text{O}_4 \cdot \text{H}_2\text{O}$	Calcium Oxalate Monohydrate
CO	Carbon Monoxide
CO_2	Carbon Dioxide
DF	Decontamination Factor
DTA	Differential Thermal Analysis
FBR.....	Fast Breeder Reactor
HLW	High Level Radioactive Waste
HRS.....	Hybrid Recycle System
LWR.....	Light Water Reactor
MoO_3	Molybdenum Trioxide
MOX	Mixed Oxide Fuel
Nb_2O_5	Niobium Pentoxide
NCAW	Neutralized Current Acid Waste
NH_4HF_2	Ammonium Bifluoride
NWPA.....	Nuclear Waste Policy Act
PID	Proportional/Integral/Differential
PUREX	Plutonium Uranium Extraction
RGR	Reactive Gas Recycle
Rh_2O_3	Rhodium (III) Oxide

RuO_2	Ruthenium (IV) Oxide
SF_6	Sulfur Hexafluoride
SRNL	Savannah River National Laboratory
SrO	Strontium Oxide
TBP	Tributyl Phosphate
TGA	Thermogravimetric Analysis
TG/DTA	Thermogravimetric/Differential Thermal Analysis
UNF	Used Nuclear Fuel
USC	University of South Carolina
UO_2	Uranium Dioxide
U_3O_8	Triuranium Octoxide
XeF_2	Xenon Difluoride
XRD	X-Ray Diffraction
ZrO_2	Zirconium Dioxide

CHAPTER 1

MOTIVATION

The growth and development of the nuclear power industry is driven by the desire for a carbon-free, sustainable, and safe energy source. Currently in the United States, nuclear power constitutes to roughly 20% of all net electricity generation, and with the construction of new plants in Georgia and South Carolina, that number is expected to increase in the near future. [1] The continued operation of current power plants and the construction of new plants pose the issue of the disposition of commercial Used Nuclear Fuel (UNF). Though the idea of a permanent repository for UNF still exists, despite the decision for Yucca Mountain efforts to cease, capacities for these facilities is very limited. If the repository at Yucca Mountain would have been constructed at its planned size, current UNF inventory at reactor sites and High-Level Radioactive Waste (HLW) stored around the nation would completely fill the structure at day one. A need would arise for additional repositories to meet the demand of current production of UNF, and with the planned price tag of Yucca Mountain somewhere between \$42.8 and \$57.1 billion, this problem would become quite costly for the nuclear industry. [2]

One solution to this problem is through reprocessing and recycling. This solution offers both political and technical issues dealing with economics, safety, non-proliferation, and waste generation. [3,4,5] If a method for reprocessing is to be accepted and adopted by both the public and industry on a large scale, then it should effectively address all of these concerns. By inserting a reprocessing technology into the nuclear

fuel cycle, not only will the capacity demand for a permanent repository decrease, but overall fuel utilization would become much higher, reducing the life-cycle costs of nuclear electricity production. [2] Further utilization of the fuel is not only important, but it will become necessary to continue nuclear power into the future as uranium resources, although plenty relative to other energy producers using fossil fuels, are limited in the world. [3]

Traditionally, the United States has used various aqueous techniques for the separation and isolation of waste streams, most notably for use in weapons manufacturing. These techniques are generally adaptations of the PUREX (Plutonium URanium EXtraction) process and are based on the affinity of uranium and plutonium for tributyl phosphate (TBP). Aqueous methods, however, produce a large amount of secondary waste volumes which does not fare well in the argument of waste minimization. Despite the increased production of secondary waste volumes, the PUREX process is very well understood and has been practiced for decades, which would allow for a greater ease of implementation into designing a closed fuel cycle. [4] Various other techniques such as fluoride volatility and pyroprocessing all have pros and cons associated with each method, and will be discussed in more detail. Further research efforts have to be conducted in order to explore adaptations to current techniques and/or the investigation of novel reprocessing strategies which will effectively address the need for a solidified reprocessing and storage solution.

One such technology proposed by Savannah River National Laboratory (SRNL) is Reactive Gas Recycling (RGR). [5,6] Similar to fluoride volatility, RGR is based on the selective volatility of various oxides in the UNF matrix when fluorinated. This is a fully

dry reprocessing scheme which offers the possibility for a severe reduction in waste streams relative to current aqueous techniques for the reprocessing of UNF while addressing the materials limitations accompanying the highly corrosive nature of fluoride volatility. This paper explores the feasibility of formation of fluorinated products upon exposure to two separate, solid-phase fluorinating agents, xenon difluoride (XeF_2) and ammonium bifluoride (NH_4HF_2), at elevated temperatures. The study will address key UNF matrix materials using the combination of surrogate oxides or metal powders as found in the UNF from typical Light Water Reactor (LWR) service. Once the basic fluorination reactions of these compounds are understood, a matrix can begin to be developed to analyze possible product streams in terms of separations between volatile and non-volatile fluorides. Chemical and thermal separations through a mixed, reactive gas environment may offer the potential for a transformational change in the national approach to closing the nuclear fuel cycle.

CHAPTER 2

LITERATURE REVIEW

2.1 United States Current Used Nuclear Fuel Policies

The potential of nuclear energy for electricity production began at the discovery of uranium fission in 1938, and by the end of the 1940's the first efforts were already being made to develop technology for safe practice. [7] With the economic break-through for nuclear electricity generation, rapid and substantial growth of nuclear capacity took place starting in the 1960's. [7] Since then, however, major efforts have been put into defining long-term nuclear waste management policies as the growing argument against building nuclear power plants in the U.S. is that there is no long-term solution to the used nuclear fuel storage program. [7,8]

The United States of America is currently at a crossroads regarding what will be our policy for the disposition of used nuclear fuel from our current and growing fleet of nuclear power reactors and for the final disposition of high level nuclear wastes and spent nuclear fuel that are owned by the federal government. [9] These wastes must be disposed of in a secure, proliferation resistant, and environmentally protective manner within an ethical and morally responsible timeframe. [4,7,9] Contrary to popular belief, the components of used fuel are not unique among industrial wastes. They are neither the only toxic, nor the only carcinogenic or mutagenic wastes produced industrially. In fact, compared with some highly stable compounds or permanently toxic inorganic compounds, the predictability of radioactive decay provides the nuclear industry with

something of an advantage; after 100 years, the level of radioactivity remaining in the used fuel is only about 1 percent of what it was one year after discharge from the reactor.

[7]

Used nuclear fuel storage is a complex matter and can be broken down into two basic types: at reactor storage and either regional or centralized storage where excess used nuclear fuel can be stored for an interim time period awaiting final disposition either directly at a repository or via a recycling facility. [9] It is noted that the first type, reactor storage, is becoming a problem as over 49 sites currently have filled their pools to capacity and have had to add dry cask storage facilities. [9,12] Even if this interim storage were to all be moved to a recycling facility, an ultimate reprocessing strategy does not negate the need for a permanent repository to store HLW; however, it does effectively increase the uranium utilization, extending the life cycle of nuclear power. This concept is crucial for the continuation of nuclear power into the future. [4] A separations process is achieved by exploiting chemical and physical property differences between the substances through the use of one or more separating agents. [4] The approximate composition of used nuclear fuel is shown in Table 2.1 below.

Table 2.1 Composition of UNF

Element or group	Percent, by weight
Uranium	95.6
Fission products, stable and short-lived	0.3
Plutonium	0.9
Cesium and strontium	0.3
Minor actinides (Np, Cm, Am)	0.1
Iodine and technetium	0.1

Near complete recycle and re-use of most of the components of used fuel including materials that are vital to U.S. needs, can be accomplished using existing technologies and focused research and development to enable the required new

capabilities and to resolve regulatory issues for restricted uses within various industries. [10] With the many existing technologies available, shown in Table 2.2, the goal for the United States is that when the time comes to choose one of these strategies, the absolute best is implemented in terms of safety, non-proliferation, economics, etc. Chandler has conducted a study to analyze the strategies either currently in use by at least one nation, planned to be in use by at least one nation, or discussed in literature as possibly viable technologies. [4]

Table 2.2 Current Reprocessing Strategies

Aqueous processes	Pyroprocesses
PUREX	LiCl-KCl
COEX	NaCl-KCl
UREX	Fluoride volatility
UREX+1	FLUOREX ^a
UREX+2	
Supercritical CO ₂	

^a FLUOREX process contains both aqueous and pyroprocess steps.

Each strategy was analyzed against a number of attributes, and then these totals were weighed using professional judgment on 7 separate scenarios, each with largely different policy choices the United States lawmakers may choose to value. [4] The differences in policies which affected the weighing of the attributes ranged from effective separations, number of steps/simplicity of the process, proliferation resistance, technical knowledge and ease of implementation, and safety. [4] The results from the various scenarios for each reprocessing strategy are shown in Table 2.3.

Table 2.3 Results from Chandler Study

Technology	1	2	3	4	5	6	7
PUREX	0.330	0.636	0.279	0.498	0.547	0.829 ^a	0.222
COEX	0.455 ^a	0.711 ^a	0.394 ^a	0.475	0.596 ^a	0.418	0.292
Supercritical	0.352	0.214	0.322	0.510	0.392	0.782	0.469
UREX	0.418	0.688	0.334	0.547	0.550 ^b	0.409	0.278
UREX+1	0.355	0.653	0.263	0.586 ^b	0.450	0.403	0.250
UREX+2	0.349	0.651	0.252	0.601 ^a	0.445	0.402	0.250
Fluoride volatility	0.439 ^b	0.696 ^b	0.353 ^b	0.559	0.452	0.825 ^b	0.555 ^a
FLUOREX	0.248	0.585	0.243	0.452	0.365	0.801	0.192
LiCl-KCl	0.399	0.237	0.333	0.536	0.258	0.390	0.512 ^b
NaCl-KCl	0.391	0.232	0.329	0.532	0.243	0.388	0.507

^a First choice.^b Second choice.

The results from Table 2.3 suggest that there is no clear reprocessing strategy that outranks the rest of the competition in every scenario posed by Chandler. This choice will inevitably fall in the hands of policymakers to determine the future of the United States fuel cycle should it ever choose to adopt a reprocessing strategy. What is not only definite, but an immediate decision that should be made is the future of a permanent repository for this waste, even if a reprocessing strategy is not chosen in time.

Worldwide, there is broad agreement that deep geological disposal is the preferred option for spent fuel and high-level waste disposal, with the intent being that the geological environments will provide long-term protection of the waste packages from degradation, and will limit the transport of radionuclides to the human environment in the event of container failure. [11]

Until recently, the course of action in the US was to license and build the geologic repository at Yucca Mountain Nevada, which is adjacent to the nuclear weapons testing station approximately 100 miles northwest of Las Vegas, Nevada. [9] Although the State of Nevada openly rejects to having the repository built in their state, this site is established in law by the Nuclear Waste Policy Act (NWP) after 20 years of intensive scientific analysis and overwhelming bipartisan votes in the House and Senate in 2002.

This site is a retrievable disposal facility that easily allows future generations to access the materials, if they so desire, or provide completely passive disposal while meeting very protective EPA and NRC environmental and safety standards for up to one million years in the future. To date, over \$10 billion has been spent on the program and there is a positive \$24 billion balance in the Civilian Nuclear Waste Fund to complete the program.

[9]

Despite all of the effort put into the Yucca Mountain project, the Obama Administration has terminated the project, and in turn, established the Blue Ribbon commission on America's Nuclear Future (BRC) to find an alternative approach.

[9,12,13,14] The BRC was appointed in January 2010 and two years later, published its findings which included a set of eight main recommendations. [12,13] These recommendations are:

- A new consent-based approach to siting future nuclear waste management facilities.
- A new organization dedicated solely to implementing the waste management program and empowered with the authority and recourses to succeed.
- Access to the funds nuclear utility ratepayers are providing for the purpose of nuclear waste management.
- Prompt efforts to develop one or more geologic disposal facilities.
- Prompt efforts to develop one or more consolidated storage facilities.
- Prompt efforts to prepare for the eventual large-scale transport of spent nuclear fuel and high-level waste to consolidate storage and disposal facilities when such facilities become available.

- Support for continue U.S. innovation in nuclear energy technology and for workforce development.
- Active U.S. leadership in international efforts to address safety, waste management, nonproliferation, and security concerns.

The Obama administration has not given a scientific or economical basis for not continuing to implement what the NWSA suggests; however, it is obvious that establishing a politically sensitive high level nuclear waste disposal site is not the most desirable political task for elected officials, so deferral to someone else in the far future is often an attractive near term political proposition. [9] What Barrett suggests is that “no decision is often the worst decision when facing challenging complex issues like disposition of used nuclear fuel and high level waste.” It is evident from the BRC report that adopting a reprocessing technology is not in the near future, citing that economics alone is enough to justify this decision. [13] The main goal for the nuclear power industry in the immediate future is to develop a long-term storage solution for the wastes the industry produces. The US and all other nations, both current and future, who use nuclear power will eventually have to adopt a strategy to reuse this material. At this time, however, the baton remains in the hands of researchers to find the absolute best method for reprocessing and have the knowledge to make it available when the time comes.

2.2 Overview of the PUREX Process

The PUREX process in the United States has long been the standard separations method for the separation and isolation of uranium and plutonium waste streams, particularly for the use of weapons manufacturing. The chemical principle of separation

is based on the mostly selective binding of plutonium (IV) nitrate and uranyl nitrate on tributyl phosphate (TBP) whose equations are shown in Figure 2.1 below. [15-18, 21]

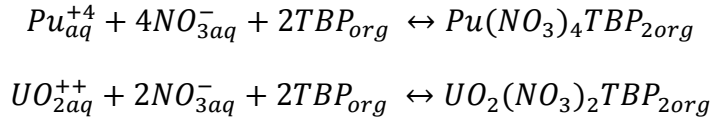


Figure 2.1 Reaction Equations for PUREX Process

This process was the man driver behind the plants at Savannah River and Hanford and has sense been modified and adapted to include additional steps which futher separate components in the waste streams. [15,18] Despite the long term practice of this technology, aqueous separation methods have a tendency to create large secondary waste volumes, which in turn have to also be disposed as HLW. [20] The increased waste is highly undesirable when looking for options to reduce the store requirements of the permanent geological repositories discussed earlier in this chapter. Efforts have been made to reduce the overall prduction of secondary wastes, simplifying the process and reducing the overall cost. [16] Also, further treatment of the secondary wastes is an option which may reduce the high level storage requirement, simplifying the treatment of spent TBP/Kerosene solvents. [19]

Process technology development efforts at the U.S. Department of Energy Hanford Site work to minimize the amount of high-level waste that may require disposal in a borosilicate glass form. After the initial separations of plutonium, uranium, and neptunium, the first solvent extraction cycle aqueous waste stream contains essentially all the fission products present in the fuel elements. This stream is denitrated and the neutralized (made alkaline) to generate neutralized current acid waste (NCAW), which is stored in underground double-wall tanks. Separation of the supernate liquid from the

solids in the NCAW slurry could allow disposal of the supernate liquid (after ^{137}Cs removal) as a low-level waste stream in grout vaults, while the TRU-bearing solids would be disposed of in a borosilicate glass form. The estimated cost of disposal of NCAW without separating the soluble slats is approximately seven-fold higher than the cost for disposal after pretreatment, \$1.5 billion, based on the processing of 2.0×10^7 L of NCAW. The economic incentive for pretreatment is, therefore, very large. [18] Figure 2.2 shows a cartoon of this process, highlighting the separations and the differences in respective storage requirements.

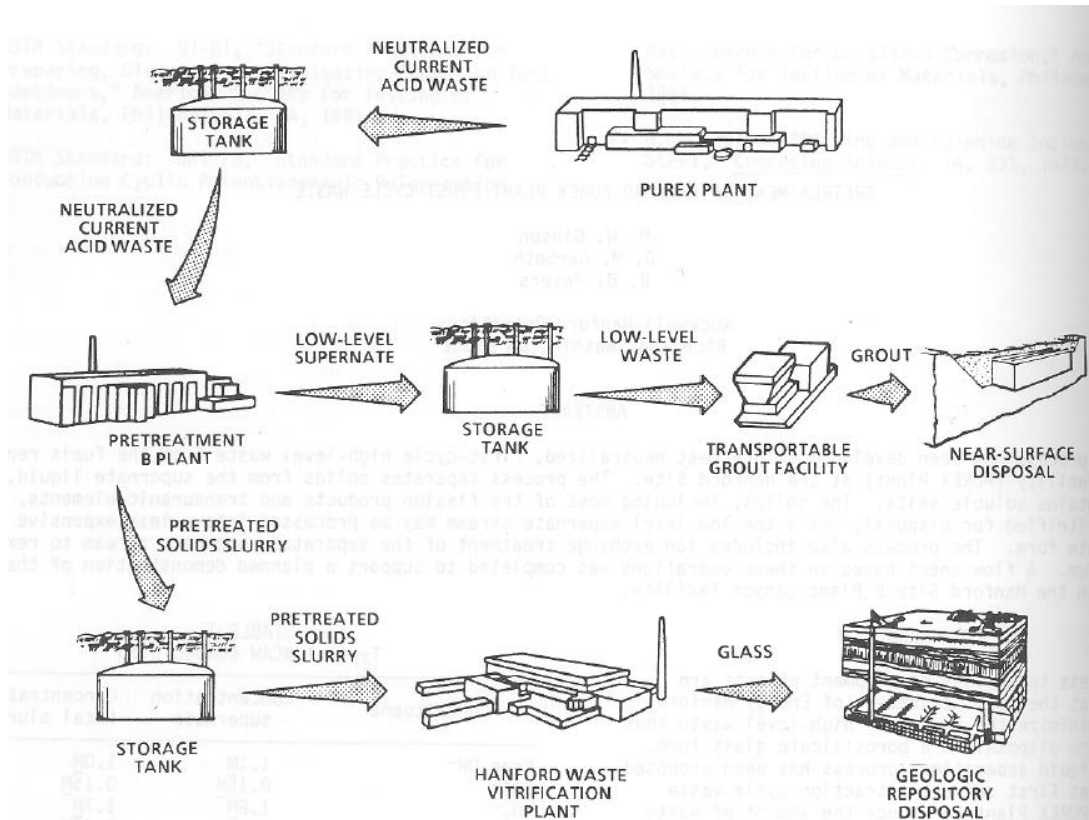


Figure 2.2 Secondary Waste Alternatives for PUREX Process

One disadvantage of the PUREX process is the difficulty in processing higher burn-up fuels with increased plutonium content which may be common for used nuclear

fuel if new generation reactors using fast neutron spectra are developed further. [17,22]

The consequences of an increased burn-up are those of increased radiolysis of organic extractant and increased quantities of volatile and non-volatile fission products. There are goals to modify the PUREX process further to accommodate much higher plutonium content and increased burnup of Fast Breeder Reactor (FBR) fuels (roughly 20% Pu, 80 MWd/kg) while simultaneously applying the results to LWR fuels. [17]

2.3 Overview of Fluoride Volatility

The volatility processes being developed offer a number of advantages over the solvent extraction processes and show promise for reducing the cost of nuclear fuel reprocessing in the future. Some of the advantages are the following: [3,22]

- Fewer, and probably simpler, processing steps
- The use of reagents with low susceptibilities to deleterious radiation effects
- Reduced criticality problems owing to the absence of neutron moderating chemicals in the process
- Radioactive waste products in solid form and small volume

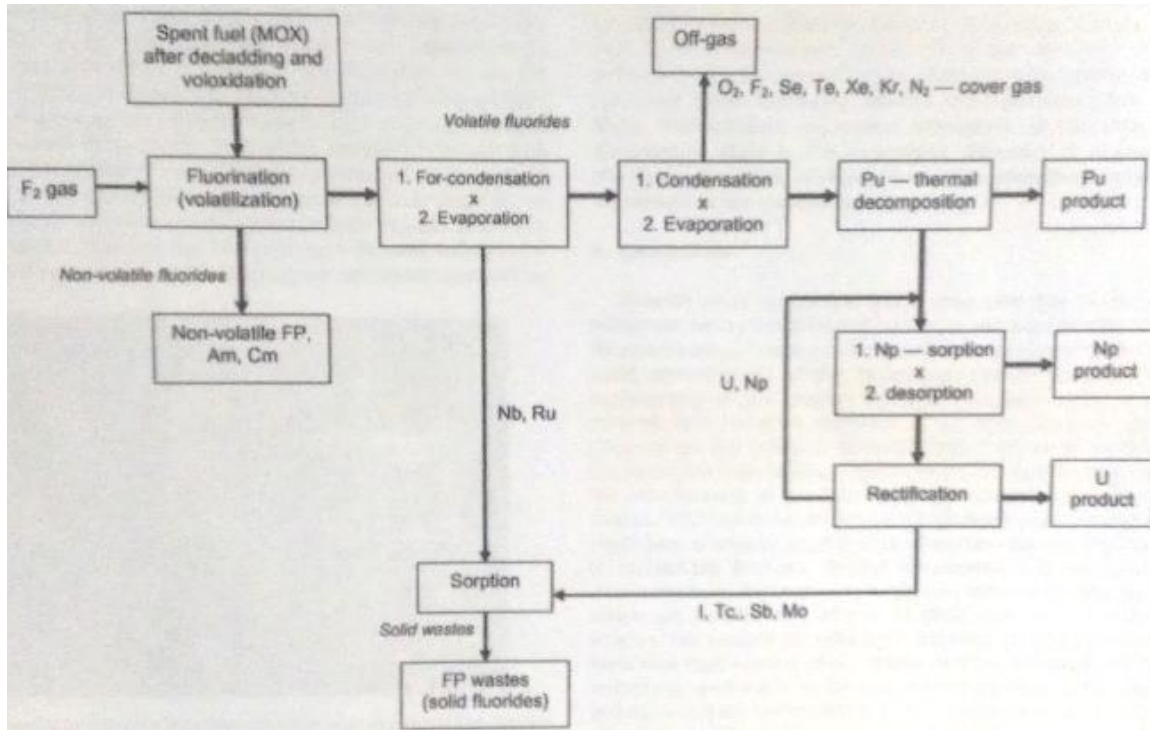


Figure 2.3 Flow Sheet for Fluoride Volatility Method [23]

As mentioned previously, this technology could also be used for the reprocessing of advanced oxide fuel types, e.g. fuels with inert matrices and/or fuels with very high burn-up, high content of plutonium, and very short cooling times. [23,25] This process is based on a separation which comes out of the specific property of uranium, neptunium, and plutonium to form volatile hexafluorides. [22,24-26] Uhlir and Marecek describe the volatility process, giving detailed analysis for the fluorination of each element found in the UNF matrix. A table of the relative volatilities of each fluoride is shown in Table 2.4. [23]

Table 2.4 Volatility of Various UNF Components

Group I (highly volatile)			Group II (volatile)			Group III (non-volatile)		
Agent	mp (°C)	bp (°C)	Agent	mp (°C)	bp (°C)	Agent	mp (°C)	bp (°C)
Kr	-157.2	-153.4	IF ₇	5	4	AmF ₄	Subl.	513
CF ₄	-184	-129	MoF ₆	17.6	33.88	RhF ₃	Subl.	600
Xe	-111.8	-108.1	NpF ₆	54.8	55.18	SnF ₄	Subl.	705
TeF ₆	Subl.	-38.6	TcF ₆	37.9	55.2	ZrF ₄	912	918
SeF ₆	Subl.	-34.5	UF ₆	64	56.5	PuF ₄	1037	927
			PuF ₆	51.9	62.2	CsF	703	1231
			IF ₅	9.4	98	RbF	760	1410
			SbF ₅	6	142.7	UF ₄	1036	1450
			NbF ₅	80	235	AmF ₃	1427	2067
			RuF ₅	101	280	CmF ₃	1406	2330
			RuF ₆	51	70	YF ₃	1136	2230
			RhF ₅	95.5	n/a	BaF ₂	1353	2260
			RhF ₆	70	73.5	EuF ₃	1276	2280
						GdF ₃	1380	2280
						CeF ₄	838	Decomp.
						CeF ₃	1430	2330
						PmF ₃	1410	2330
						SmF ₃	1306	2330
						SrF ₂	1400	2460

Progress has also been made for the use of advanced fluoride volatility methods, as seen with Kamoshida et. al. in the proposed Hybrid Recycle System (HRS). This advanced recycle system uses improved fluoride volatility reprocessing and a vibration packing scheme for MOX fuel fabrication. [3] The goal behind this process is to produce an isolated uranium stream with a high Decontamination Factor (DF), minimizing storage requirements and enabling the production of MOX fuel, while yielding a plutonium stream with a low DF to minimize the issue of non-proliferation. The “dirty Pu” can still be used as fuel in a FBR scheme. [3] The creation of the two product streams occurs in a multiple stage process by varying the concentration of the F₂ gas used as the fluorinating agent. Uranium is more easily volatilized than Pu, and can be fluorinated/volatilized with a diluted fluorine stream. Once the majority of the uranium is gone from the spent fuel, a more concentrated fluorine stream is needed to volatilize the Pu. The basic concept of the HRS system is illustrated in Figure 2.4. [3]

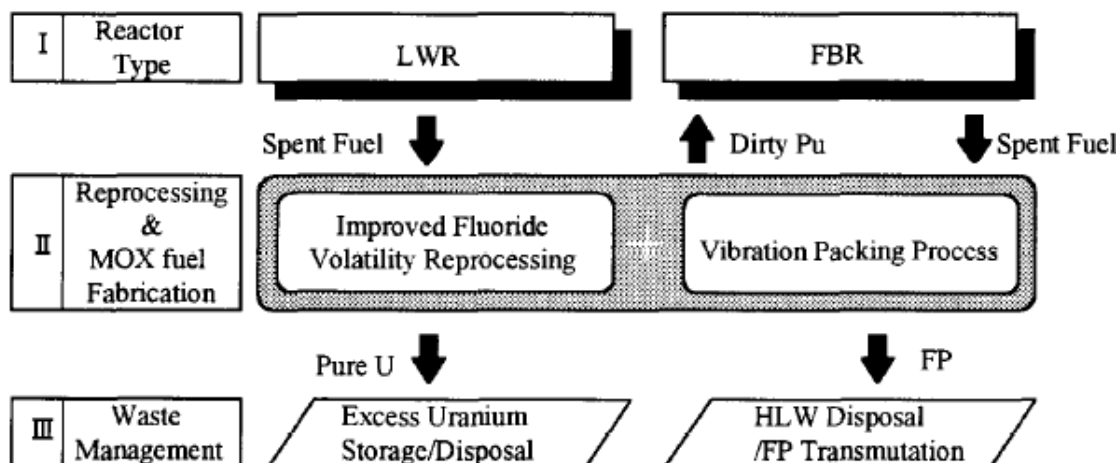


Figure 2.4 Basic Concept for HRS

Overall, fluoride volatility shows promise in the ability to successfully separate product streams of the UNF matrix while minimizing waste volumes. [4] This will allow for a drastic reduction in volume and radiotoxicity of the waste for final disposal in a geological repository. [4,27] The biggest disadvantage seen with the fluoride volatility method is the nature of the fluorinating agents used in the process. Pure fluorine gas streams require extremely corrosive resistant materials which increase the associative hazards in operation. [4,31] Constant maintenance and inspections would need to be conducted to ensure the safety of the plant.

2.4 Investigation of Alternate Fluorinating Agents

2.4.1 Nitrogen Trifluoride (NF₃)

The testing of an alternate fluorinating agent has been investigated as seen with Scheele's work using thermal NF₃. [28,29] The primary fluorinator NF₃ works on the same principles as a traditional fluoride volatility process where differences in the volatility of the various constituents of the used nuclear fuel matrix are exploited to construct an effective separations mechanism. Nitrogen trifluoride is advantageous due

to its relatively low chemical toxicity, minimal room temperature reactivity hazard, and temperature dependent (thermally sensitive) nature of its reactivity. These reasons may promote the use of NF_3 over traditional fluoride volatility fluorinators. Overall, the basic principle of fluoride volatility is receiving new interest as the search for a reprocessing scheme addressing the issues of cost, proliferation resistance, compactness, as simplified design needs to arise to meet the growing problem of used nuclear fuel inventory. [28,29]

For the research into NF_3 , Seiko thermogravimetric (TG) and differential thermal analyzers (DTA) were installed, models 320 and 6200, to carry out the fluorination reaction at elevated temperatures. Argon gas was flowed through each machine, in addition to the NF_3 gas reactant, to ensure a stable and controllable working environment. Where contamination issues posed increased risk, the TG/DTA (model Seiko 6200) was placed in an actinide glovebox with the gas exhaust also passing through a water bubbler. These studies were carried to a maximum temperature of 600 °C; however, degradation issues eventually leading to failure of the thermocouples arose as NF_3 becomes more chemically aggressive in nature with increased temperature. [28]

Calculated reaction enthalpies and free energies changes suggest that the fluorination of the fission products and actinides will be exothermic and spontaneous in nature making these reactions thermodynamically favorable and thus have a strong likelihood of occurring. These reaction enthalpies are shown in Table 2.5 [28,29]

Table 2.5 Expected Fluorination Reactions with NF₃

Postulated reaction	ΔH (kJ/mol metal)	ΔG (kJ/mol metal)
$\text{La}_2\text{O}_3 + 2\text{NF}_3(\text{g}) = 2\text{LaF}_3 + \text{N}_2(\text{g}) + 1.5\text{O}_2(\text{g})$	-669	-690
$\text{CeO}_2 + \text{NF}_3(\text{g}) = \text{CeF}_3 + 0.5\text{N}_2(\text{g}) + \text{O}_2(\text{g})$	-464	-522
$\text{CeO}_2 + 1.33\text{NF}_3(\text{g}) = \text{CeF}_4 + 0.66\text{N}_2(\text{g}) + \text{O}_2(\text{g})$	-579	-630
$0.5\text{Nb}_2\text{O}_5 + 1.67\text{NF}_3 \rightarrow \text{NbF}_5(\text{g}) + 0.83\text{N}_2 + 1.25\text{O}_2$	-571	-705
$0.5\text{Nb}_2\text{O}_5 + \text{NF}_3 \rightarrow \text{NbOF}_3(\text{g}) + 0.5\text{N}_2 + 0.75\text{O}_2$	-277	-412
$\text{Mo} + 1.66\text{NF}_3(\text{g}) = \text{MoF}_5(\text{g}) + 0.833\text{N}_2(\text{g})$	-1023	-1057
$\text{Mo} + \text{NF}_3(\text{g}) = \text{MoF}_3 + 0.5\text{N}_2(\text{g})$	-773	-725
$\text{Mo} + 2\text{NF}_3(\text{g}) = \text{MoF}_6(\text{g}) + \text{N}_2(\text{g})$	-1291	-1291
$\text{MoO}_2 + 2\text{NF}_3(\text{g}) = \text{MoF}_6(\text{g}) + \text{N}_2(\text{g}) + \text{O}_2(\text{g})$	-706	-810
$\text{MoO}_2 + 1.66\text{NF}_3(\text{g}) = \text{MoF}_5(\text{g}) + 0.833\text{N}_2(\text{g}) + \text{O}_2(\text{g})$	-262	-345
$\text{MoO}_2 + \text{NF}_3(\text{g}) = \text{MoF}_3 + 0.5\text{N}_2(\text{g}) + \text{O}_2(\text{g})$	-188	-243
$\text{MoO}_2 + 1.33\text{NF}_3(\text{g}) = \text{MoF}_4 + 0.666\text{N}_2(\text{g}) + \text{O}_2(\text{g})$	-186	-336
$\text{MoO}_3 + 2\text{NF}_3(\text{g}) = \text{MoF}_6(\text{g}) + \text{N}_2(\text{g}) + 1.5\text{O}_2(\text{g})$	-550	-694
$\text{MoO}_3 + 1.66\text{NF}_3(\text{g}) = \text{MoF}_5(\text{g}) + 0.833\text{N}_2(\text{g}) + 1.5\text{O}_2(\text{g})$	-281	-459
$\text{MoO}_3 + 1.33\text{NF}_3(\text{g}) = \text{MoF}_4 + 0.666\text{N}_2(\text{g}) + 1.5\text{O}_2(\text{g})$	-30	-220
$\text{MoO}_3 + 2\text{NF}_3(\text{g}) = \text{MoF}_3 + 0.5\text{N}_2(\text{g}) + 1.5\text{O}_2(\text{g})$	-32	-127
$\text{RuO}_2 + 1.33\text{NF}_3 \rightarrow \text{RuF}_4 + 0.67\text{N}_2 + \text{O}_2$	-477	-530
$\text{RuO}_2 + 1.67\text{NF}_3 \rightarrow \text{RuF}_5(\text{g}) + 0.83\text{N}_2 + \text{O}_2$	-289	-406
$0.5\text{Rh}_2\text{O}_3 + \text{NF}_3 \rightarrow \text{RhF}_3 + 0.5\text{N}_2 + 0.75\text{O}_2$	-425	-456
$0.5\text{Rh}_2\text{O}_3 + 1.33\text{NF}_3 \rightarrow \text{RhF}_4 + 0.67\text{N}_2 + 0.75\text{O}_2$	-590	-616
$\text{UO}_2 + 2\text{NF}_3(\text{g}) = \text{UF}_6(\text{g}) + \text{N}_2(\text{g}) + \text{O}_2(\text{g})$	-799	-901
$\text{TeO}_2 + 1.33\text{NF}_3 \rightarrow \text{TeF}_4(\text{s}) + 0.67\text{N}_2 + \text{O}_2$	-325	-427
$\text{TeO}_2 + 1.33\text{NF}_3 \rightarrow \text{TeF}_4(\text{g}) + 0.67\text{N}_2 + \text{O}_2$	-454	-588
$\text{TeO}_2 + 1.67\text{NF}_3 \rightarrow \text{TeF}_5(\text{g}) + 0.83\text{N}_2 + \text{O}_2$	-621	-734
$\text{TeO}_2 + 2\text{NF}_3 \rightarrow \text{TeF}_6(\text{g}) + \text{N}_2 + \text{O}_2$	-655	-721
$\text{UO}_2 + 2\text{NF}_3(\text{g}) = \text{UF}_6(\text{g}) + \text{N}_2(\text{g}) + \text{O}_2(\text{g})$	-799	-901
$\text{UO}_2 + 1.33\text{NF}_3(\text{g}) = \text{UF}_4 + 0.666\text{N}_2(\text{g}) + \text{O}_2(\text{g})$	-983	-1044
$\text{UO}_2 + 1.333\text{NF}_3(\text{g}) = \text{UO}_2\text{F}_2 + 0.666\text{N}_2(\text{g}) + \text{F}_2(\text{g})$	-391	-417
$\text{U}_3\text{O}_8 + 6\text{NF}_3(\text{g}) = 3\text{UF}_6 + 3\text{N}_2(\text{g}) + 4\text{O}_2(\text{g})$	-708	-806
$\text{U}_3\text{O}_8 + 4\text{NF}_3(\text{g}) = 3\text{UF}_4 + 2\text{N}_2(\text{g}) + 4\text{O}_2(\text{g})$	-551	-618
$\text{U}_3\text{O}_8 + 2\text{NF}_3(\text{g}) = 3\text{UO}_2\text{F}_2 + \text{N}_2(\text{g}) + \text{O}_2(\text{g})$	-374	-374
$\text{PuO}_2 + 2\text{NF}_3(\text{g}) = \text{PuF}_6(\text{g}) + \text{N}_2(\text{g}) + \text{O}_2(\text{g})$	-450	-516
$\text{PuO}_2 + 1.33\text{NF}_3(\text{g}) = \text{PuF}_4 + 0.666\text{N}_2(\text{g}) + \text{O}_2(\text{g})$	-815	-880
$\text{NpO}_2 + 1.33\text{NF}_3(\text{g}) = \text{NpF}_4 + 0.666\text{N}_2(\text{g}) + \text{O}_2(\text{g})$	-303	-438
$\text{NpF}_4 + 0.666\text{NF}_3(\text{g}) = \text{NpF}_6(\text{g}) + 0.333\text{N}_2(\text{g})$	+20.4	-39.2
$\text{PuF}_4 + 0.666\text{NF}_3(\text{g}) = \text{PuF}_6(\text{g}) + 0.333\text{N}_2(\text{g})$	+113.2	+54.1

Previous experiments showed that U₃O₈ did not react at lower temperatures, and the exothermic reaction with NF₃ to produce volatile UF₆ began around 530 °C without

any observable mass gain as a result of the fluorination. The experiments did show that 80% of the U_3O_8 had volatilized from 400-600 °C when heating at a rate of 5 °C/min, but the conversion to UF_6 was much slower than with the UO_2 samples studied. The experiments with UO_2 again showed an exothermic reaction with NF_3 around 360 °C where the sample continued to gain mass until a temperature of 570 °C was reached. At this temperature, a strong exothermic reaction which produced volatile UF_6 initiated, completely volatilizing the entire sample after 10 minutes. [28]

Upon exposure to 5% NF_3/Ar at 40°C, Scheele reports that Nb_2O_5 reacted almost immediately as suggested by the increasing mass on the TGA curve. The DTA curve indicated that the reaction was highly exothermic suggesting the formation of NbF_5 , which has a boiling point of 235°C. The experiments indicated that the fluorinator NF_3 is sufficiently strong enough to convert Nb_2O_5 to a volatile fluoride before it is fully converted to an intermediate, non-volatile form. Scheele also reports that the closeness of the volatilization temperatures for uranium and Nb may suggest that both compounds will volatilize simultaneously when treated with thermal NF_3 . [28]

When exposed to 5% NF_3/Ar , molybdenum compounds began to react exothermically near 300 °C and complete volatilization of the samples were observed. Comparison of the reaction profiles of the Mo compounds with those of uranium oxides finds significant differences in behavior, suggesting a thermal window may be present to separate Mo from uranium oxides. The volatilization temperatures of the uranium samples was far greater than that of molybdenum, so as long as the reaction temperature is able to be maintained around 300 °C, molybdenum should volatilize away from UNF before uranium. [28]

Investigation on the fluorination of RuO_2 by reacting with thermal NF_3 found that although fluorination and subsequent volatilization was possible (raid mass loss around 500°C), the reaction temperatures were quite close to those of uranium compounds. This suggests that separations based solely on reaction temperature may be difficult. Scheele et al. suggest that further isothermal testing should be conducted to provide a more precise thermal reaction profile and develop the kinetic models needed for further analysis. [28]

The fluorination and subsequent volatilization of Rh_2O_3 by using thermal NF_3 proved unsuccessful at temperature ranges below 550°C . It was reported that although Rh has volatile fluorides, NF_3 was not a sufficiently strong fluorinating and oxidizing agent to produce a volatile fluoride. In a separations process, a fluorination reaction with this oxide would occur, but the intermediate fluoride species would be formed, leaving the sample in a non-volatile fraction. [28]

A complete list of the oxides tested by Scheele et al. is shown in Table 2.6.

Table 2.6 Reaction Onset and Volatilization Temperatures using NF_3

Test material	Onset temperature (s) ($^\circ\text{C}$)	Volatilization temperature ($^\circ\text{C}$)
UO_2	360, 570	570
U_3O_8	530	530
La_2O_3	230, 330	NA
CeO_2	320, 400	NA
Nb_2O_5	360, <540	<540
Mo metal	300	300
MoO_2	260	260
MoO_3	320	320
RuO_2	330, 460, 500	330, 500
Rh_2O_3	220, 350	NA
TeO_2	260	260
PuO_2	450	NA
NpO_2	420	550

2.4.2 Ammonium Bifluoride (NH_4HF_2)

Recent work using ammonium bifluoride as a potential fluorinating agent gives promise to the formation of desired compounds when reacting with oxides of the used nuclear fuel matrix. [2,29,30] By simply mixing ammonium bifluoride with UO_2 in a ball mill at room temperature, tetravalent ammonium uranium fluorides were successfully formed. These fluorides were then reacted in an ammonia atmosphere at $800\text{ }^\circ\text{C}$ to form hexavalent UN_2 . Visual evidence from these experiments is shown in Figure 2.5. [30]

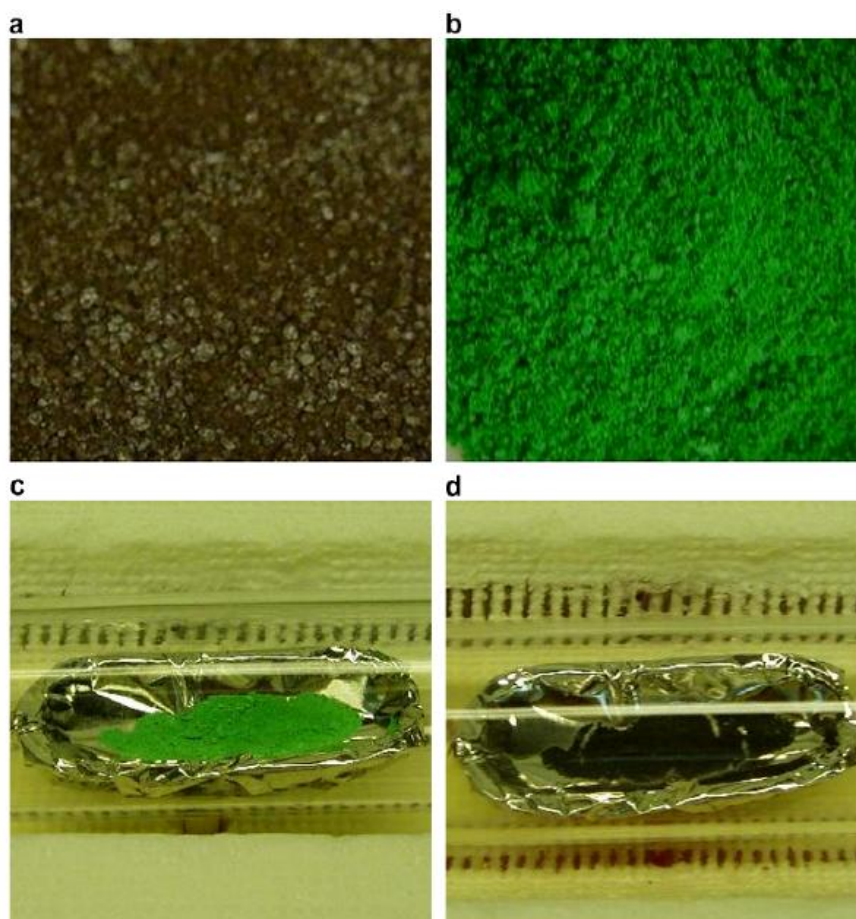


Figure 2.5. Reaction of UO_2 with NH_4HF_2 to Produce UN_2

The formation of UN_2 is desirable because this compound can be easily decomposed to UN at $1100\text{ }^\circ\text{C}$ under argon through an intermediate phase of U_2N_3 . [30]

Uranium mononitride (UN) has a number of favorable nuclear fuel properties, such as high fissile atom density, high melting point, and a high thermal conductivity. [30] The reaction pathway using ammonium bifluoride and UO_2 to create this compound is much simpler than current routes to form these nitrides which require very high temperature and pressure. [30]

Fluorination profiles of other oxides, such as the rare earth oxide Y_2O_3 , have been studied using TGA and DTA analysis at elevated temperatures. [31] Mukherjee et al. report during the mixing of the fluorinating agent with the surrogate oxide powder, all of the samples became reasonably warm alluding to the occurrence of an exothermic chemical reaction even at room temperature. Also, the sealed bags used to store the mixtures became inflated after some time, indicating the reactions had a gaseous product. [31] During the study of high temperature reactions, it was found that substantial evaporation of ammonium bifluoride led to the inability of the fluorinating agent to react with the Y_2O_3 sample. [31]

2.4.3 Xenon Difluoride (XeF_2)

The fluorination of uranium and zirconium oxides by using XeF_2 was reported by Mayhew and Boyle. Their findings suggest that at ambient pressure, mixtures of XeF_2 with UO_2 or ZrO_2 do not need to be heated to elevated temperatures in order to produce UF_6 and ZrF_4 respectively. [32] What is required, however, is the addition of a drop of water to insinuate a violent exothermic reaction which fluorinates these oxides at room temperature. It was also noted that U_3O_8 can be made to react with XeF_2 in the same way. [32] A summary of the observations recorded by this research is shown in Figure 2.6.

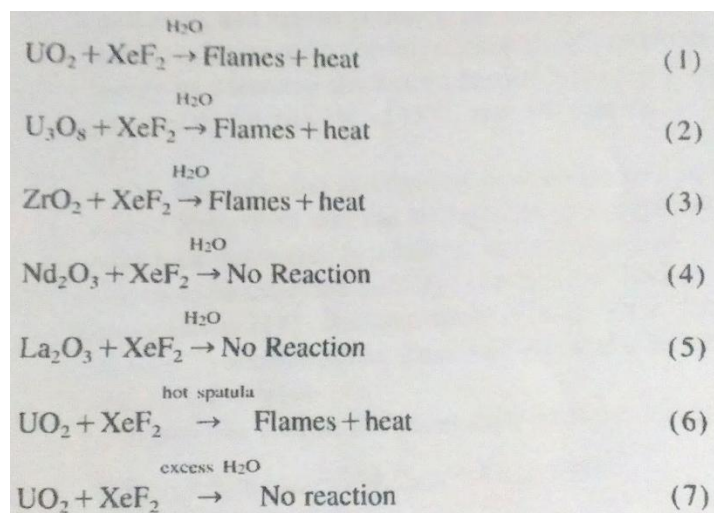


Figure 2.6 Observations Using XeF_2 as Fluorinating Agent

The use of a fluidized bed reactor has been investigated for the fluorination reaction between XeF_2 and UO_3 . [33] It was found that the fluorination reaction proceeded in two steps by forming the intermediate UO_2F_2 in the process and the fluorination rate was higher than for pure F_2 gas using temperatures below 150°C . [33] The intermediate UO_2F_2 was converted to UF_6 at temperatures above 300°C . One interesting note is that the exothermic reactions were so large and violent that mixtures of XeF_2 and UO_3 needed to be diluted with Al_2O_3 to absorb the thermal shock at the onset of reaction. This is attributed to the largely negative heat of formation with the uranium fluorides. Every fluorinating agent has their respective advantages and disadvantages, most of which pertain to availability, handling problems, toxicity, reaction rate, and product separation and recovery. [33]

CHAPTER 3

METHODOLOGY

Experimental Setup – Non Radioactive (Savannah River National Laboratory)

For all experiments using non-radioactive, surrogate oxides of the used nuclear fuel matrix, experiments were carried out using a Shimadzu DTG-60 Simultaneous Thermogravimetric/Differential Thermal Analysis (TG/DTA) machine, which was installed in one of the clean laboratories at SRNL. Capable of reaching temperatures of 1100 °C from ambient, the DTG-60 is completely sufficient for the temperature range of interest for this research (< 1000 °C). The instrument comes installed with a built-in cooling fan coupled with a low mass furnace too allow for high sample throughput and reasonable experiment runtimes. The heightened sensitivity of the machine is a result of a unique balance mechanism (Roberval Mechanism) that prevents small changes caused by factors such as thermal expansion. The fulcrum used for the balance is made of lightweight materials which possess small thermal coefficients and have extremely low friction and resistance. The measurable ranges for the DTG-60 is ± 500 mg (TG) with a readability of 0.001 mg and ± 1000 μ V (DTA). Data acquisition is done by the TA-60WS equipment, and the programming of all experiments is built through the included software package for the machine. [34]

The atmosphere of the DTG-60 furnace was maintained using a high purity argon gas bottle connected to the machine using a regulator, safety relief valve, and standard swagelok tube fittings. Gas flow was maintained using an Alicat Scientific MC Series

Mass Flow Controller to push 40 standard cubic centimeters of argon gas through the furnace during all experiments. The entire machine was installed under a fume hood, so any off gases were safely expelled from the TG/DTA out of the laboratory. With the decomposing nature of the alternate fluorinating agents tested throughout this research, an inert glovebox was used for both sample storage and preparation. The glovebox and fume hood in which the TG/DTA was installed are both located in the same laboratory room which allowed for minimal transition time when moving from one to another.

Figure 3.1 shows the DTG-60 as it was installed in the laboratory.



Figure 3.1. Installation of DTG-60

Although there were a variety of sample pans available for use, generally experiments were conducted using platinum sample pans capable of withstanding

maximum furnace temperature, a much higher temperature than aluminum or stainless steel sample pans can safely operate. With highly exothermic reactions expected during the fluorination of the various surrogate oxides, localized sample temperatures may rise much higher than the controlled, bulk furnace temperature; therefore, it was much safer to go with the platinum pans despite all experiments using these oxides being held below 600 °C. Alumina powder (Al_2O_3) was used as a reference material in all cases due to its severely inert nature and thermal stability. If any sample residues remained at the conclusion of each experiment, they were stored in labeled, glass vials for future analysis or disposal.

Powder X-ray Diffraction (XRD) was performed on starting materials and on compositions after each experiment. Products were packed onto a glass slide and sealed with a Kapton film as seen in Figure 3.2. XRD data was collected using $\text{Cu-K}\alpha$ radiation from a PANalytical Xpert Pro X-ray diffractometer. Further instrument parameters for the XRD analysis are shown in Table 3.1.

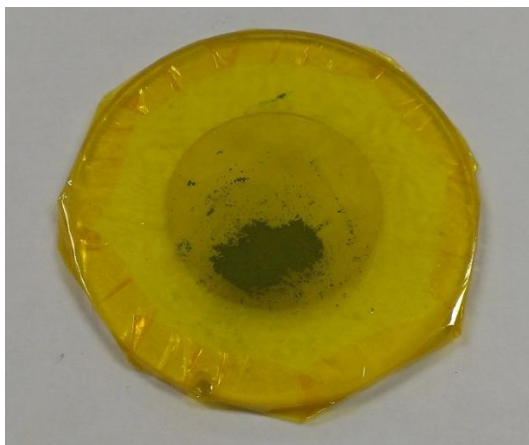


Figure 3.2. XRD Slide Preparation

Table 3.1. XRD Instrument Parameters

Radiation Source	CuK α X-ray
Source Power	45 kV, 40 mA
Wavelength	1.5405982 Å
Goniometer	PANalytical X'pert Pro
Divergence Soller Slit	0.04 rad
Divergence Slit	1/2°
Beam Mask	10mm
Divergence Antiscatter	1°
Specimen Rotation	No
Diffacted Beam Antiscatter (short)	3.4
Diffacted Beam Antiscatter (long)	5.5
Filter	Nickel
Detector	X'Celerator
Active Length	2.122°
2 θ Range	5° - 70°
Step Interval	0.0167° (2 θ)
Fixed counting Time	99.965 s/step

TG/DTA Calibration (SRNL)

Because the TG/DTA was newly installed in the laboratory, initial setup/calibration needed to be done to ensure proper functionality of the machine. First, a burnout of the furnace was initiated by taking the machine to maximum temperature (1100 °C) with a high argon gas flow rate and no samples present. The goal in doing so was to remove any residue which may be present on the inside of the furnace leftover from factory construction. Next, an experiment was conducted, again without a sample present, for a baseline hold at 200 °C for a length of 30 minutes. The goal for this run was to ensure the proportional-integral-derivative controls (PID) which are built into the machine's system were functioning within acceptable limits. It was found that the TG/DTA fell 8.08 °C short of the intended setpoint, and a correction needed to be implemented. Results from this run are shown in Figure 3.3 below.

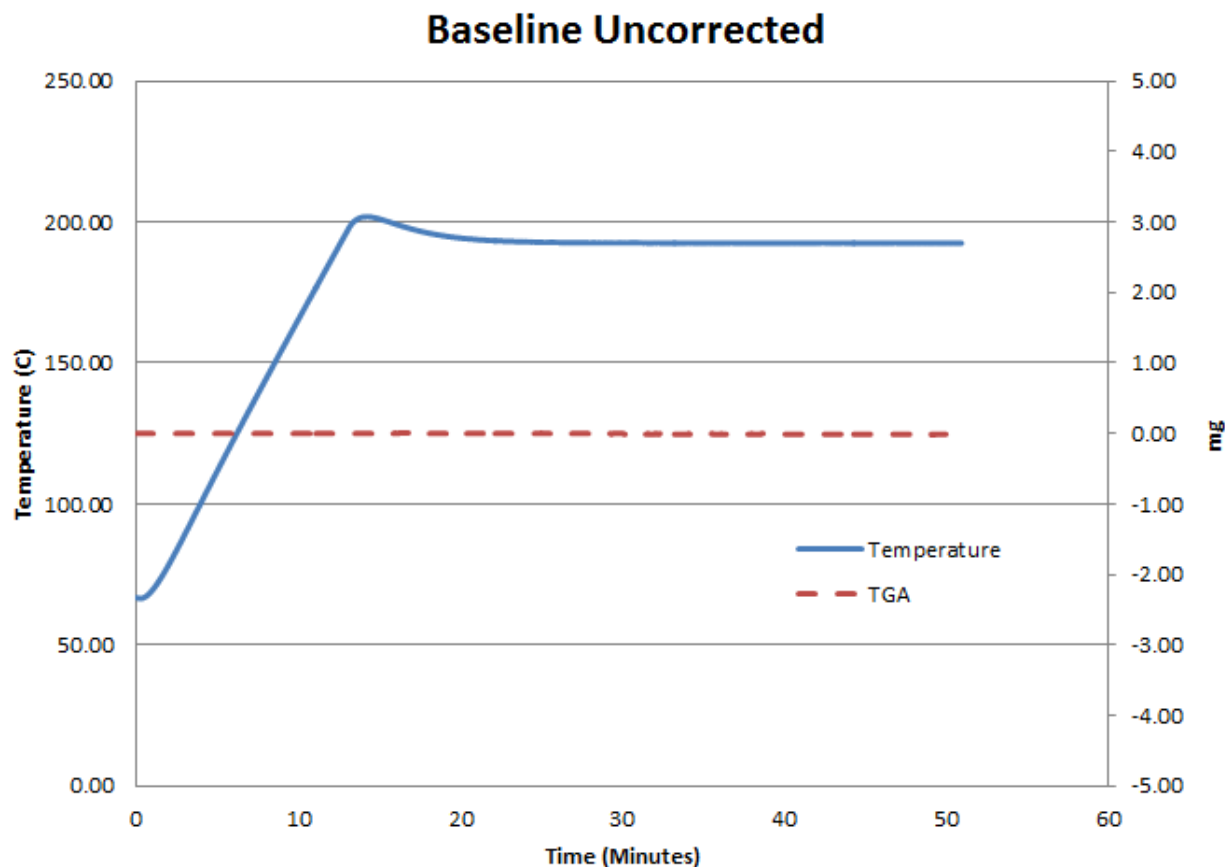


Figure 3.3. Baseline Heating Results Prior to Adjustment

A temperature correction could be easily adjusted using the provided software, and a follow-up run was needed to prove the correction successful. For the corrected experiment, a temperature hold was set at 250 °C for the duration of an hour, and the results are plotted in Figure 3.4 below. Comparing Figures 3.3 and 3.4 shows a distinct difference in the ability to hit the desired setpoint, with the corrected test agreeing perfectly with the initial experimental input. It can also be noted that the PID parameters remained at their default factory setting, and the temperature adjustment was implemented using additional control options. Although the graphed furnace temperature does rise past the intended setpoint only to fall and reach the exact value 5-10 minutes later, the severity was not large enough to warrant changing and optimizing the PID

parameters. In all of the baseline tests and burnout experiment, the controlled heating rate remained stable and consistent throughout all temperature ranges.

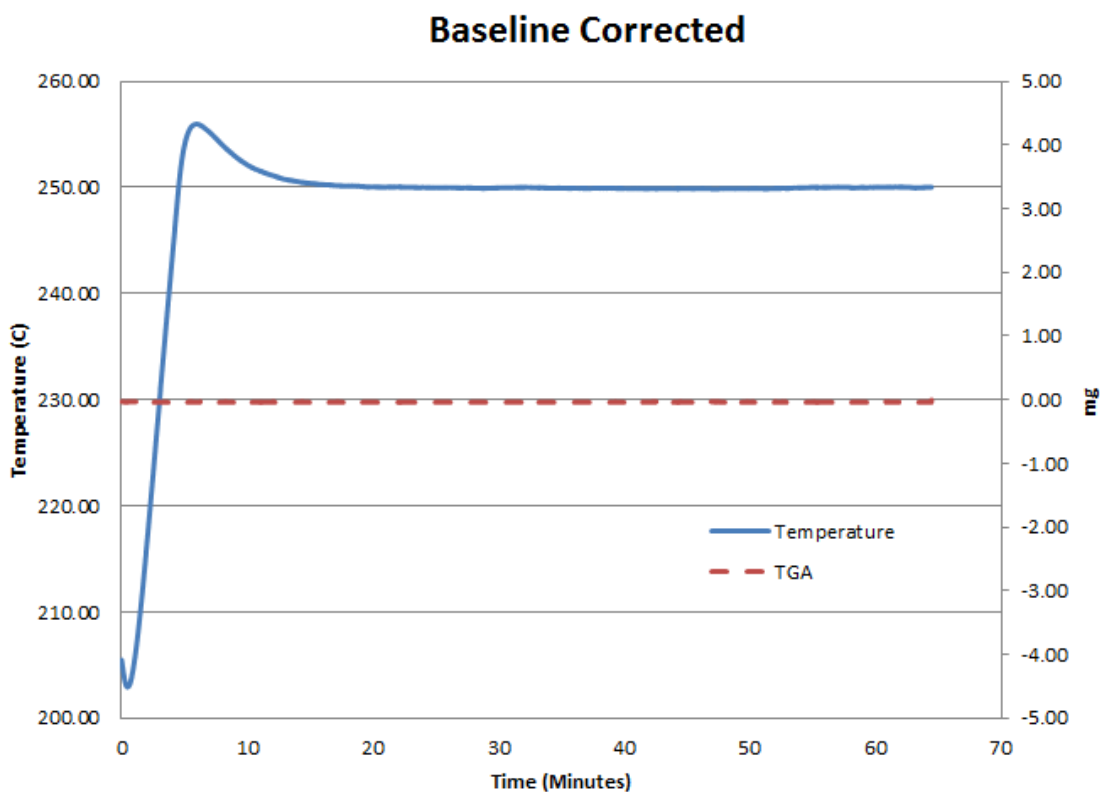


Figure 3.4. Baseline Heating Results Post Adjustment

The Shimadzu DTG-60 comes standard with reference materials to perform temperature calibrations. Experiments were conducted using a sample of Tin (Sn), and the experimental temperature for melting was compared with published data on the melting point (231.9 °C). [34] A melt should clearly be shown as an endothermic reaction on the DTA curve as energy is required to break the bonds of the structure to perform the phase change. If needed, adjustments could be made to make the expected and experimental melting points agree, but upon inspection, the DTG-60 appeared to be functioning well within the required limits for error. Results from the melting of Tin are shown in Figure 3.5. This experiment was conducted using a 22.3 mg sample heated at a

rate of 10 °C/min until a temperature of 250 °C was reached and melting of the sample was observed.

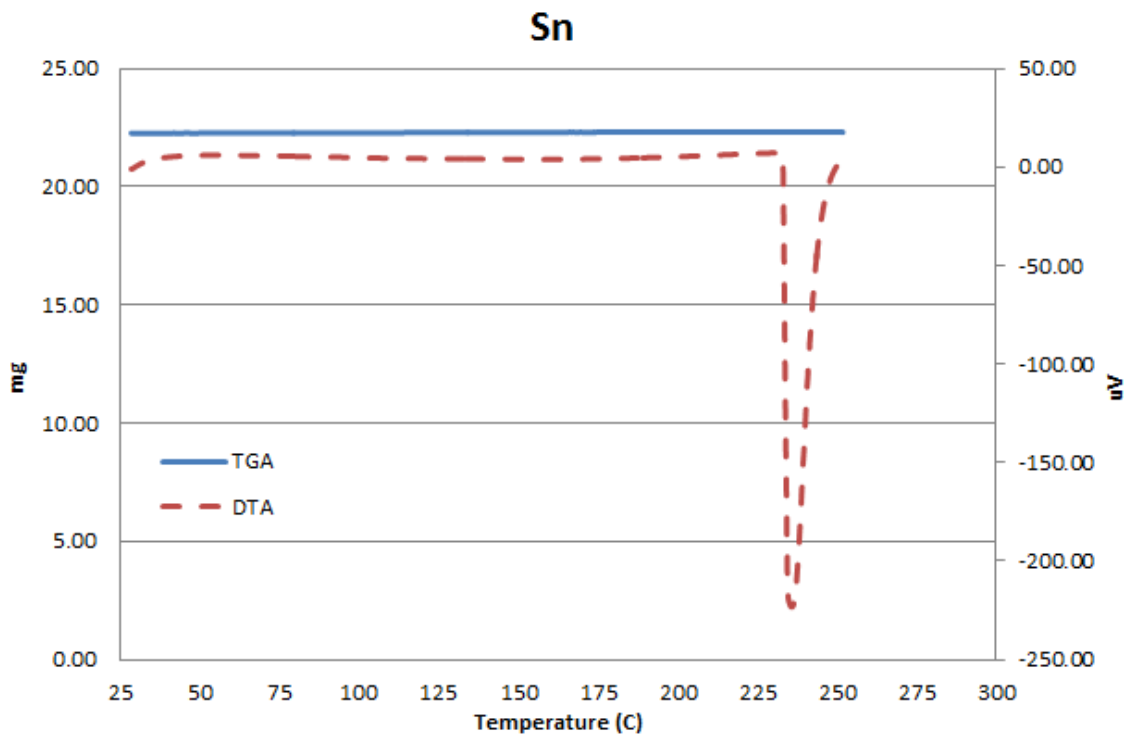


Figure 3.5. TG/DTA Data for Melting of Tin

The use of calcium oxalate monohydrate ($\text{CaC}_2\text{O}_4 \cdot \text{H}_2\text{O}$) as a calibration tool is well publicized in literature for use in a TG-DTA apparatus. [35] Its thermal decomposition is well defined at three specific locations; giving off water (H_2O), carbon monoxide (CO), and carbon dioxide (CO_2) at predictable temperature ranges. [35] A series of three experiments using calcium oxalate monohydrate were conducted for the initial setup of the machine; two in an argon environment and one in an air environment. The difference when exposed to argon vs. air is that while argon is pushed through the furnace, the second reaction is endothermic. Alternatively, when air is pushed through the furnace, the second reaction exhibits an exothermic peak on the DTA graph. The results

of these three runs along with the baseline hold corrections and reference material melting proved the machine was in good working order. Additional runs decomposing calcium oxalate monohydrate in an argon environment were completed weekly throughout the duration of the research to ensure the consistency of the machine. All of the runs using $\text{CaC}_2\text{O}_4 \cdot \text{H}_2\text{O}$ were completed using roughly 30 ± 5 mg samples in a Pt sample pan heated at a rate of $10^\circ\text{C}/\text{min}$ until termination at 1000°C . Sample TG-DTA data for calcium oxalate monohydrate in an argon environment is shown in Figure 3.6.

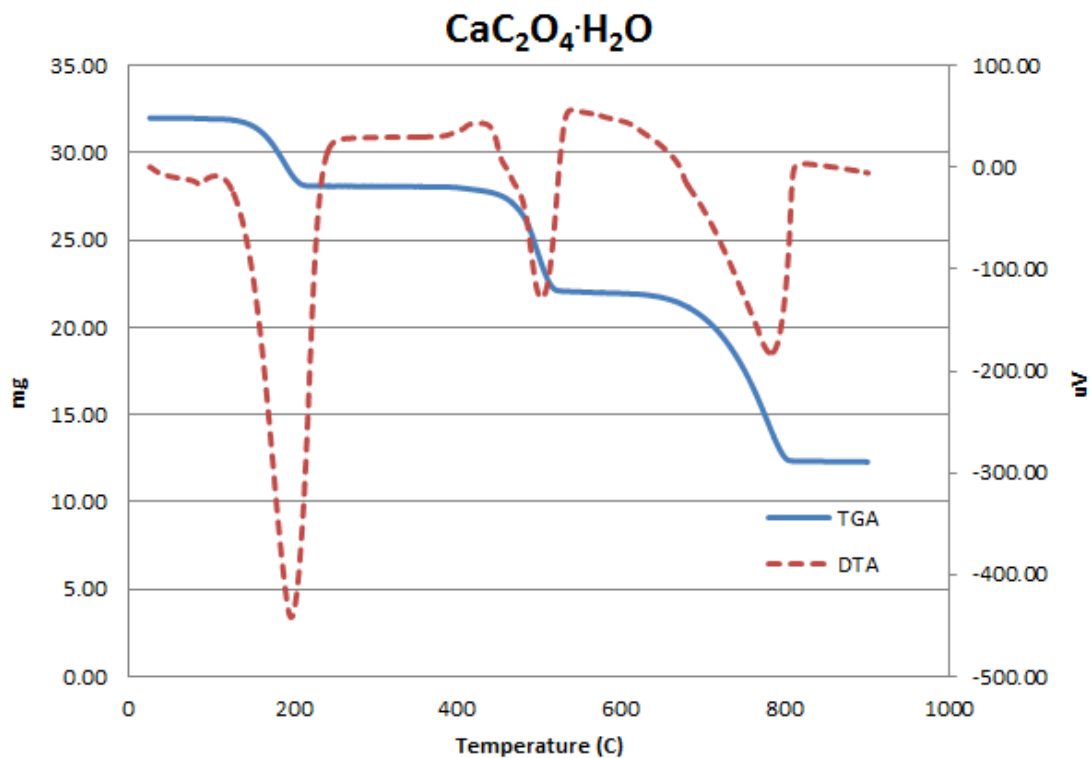


Figure 3.6. TG/DTA Data for Calcium Oxalate Monohydrate ($\text{CaC}_2\text{O}_4 \cdot \text{H}_2\text{O}$)

Sample Preparation (SRNL)

The surrogate oxides and fluorinating agents used in these experiments came from chemical storage stocks used in previous research at SRNL and were all of very high purity (> 99%). As they were needed, the oxide materials were transferred to the glovebox where the fluorinating agents were stored to be weighed and mixed in the sample pans. Samples were prepared in excess of fluorinating agent, typically on a 2:1 scale of fluorinator to surrogate oxide respectively. The target weight for each run was roughly 30 mg total; however, small deviations from this approach may have been inevitable and will be explained as they are presented later in this report. The components were lightly mixed using a scupula and/or tongs in attempt to create more homogenous mixture through the sample pan. This would help promote the reaction pathways necessary for a solid-solid reaction to take place.

One variation to the standard sample preparation procedure was used during some experiments with ammonium bifluoride against molybdenum trioxide (MoO_3) and again with strontium oxide (SrO). The variation lies within the sample pan used during the experiments. Available for use were stainless steel sample pans which came with an option to use a fitted lid during the experiment. Although not completely airtight, especially at elevated temperatures, the new sample pan would hopefully better contain the reactants throughout the heating in the TG/DTA furnace, promoting the fluorination reaction. Samples were still prepared at a 2:1 ratio totalling roughly 30 mg and lightly mixed before they were inserted into the TG/DTA.

Experimental Setup –Radioactive (SRNL)

Experiments testing radioactive samples against the fluorinating agents had to be conducted on a separate TGA machine located in the RAD labs at SRNL. This machine, a modified Dupont 951 TGA shown in Figure 3.7, was used in previous research studying sulfur hexafluoride (SF_6) as a potential fluorinating agent for use in Reactive Gas Recycle. [5,6] Although the general idea for fluorination/volatilization of the oxides is the same no matter what reactant used, the major difference in SF_6 as opposed to XeF_2 or NH_4HF_2 is that SF_6 exists as a gas at room temperature as opposed to latter two solid-phase fluorinators. Because of this, the TGA machine/reactor already installed in the lab was setup in a flow through design meant for a gas reactant. The machine could still be used without modification; however, both the oxide of interest and fluorinating agent would now rest in the sample pan. Previous research with SF_6 simply had the oxide rest in the sample pan and then flow a mixture of argon and SF_6 gas directly onto the sample. [5,6] This allowed for a constant supply of fluorinating agent throughout the entire experiment (i.e. all temperature ranges); whereas, if the solid phase fluorinating agents used in the current research were to decompose prior to fluorination, there would be none left to react once the appropriate temperature was reached. This is particularly visible when reacting with uranium and zirconium oxides which require elevated temperatures to initiate the fluorination reaction.

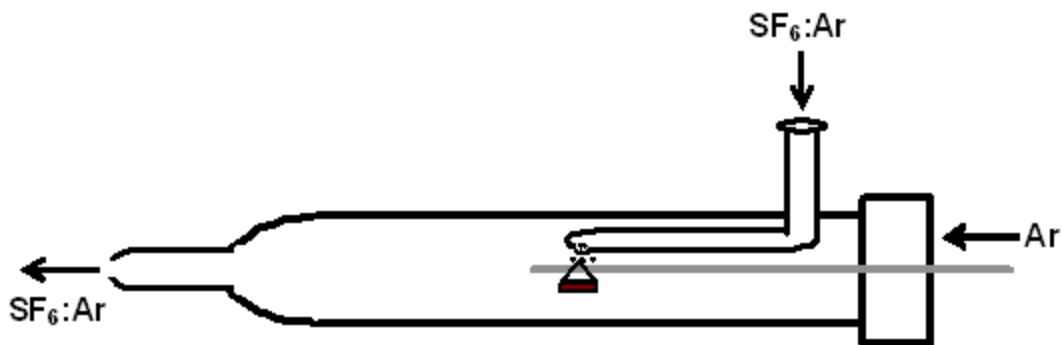


Figure 3.7 Modified Dupont 951 TGA

Samples were prepared similarly to the previous experiments in the clean laboratory with all samples containing an excess of fluorinating agent at roughly a 2:1 ratio. All experiments were conducted with a constant stream of 40 sccm argon gas through the reactor at all times. The TGA furnace was heated at a rate of 10 °C/min until the final temperature was reached; no temperature holds were used with this machine. As needed calibration runs were conducted using the same methods as mentioned with the clean TG/DTA machine using calcium oxalate monohydrate.

Experimental Setup (USC)

The experiments conducted in the laboratories at USC were done so in a two part process using the help of a CM Model 1730-12 HTF Tube Furnace and Netzsch STA 409 TGA. By using a two-step approach, both closed and open systems were utilized to study the fluorination and volatilization profile of U_3O_8 . Further detail for each approach will be outlined later in this report.

The 1700 series CM tube furnaces are capable of reaching temperatures up to 1700 °C at rapid heating and cooling rates. The fast thermal cycling is a result of the low thermal conductivity and light weight nature of the high purity alumina fibers used as

insulation in the furnace. [36] Installed in the laboratory is a Model 1730 HTF Horizontal Tube configuration as shown in Figure 3.8. A cooling water jacket was also installed on both ends of the tube which extrudes from the active volume of the furnace, shown in better detail in Figure 3.9. The instrument is controlled by a large power supply and input screen which exists as a separate unit from the figures below. Preset experimental parameters using multiple different segments of various heating/cooling rates and hold times may be input to the machine, or the user can choose to operate in manual mode. Parameters were set to emulate the work at SRNL with non-radioactive, surrogate oxides to maintain consistency throughout all experimentation.

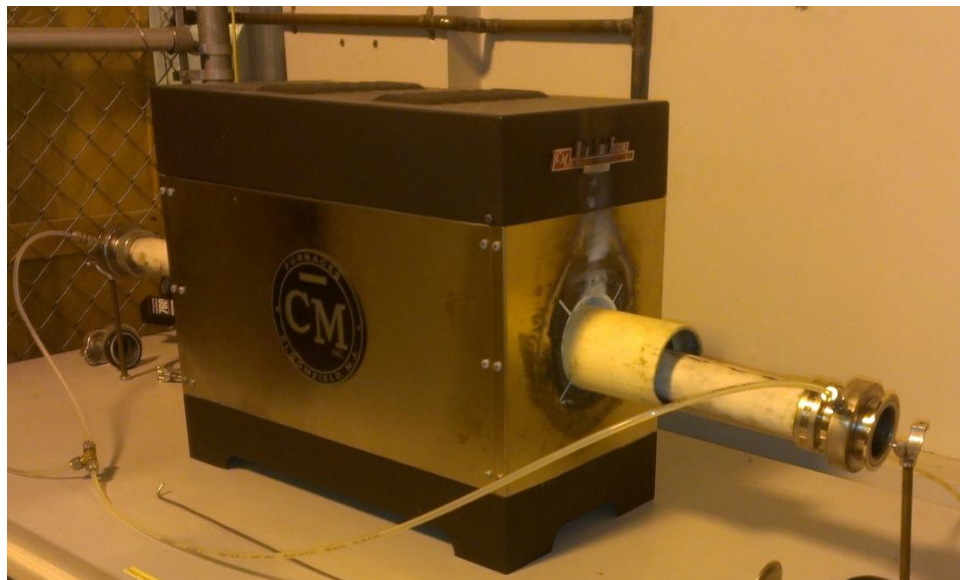


Figure 3.8. CM 1730-12 HTF Tube Furnace



Figure 3.9. Close-up of Cooling Water Jacket and End Caps

To construct a closed system which would be used in the tube furnace, stainless steel swagelok tube fittings were pieced together to form a sealed volume for the sample material. A single SS-400-6 union was capped on both ends by two SS-400-P plugs to create this small volume. These fittings would hopefully contain the reactants, addressing the problem of XeF_2 escaping through decomposition, while the furnace reached elevated temperatures where fluorination reactions are better promoted. Upon cooling, the volume would be removed from the furnace, opened, and the now fluorinated sample could be transferred to the TGA for further analysis. When any sample was inserted in the furnace, a molybdenum boat was utilized to easily transfer the sample to the active volume of the furnace located directly in the middle of the tube. These boats were manufactured by R.D. Mathis Company and are model number SB-7A-.010MO.

Once the samples were removed from the sealed swagelok fittings after step one in the tube furnace, the material was then sent to undergo thermogravimetric analysis using a Netzsch STA 409 TGA. This machine was already in use and in good working order for other ongoing research in the laboratory at USC, so no initial setup was necessary. The particular model used has a sensitivity of 5 μg up to a maximum sample weight of 15 g and capability of reaching temperatures from ambient to 1600 $^{\circ}\text{C}$, well within the limits for this research. [37] Detailed control of the atmospheric conditions inside the furnace was available, but not fully exploited as they were not deemed necessary for the reactions in question. That being said, however, the furnace volume was vacuumed down after each opening and replenished with argon gas. Also, a steady flow of 40 sccm argon gas flowed through the furnace during all experimentation. The machine, as installed in the laboratory, is shown in Figure 3.10.



Figure 3.10. Netzsch STA 409 TGA

Baseline tests had to be conducted using the Al_2O_3 crucible which would be used for all powdered sample experiments in the TGA. The purpose in doing a baseline test is to negate the buoyancy effects which occur at the onset of gas flow at the start of data acquisition. When an experiment is initiated, the 40 sccm of argon gas flows from the bottom of the furnace, exerting an upward force on the bottom of the crucible, and then exists out of the top of the machine. This upward force causes the sample to appear lighter to the TGA, skewing the results. It is also noted that these effects are temperature dependent, so the baseline test has to be done at the exact parameters as will be used in the real experiments. Once the baseline test is completed, all experiments from then on, assuming all experimental parameters remain constant, will automatically have the buoyancy effects subtracted from the results.

The baseline experiments were run from room temperature and heated at a rate of $25\text{ }^\circ\text{C}/\text{min}$ until a temperature of $800\text{ }^\circ\text{C}$ was reached. Once at final temperature, the furnace was maintained for one before allowed cooling. As mentioned previously, the crucible was made of aluminum oxide and industrial argon gas (40 sccm) was flowed through the machine at all times. For the greatest consistency between experiments, the furnace volume of the TGA was vacuumed out after each opening of the machine. Once at vacuum, the industrial argon gas was pushed into the chamber until the volume was brought back to atmospheric pressure. Once this step was completed, the experiment was allowed to begin. A total of three baseline experiments were completed, and the best results were chosen. All three baseline experiments were very similar; however, the second experiment showed the smallest margin of drift in the data. Results from the second baseline experiment are shown in Figure 3.11.

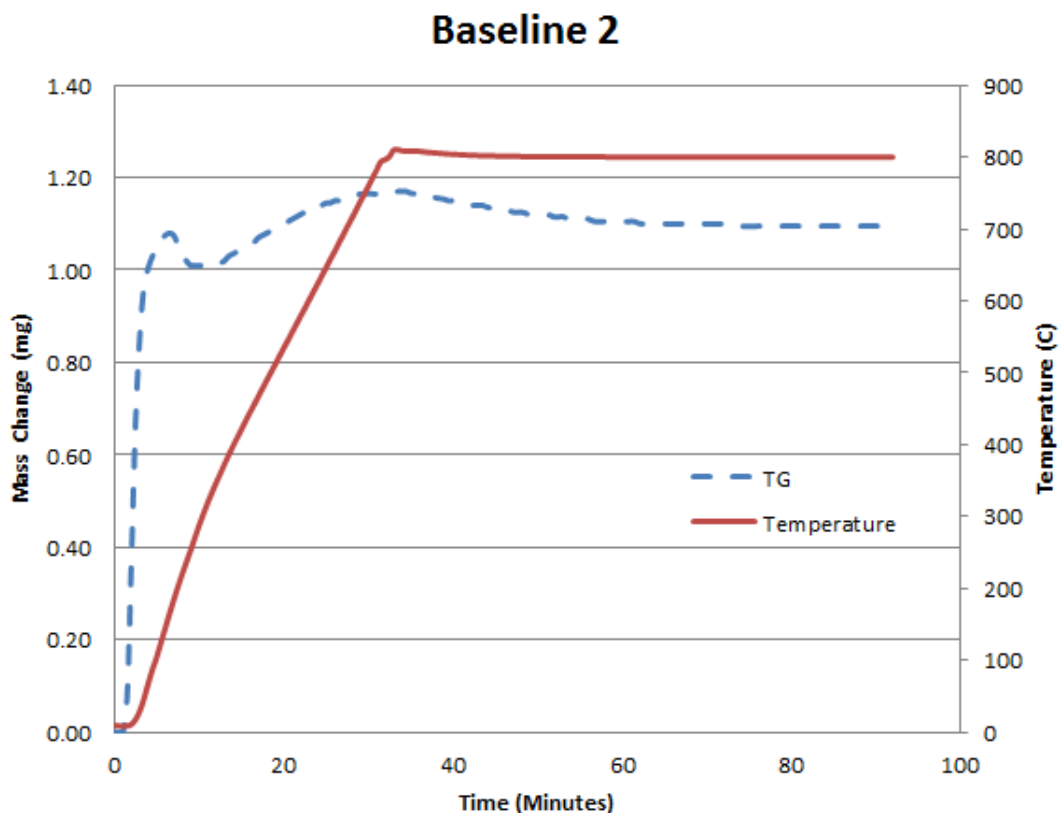


Figure 3.11. Baseline 2 TGA Results

Sample Preparation (USC)

The laboratory at USC already possessed a large quantity of uranium material which was made available for use in this study. The stockpile that was chosen was labeled and documented as natural uranium in the form of small metal chunks ranging from roughly 0.2 – 2.6 grams in size. In its current state, large solid pieces of metal material are not as favorable in terms of reaction kinetics to promote the fluorination reaction aimed by mixing the material with XeF_2 . To alleviate this problem, 11.3926 g of the natural uranium material was to be heated in the furnace to completely oxidize the material to a fine, uniform U_3O_8 powder. Two runs in the tube furnace were set up to complete the oxidation of this material. The first run was heated to a temperature of 750

°C from ambient at a rate of 600 °C/hr and held for one hour. This temperature setpoint, as reported by Thein and Bereolos, is completely sufficient to ensure the conversion of both UO_2 and UO_3 to U_3O_8 , a much more stable compound in oxidizing atmospheres. [38] The metal chunks were placed in the molybdenum boats, as shown in Figure 3.12, and inserted into the furnace for heating. Upon completion of the first run, the sample was removed from the furnace only to find that a couple of the larger metal chunks had severely decreased in size but not completely oxidized to powder form. This was the motivation behind the second run in the furnace, which was conducted from ambient to 800 °C at a rate of 600 °C/hr for a three hour hold. The longer duration would hopefully ensure that all of the material would be reduced to powdered form.

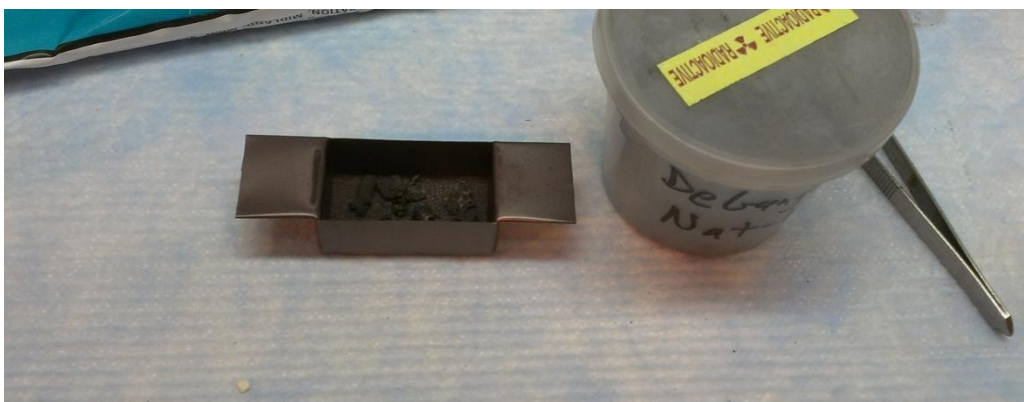


Figure 3.12. Metal Chunks of Uranium Prior to Oxidation in Furnace

After the second run in the furnace was complete, the now U_3O_8 powder was collected and stored in a glovebox until it was needed for the experiments with XeF_2 . For a sense of verification that the powder was indeed completely oxidized, a small sample of the U_3O_8 powder was heated in the TGA for analysis. Using roughly 500 mg of the U_3O_8 powder, the sample was placed in the Al_2O_3 crucible and heated from ambient to 800 °C at a rate of 25 °C/min and then held at temperature for one hour. These are the same

parameters as chosen in the second baseline experiment as mentioned above, and the TGA software will automatically incorporate the results of the baseline into the experimental results. The results of this experiment are shown in Figure 3.13.

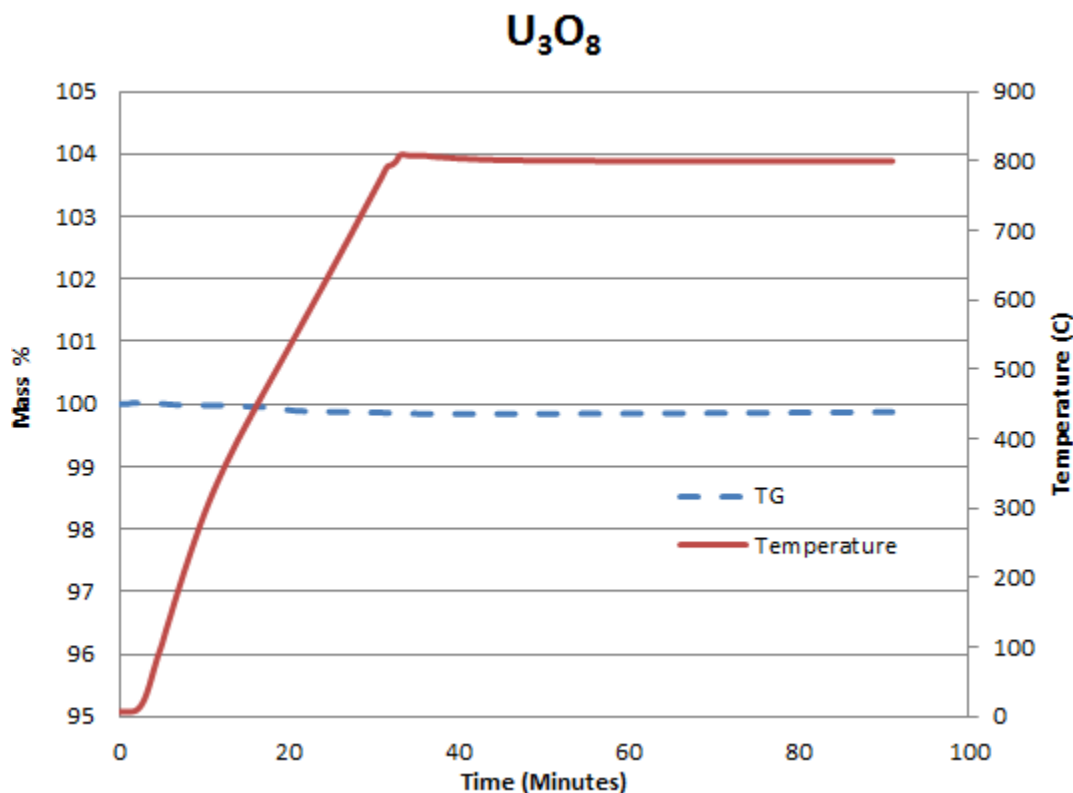


Figure 3.13. Verification of U₃O₈ Material

Upon analysis of Figure 3.13, it is clear that there is very little change in the mass balance of the sample, and one can be reasonably assured that U₃O₈ powder was indeed formed as a result of the two runs in the tube furnace. This is the material that will be used to study the fluorination and subsequent volatilization profile of U₃O₈ when mixed with XeF₂ at elevated temperatures.

CHAPTER 4

RESULTS AND DISCUSSION

4.1 Thermal Decomposition of XeF_2

Xenon difluoride (XeF_2) exists as solid, white crystals at room temperature and is maintained in an inert environment, usually packed under argon for shipment to the laboratory. When exposed to air, particularly moisture in the air, XeF_2 decomposes with a very strong odor. The compound has an atomic mass of 169.29 g/mol with a density of 4.32 g/cc.

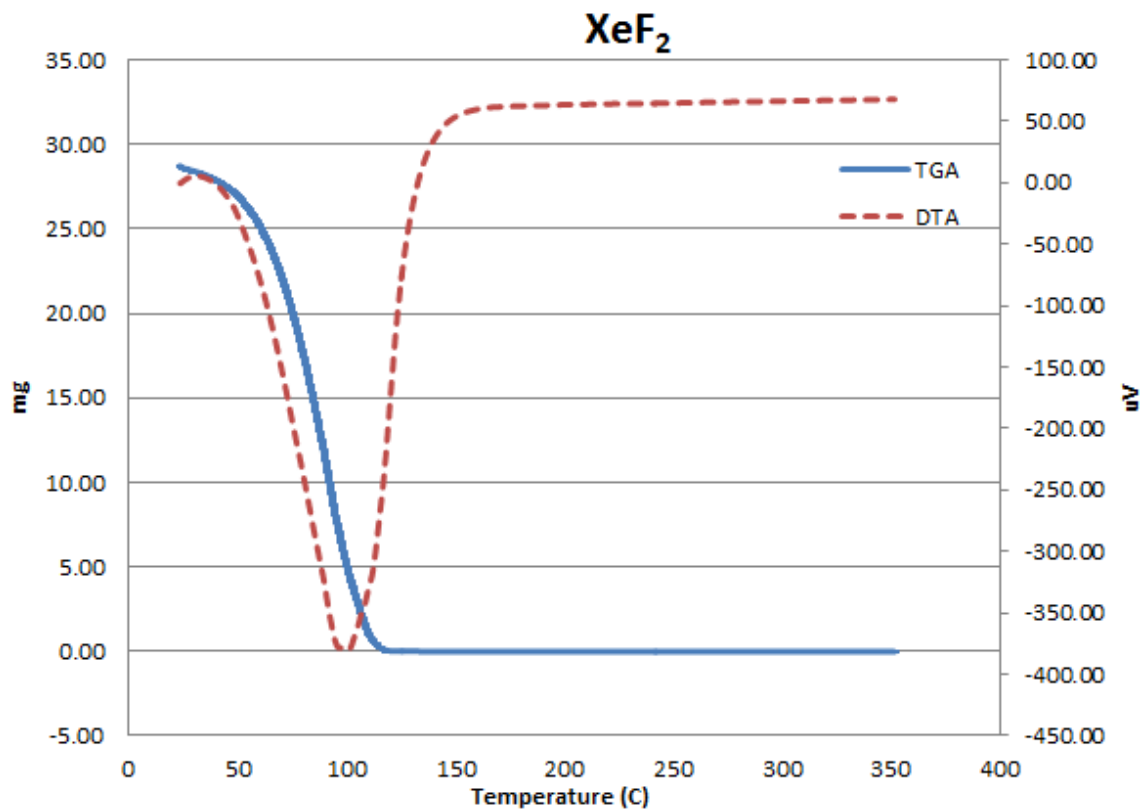


Figure 4.1. Thermal Decomposition of XeF_2

Before XeF_2 was tested against any oxides of the simulated UNF matrix, its thermal decomposition was analyzed in the TG/DTA. Approximately 30 mg, 28.72 mg by the onset of data collection due to slight decomposition in air on transfer, of XeF_2 was placed in a platinum sample pan and allowed to decompose under increasing temperatures at a rate of $10\text{ }^\circ\text{C}/\text{min}$ until a temperature of $350\text{ }^\circ\text{C}$ was reached. Results from this experiment are shown in Figure 4.1.

In analyzing the graph above, it is apparent that the decomposition and sublimation of XeF_2 is a single, smooth event that is completed by roughly $120\text{ }^\circ\text{C}$. This decomposition reaction is highly endothermic as noted by the DTA curve, and once the reaction is completed, the signal returns to a nominal constant value. It is also noted that the rate of decomposition is increasing with further elevated temperatures as expected. This raises concern because the TG/DTA used at SNRL is an open system, and there may be a possibility that the reactant, XeF_2 , may be eliminated from the sample pan before the fluorination of the oxides can take place. Care will be given to make sure the sample materials are properly mixed to better incorporate the fluorinator to each surrogate oxide. This will ensure that even when XeF_2 decomposes into a gas, it will still come into contact with the oxide material before it exists the sample pan.

4.2 Thermal Decomposition of NH_4HF_2

Ammonium bifluoride (NH_4HF_2) exists as flaky, white crystals with an atomic mass of 57.04 g/mol and a density of 1.50 g/cc . Like XeF_2 , NH_4HF_2 decomposes when exposed to air, and in turn, has to be packed under argon and stored in an inert environment.

Approximately 31.68 mg of NH_4HF_2 was decomposed in the TG/DTA at a heating rate of $10\text{ }^\circ\text{C}/\text{min}$ under 40 sccm of argon gas until a temperature of $850\text{ }^\circ\text{C}$ was reached. The results from this experiment are shown in Figure 4.2. The TGA signal shows NH_4HF_2 decomposing in a relatively smooth nature before $220\text{ }^\circ\text{C}$ despite many DTA peaks throughout this temperature range. These DTA peaks may be attributed to either phase changes or a variation in the compounds that ammonium bifluoride decomposes into at various temperatures. There appears to be a slight change in the rate of decomposition around $250\text{ }^\circ\text{C}$ when weight loss was slowed for a short time. Rapid weight loss resumed after a large exothermic peak on the DTA curve, and it continued until most of the sample had decomposed by $330\text{ }^\circ\text{C}$. The large exothermic spike was the clear reaction which led to most of the ammonium bifluoride decomposing and leaving the furnace. A simple decomposition in the compound would show as an endothermic event, so the reverse case suggests that the ammonium bifluoride reacted with something in its environment. Inert argon gas was being channeled through the furnace throughout the duration of the experiment; however, the flow rate may not have been completely sufficient to maintain a totally inert environment. Another small event occurred at $500\text{ }^\circ\text{C}$ where slight mass loss was accompanied by a very small, relatively speaking, endothermic reaction. The severity of both the DTA and TGA peaks may be a result of the very small sample left at this point in the experiment. It was noted that there was a small amount of residue upon completion of the experiment; therefore, the sample does not completely decompose by $850\text{ }^\circ\text{C}$.

By simply inspecting the results of the TG/DTA analysis, one cannot be sure of the exact decomposition pathway of this fluorinating agent. If this is to be better

understood, additional pieces of equipment such as a residual gas analyzer should be employed to know exactly what compounds come off at the respective temperature ranges as it is highly unlikely that the compound decomposes as a whole. Comparing the results from Figures 4.1-2, one can project that xenon difluoride will be a more volatile and reactive fluorinating agent when mixed with these surrogate oxides. That being said, ammonium bifluoride did reach much higher temperatures in the TG/DTA before most of the sample had decomposed, which may be beneficial for oxides requires such conditions.

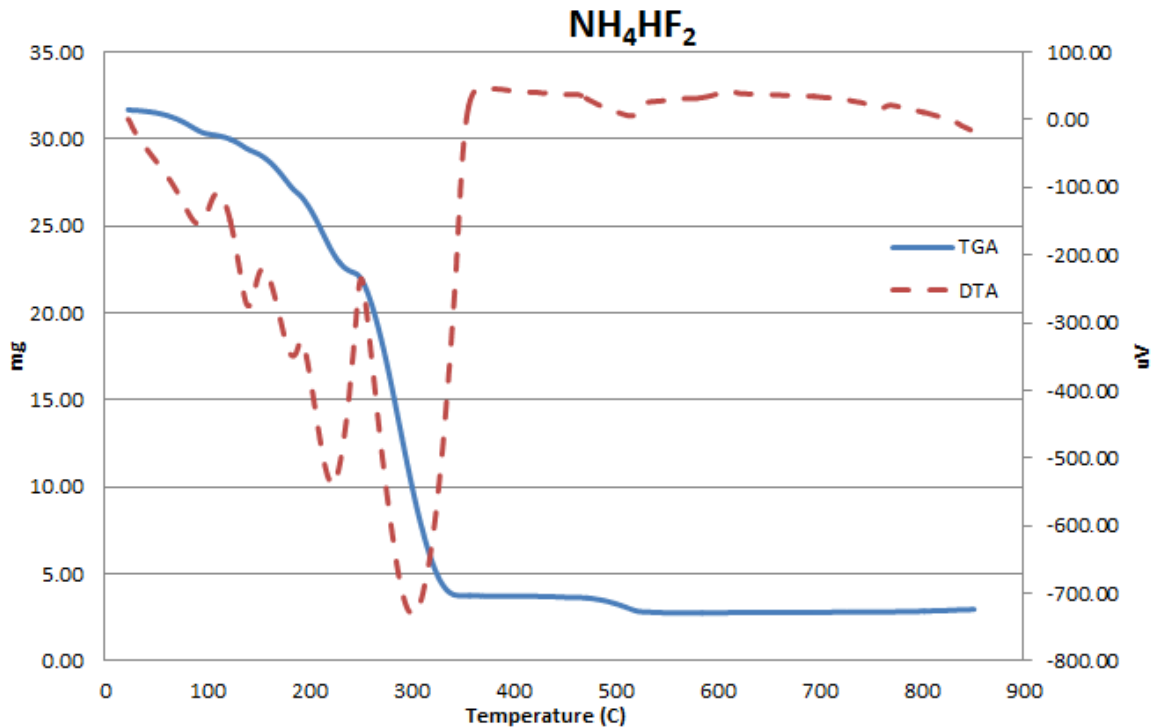


Figure 4.2. Thermal Decomposition of NH_4HF_2

4.3 Strontium Oxide (SrO)

The first surrogate oxide of the UNF matrix tested in this research was strontium oxide, a brittle, white crystalline solid with an atomic mass of 125.62 g/mol and a density

of 4.24 g/cc. The expected fluoride formation is strontium fluoride (SrF_2) with a heat of formation of $\Delta H_f = -1213.4 \text{ kJ/mol}$, a highly exothermic reaction which may severely raise local temperatures at the onset of reaction (much higher than that of the graphed, bulk furnace temperature). Of the multiple oxides presented in this research, strontium oxide is one of only two which form a non-volatile fluoride with a melting and boiling point of 1477°C and 2460°C respectively. If successfully formed, the non-volatile fluoride should remain in the sample pan at the conclusion of the experiment and will be available for XRD analysis.

In order to ensure the non-volatility of the oxides themselves (without a fluorinating agent present) all of the surrogate oxides were run in the TG/DTA prior to any experimentation with XeF_2 or NH_4HF_2 . Approximately 30.30 mg of SrO was heated in the TG/DTA at a rate of 10°C/min in a platinum sample pan with 40 sccm of argon gas flowing through the furnace. The results from this experiment are shown in Figure 4.3. Upon inspection of Figure 4.3, it is clear that strontium oxide is not volatile in nature by itself. In fact, the sample experienced around 2 mg of mass gain throughout the duration of this experiment, which was verified through additional runs of the same nature. The rise in mass may be from slight oxygen gain from the furnace environment. Again, 40 sccm of inert argon gas was flowing through the furnace throughout the duration of the experiment, but a small amount of air may have remained as the flow rate was not overly large for the size of the furnace. The DTA curve shows some movement, but the scale of the slight peaks is rather small and is not suggestive of any significant event at temperature ranges below 500°C . The fluorination and volatilization reactions expected when this surrogate oxide is mixed with a reactant will largely outweigh the

magnitude of the DTA peaks shown in Figure 4.3. This experiment, along with the results from the thermal decompositions of the fluorinating agents, will be used as comparison when binary experiments using both the surrogate oxide and fluorinating agent present are conducted.

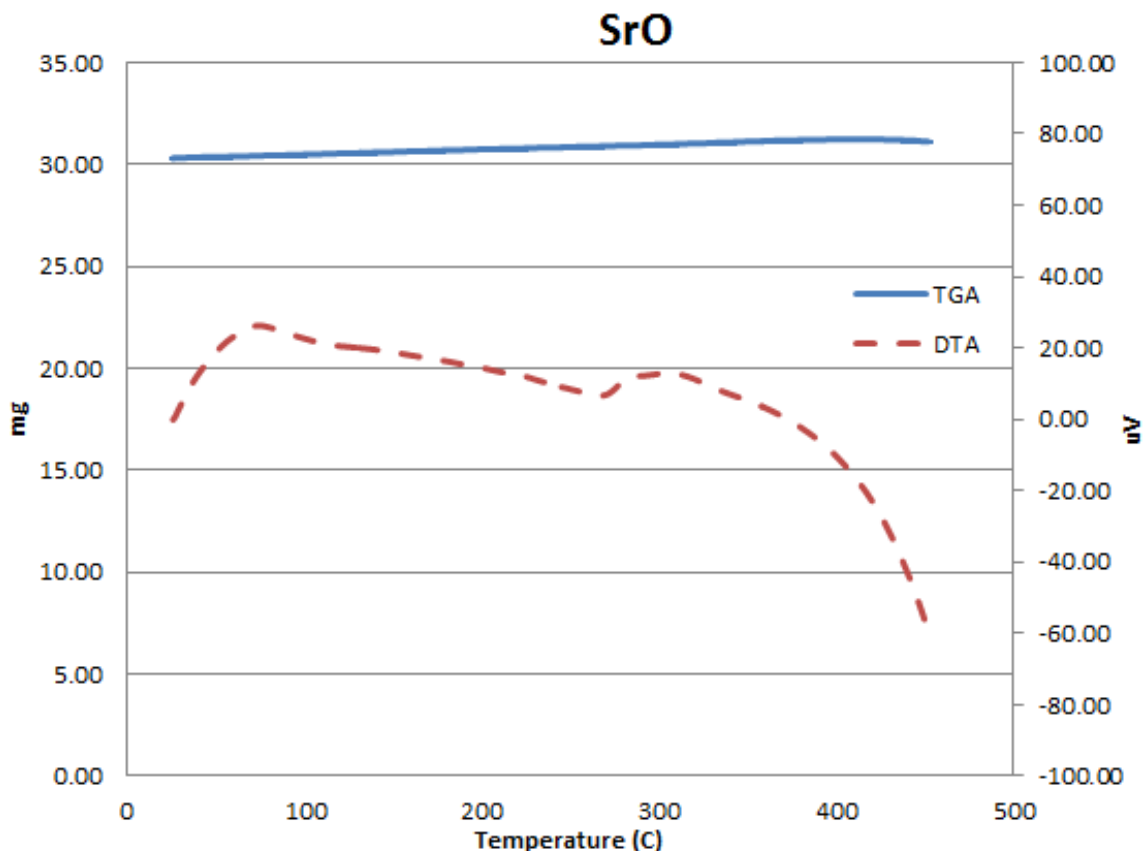


Figure 4.3. TG/DTA Data for SrO

Next the oxide was tested against XeF_2 as the potential fluorinating agent. A 28.52 mg sample was lightly mixed at approximately a 2:1 ratio of XeF_2 to SrO and quickly inserted into the TG/DTA for data acquisition. There are two things which are very noteworthy of the last sentence. The terms “lightly mixed” and “quickly inserted” are used and are probably understatement as the reaction between XeF_2 and SrO

appeared immediate and very violent. Upon sufficient contact, the two exhibited an easily visible reaction accompanied by a large release of heat. To try and capture this reaction in the TG/DTA, measures had to be taken to ensure all of the instrumentation was ready for when the samples were placed in the sample pan and then transferred to the furnace. The sample was heated at a rate of 10 °C/min until a temperature of 400 °C was reached, and the results from this experiment are shown in Figure 4.4. Of the roughly 10 mg of SrO and 20 mg of XeF₂ initially present, 21.57 mg remained at the conclusion of this case. Since it is known that separately XeF₂ decomposes in its entirety, the resulting 21.57 mg is suggestive of the formation of a non-volatile compound through contributions of both reactants. Further evidence to suggest the predicted reaction is shown through the large exothermic peak on the DTA curve in Figure 4.4, drastically different than the previous experiment with simply XeF₂.

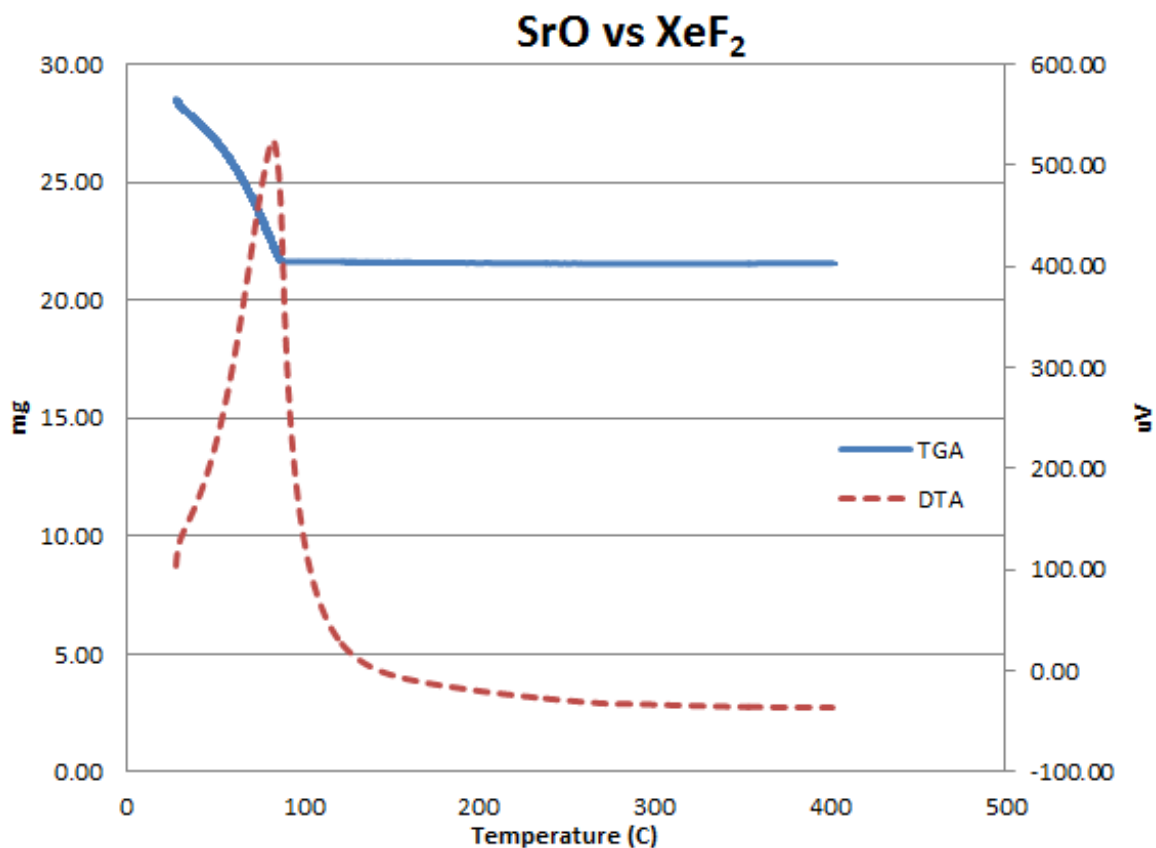


Figure 4.4. TG/DTA Data for SrO/XeF₂

Once the experiment was complete, the sample pan was removed from the TG/DTA furnace and its contents were emptied in a glass vial for storage. The decision was made to have this residue tested using XRD analysis to verify the reaction between XeF₂ and SrO did indeed produce the expected fluoride, SrF₂. The XRD slide was prepared as mentioned in Chapter 3 of this report. The results of the XRD tests were analyzed by Dr. Joe Teprovich of SRNL, and it was concluded that the peaks matched up perfectly with the database showing SrF₂, shown in Figure 4.5.

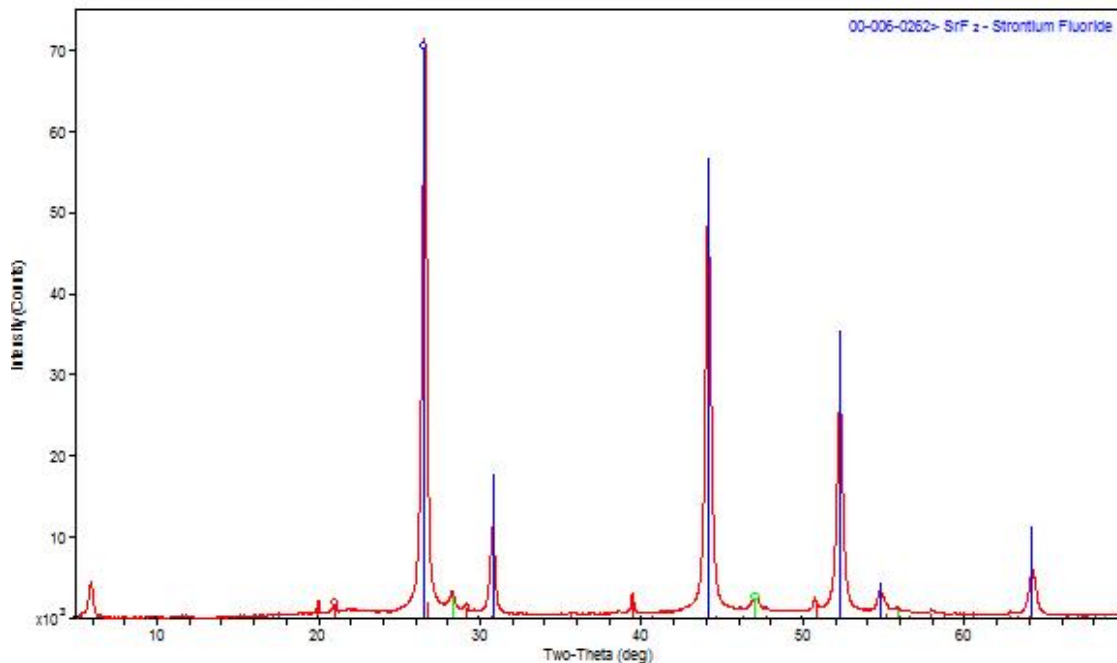


Figure 4.5. XRD Analysis for SrO/XeF₂

One additional experiment was conducted using XeF₂ and SrO as a response to the results in Figures 4.4-5, but this time the sample was not placed in the TG/DTA for analysis. Roughly 30 mg of SrO was heavily mixed in a large excess of XeF₂ in a glass vial as an attempt to procure this solid-solid reaction at room temperature. This experiment was conducted in an inert glovebox with extremely low moisture content, ensuring that whatever reaction would occur as a result of only the two materials mixed together. When mixed, the samples immediately reacted with great severity and released such a large amount of heat that the sample glowed an orange-red as the reaction took place. The sample reached a great enough temperature that the excess XeF₂ was immediately converted to a gas, and all that remained was SrF₂ powder. The residue was also analyzed using XRD, shown in Figure 4.6, and indeed was confirmed to be the non-

volatile fluoride. It was evident that this reaction did not require any kind of elevated temperature or moisture content to take place.

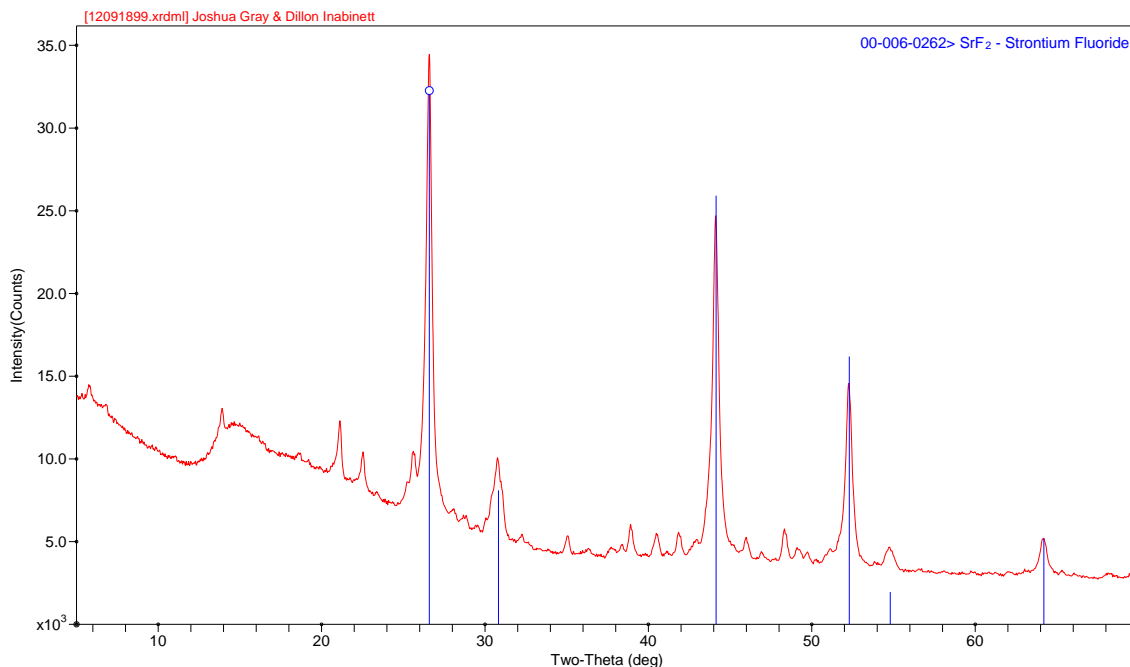


Figure 4.6. XRD Analysis for SrO/XeF₂ - No TG/DTA

Once the experimentation with XeF₂ as the potential fluorinating agent was completed, NH₄HF₂ was also used against SrO to see if fluorination would occur. As mentioned in Chapter 3, experiments with ammonium bifluoride were conducted with a different sample pan than used with XeF₂, giving the user the option to use a fitted lid to better contain the reactants throughout the duration of the experiment. These efforts were taken as a result of preliminary experimentation with SrO/NH₄HF₂, using the same methods as used with XeF₂, showing very little reactivity together, even at elevated temperatures. The resulting TGA and DTA curves appeared just as the curves did when simply ammonium bifluoride was present in the sample pan, suggesting no interaction whatsoever with the SrO. The idea behind the new sample pan was that the ammonium

bifluoride would escape much more slowly when decomposed, giving additional time for the possible fluorination of the surrogate oxide.

The re-testing of $\text{SrO}/\text{NH}_4\text{HF}_2$ with the stainless steel sample pan was done so in two parts, one without the lid and one with the fitted lid. The first experiment was conducted at roughly 32 mg total material with a 2:1 ratio of fluorinator to surrogate oxide respectively. The furnace was heated from ambient to 350 °C at a rate of 10 °C/min, and the results from the $\text{SrO}/\text{NH}_4\text{HF}_4$ No Lid experiment are shown in Figure 4.7. In analyzing the graph, the major peaks on the DTA curve still resemble the results from the experiment with just ammonium bifluoride. It is noted that the peaks are much more drawn out than in Figure 4.2, which may be a result of two phenomena. First, the much slower kinetics may be a result of the now limited mobility when ammonium bifluoride is mixed with the surrogate oxide. Second, the stainless steel sample pans are much larger and thicker than the platinum sample pans used in all of the other experiments. The additional material would display a much slower response in transferring the heat to the sample pan and consequently would be measured more slowly by the thermocouple on the end of the float it sits on. On the TGA curve, the mass loss is a single smooth event which also appears much slower than seen in Figure 4.2. It appears that the experiment should have been carried out to much higher temperatures to see if indeed the reaction/decomposition was complete. The decision to only go to 350 °C was made in analyzing the thermal decomposition graph in Figure 4.2 which suggests all of the major events with ammonium bifluoride occur before this temperature; however, more account should have been given to the slower kinetics and new sample pan.

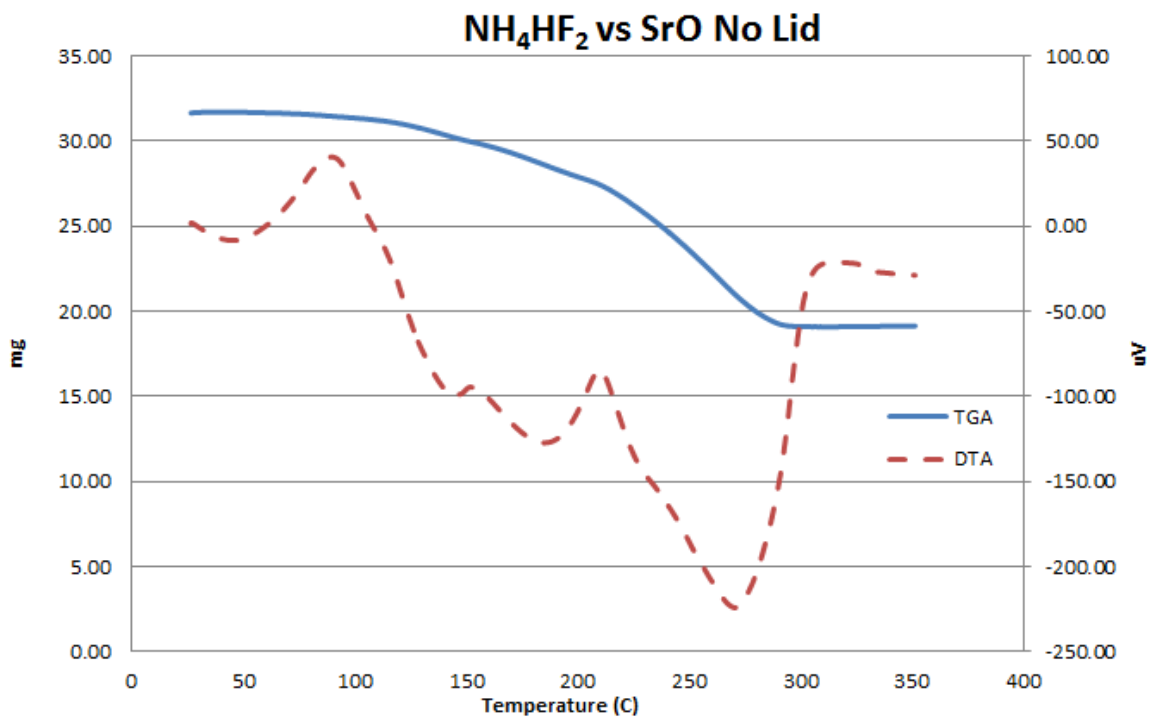


Figure 4.7. TG/DTA Data for SrO/NH₄HF₂ No Lid

The experiment testing SrO against NH₄HF₂ using the stainless steel sample pan with fitted lid was done so using roughly 28.5 mg total material with a 2:1 ratio of fluorinator to surrogate oxide respectively. The furnace was heated from ambient to a temperature of 400 °C at a rate of 10 °C/min. The increase in 50 °C from the experiment with no lid on was for reasons mentioned previously, in hopes that the reaction would be complete by this temperature. Results from the SrO/NH₄HF₄ Lid On experiment are shown in Figure 4.8.

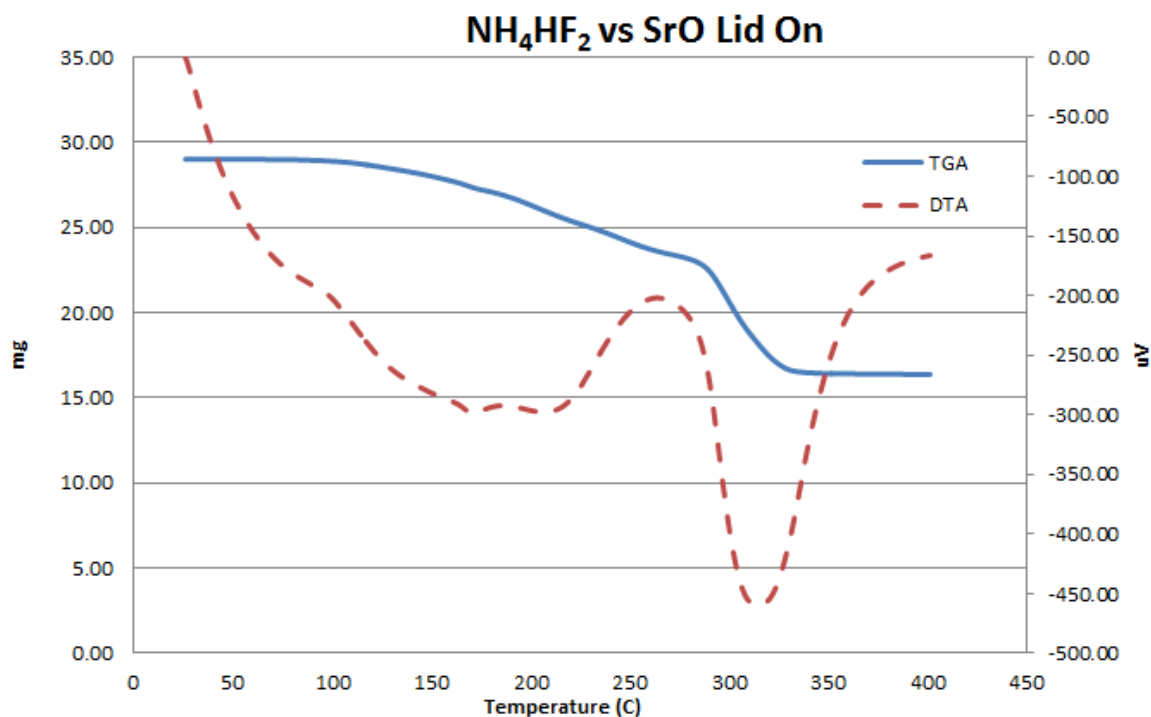


Figure 4.8. TG/DTA Data for SrO/ NH_4HF_2 Lid On

The effects the fitted lid, relative to the experiment without, were as expected. The decomposition of ammonium bifluoride appeared more drawn out as expressed by both the TGA and DTA signals. Because the lid was not completely airtight, the ammonium bifluoride was still able to escape from the sample pan. In terms of whether or not SrO was fluorinated using NH_4HF_2 , conclusions are very hard to draw from these two experiments. In both figures, there is no characteristic large exothermic spike on the DTA signal one would expect if SrF_2 was being produced, as seen when mixed with XeF_2 . XRD analysis was conducted on the sample residues from both experiments; however, no clear confirmation was able to be matched with the database of materials. That being said, when one looks at the actual mass loss for both experiments in Figures 4.7-8, an argument could be made for the formation of a non-volatile fluoride. Since 30

mg at 2:1 ratio of fluorinator to surrogate oxide was used, and given that most all of ammonium bifluoride would decompose on its own at these respective temperatures, one would expect roughly 10 mg of sample to be left over at the conclusion of the experiment. A result of this nature, when testing against an oxide which should form a non-volatile fluoride, would suggest that the fluorinator did not react with the oxide and simply decomposed. In the two experiments presented here, however, over 10 mg of sample was left at the conclusion of the experiment. In order for this to happen, some mass contribution would have to be made from both the ammonium bifluoride and the strontium oxide. Since it is known that on its own, ammonium bifluoride would have left the sample pan completely, the evidence is suggestive of an interaction between the two compounds. Further experimentation should be done to investigate this claim, although one can state that relative to XeF_2 , NH_4HF_2 appears to be a weaker fluorinating agent when mixed with SrO in this setting.

4.4 Molybdenum Trioxide (MoO_3)

The second oxide tested in this research was molybdenum trioxide, or MoO_3 . This compound is a greyish powder with a molar mass of 143.94 g/mol and a density of 4.69 g/cc. The respective melting and boiling points of the oxide itself are 795 °C and 1155 °C. The fluorination of a molybdenum species should result in the formation of molybdenum hexafluoride (MoF_6) with a heat of formation of $\Delta H_f = -1561.05 \text{ kJ/mol}$. This heat of formation is largely exothermic, similar to the fluorination reaction seen with strontium oxide. Unlike the fluoride formed with strontium, molybdenum hexafluoride has a melting point of 17.5°C and boiling point of 34.0°C enabling it to be volatile at very low temperatures.

Again, to ensure the non-volatility of the oxides themselves, approximately 16 mg of MoO_3 was placed in a platinum sample pan and heated from ambient to a temperature of 525 °C at a rate of 10 °C/min under 40 sccm argon gas. Results from this experiment are shown in Figure 4.9. As expected, both the TGA and DTA curves are unwavering throughout the duration of the experiment. The minor movement in the DTA signal can be neglected as any reactions expected with the fluorination of MoO_3 should be of a much larger scale than the signal shown in the curve below. This experiment successfully confirmed the non-volatility of molybdenum trioxide at temperatures below 600 °C.

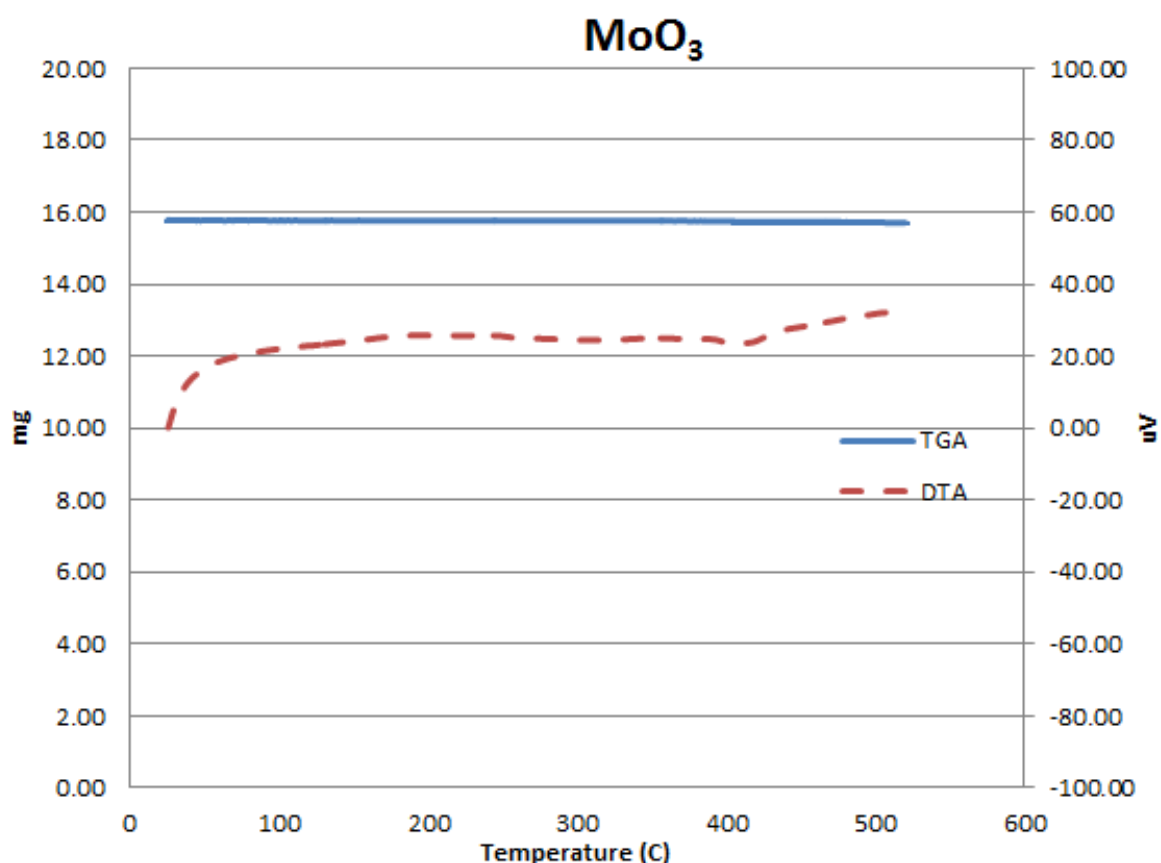


Figure 4.9. TG/DTA Data for MoO_3

Next, molybdenum trioxide was tested against XeF_2 as the potential fluorinating agent. A 30 mg sample was prepared at approximately a 2:1 ratio of XeF_2 to MoO_3 and inserted into the TG/DTA for data acquisition. The sample was heated at a rate of $10^\circ\text{C}/\text{min}$ until a temperature of 300°C was reached, and the results from this experiment are shown in Figure 4.4.

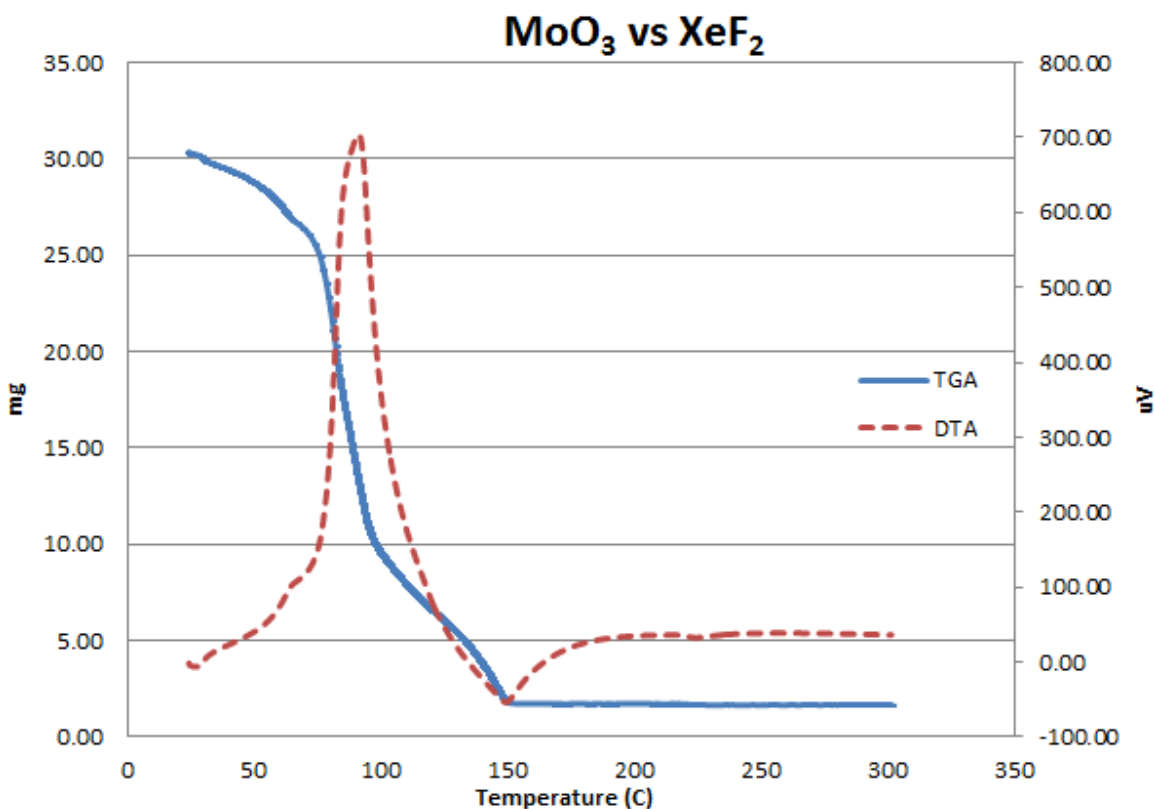


Figure 4.10. TG/DTA Data for $\text{MoO}_3/\text{XeF}_2$

Of the initial 8.9 mg of MoO_3 in the sample pan, none was left at the conclusion of the experiment. Unlike the experiments with SrO , the reaction between MoO_3 and XeF_2 was not immediate and required slightly elevated temperatures. Steady weight loss, as seen with the decomposition of XeF_2 , occurred until slightly below 80°C when a large exothermic spike coupled with rapid weight loss was observed. This sudden change

denotes a significant reaction, a reaction that is believed to be the fluorination and subsequent volatilization of MoO_3 to MoF_6 . This period of rapid weight loss appeared finished by roughly 100°C , but the TGA curve still continued to fall until the entire sample was gone. The slower weight loss at the end of the experiment can be attributed to the excess XeF_2 decomposing and leaving the furnace. No explicit confirmation of the fluorination can be shown since the entire sample was off-gassed and no residual gas analysis was available in this experimental setup. One can, however, be reasonably assured that the predicted reaction did take place through inferences made in analyzing the TG/DTA curve.

Like SrO , MoO_3 was also tested against NH_4HF_2 as a potential fluorinating agent. The same experimental setup was used in relation to using two separate experiments to test the effects of the fitted lid on the stainless steel sample pan. The first experiment without the fitted lid used 31.06 mg total sample weight at roughly a 2:1 ratio of fluorinating agent to surrogate oxide respectively. The sample was placed in the TG/DTA and heated from ambient to 700°C at a rate of $10^\circ\text{C}/\text{min}$. The much higher temperature setpoint was used in this experiment to ensure there were no questions as to if the reaction was complete by the end of the experiment. Results from the experiment testing NH_4HF_2 against MoO_3 without the fitted lid are shown in Figure 4.11. The analysis for this experiment is very simple, as both the TGA and DTA curves exactly resemble that of Figure 4.2 when only ammonium bifluoride was present. It appears that the fluorinating agent was unreactive with the surrogate oxide, and of the roughly 10 mg of MoO_3 present at the start of the experiment, the data suggests all of it was left over at the conclusion. It is known that MoO_3 should form the volatile MoF_6 when fluorinated,

so if this would have happened in this experiment, less than 10 mg needed to be left at the conclusion of the experiment to even begin to suggest successful fluorination and subsequent volatilization of the compound. Even so, both of the curves do not show any sign of this reaction, leaving one to suggest that NH_4HF_2 is not likely to produce a fluorination reaction with MoO_3 in these conditions.

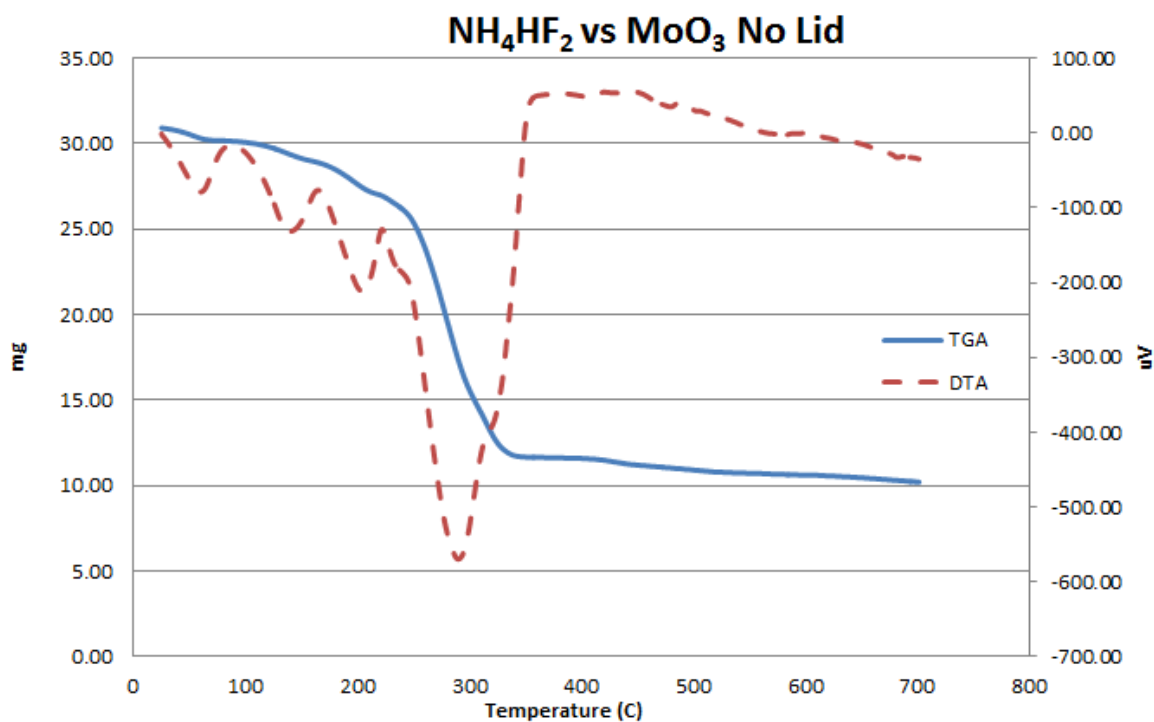


Figure 4.11. TG/DTA Data for $\text{MoO}_3/\text{NH}_4\text{HF}_2$ No Lid

The previous experiment was repeated, but this time the fitted lid was placed on the sample pan. Using 26.60 mg total sample weight, the furnace was heated from ambient to 400 °C at a rate of 10 °C/min. The results from this experiment are shown in Figure 4.12.

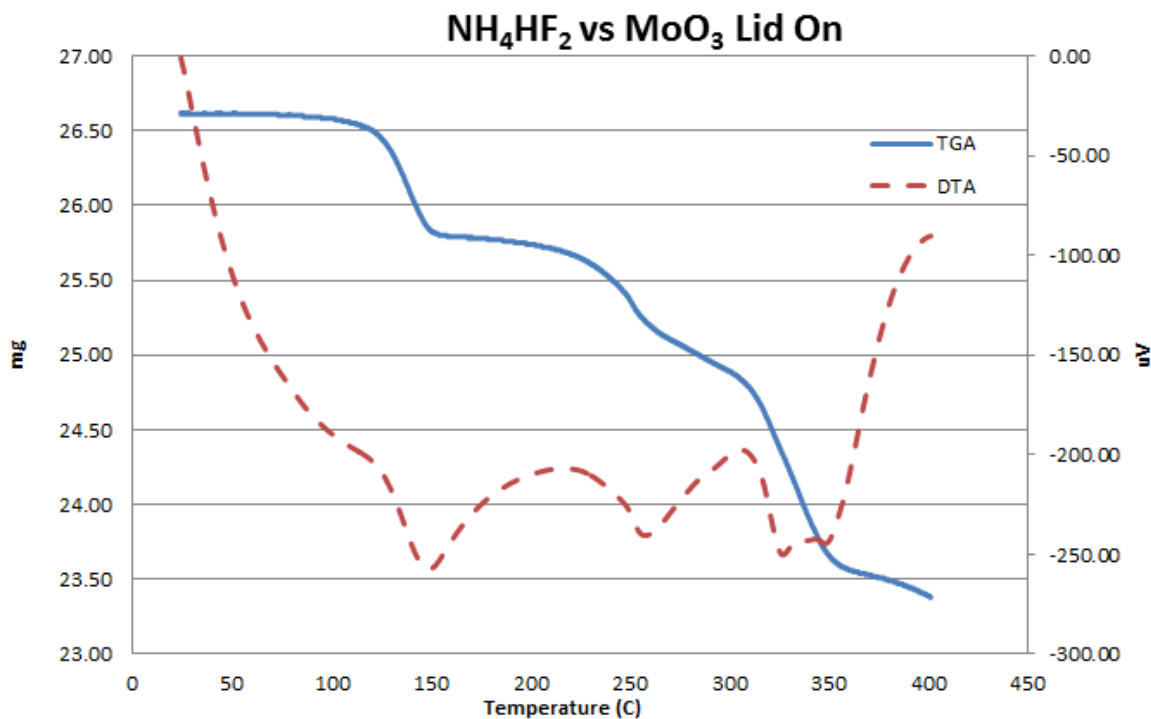


Figure 4.12. TG/DTA Data for MoO₃/NH₄HF₂ Lid On

Comparing Figure 4.11 and 4.12 shows how the fitted lid has a drastic effect on the TGA and DTA curves at temperatures ranges below 400 °C. In the fitted lid experiment, the mass loss appeared in separate stages, seemingly accompanied by respective DTA events. This experiment was only run to a final temperature of 400 °C because the previous experiment without the lid suggested the reactions would have been completed by this point. In Figure 4.12, however, the addition of the fitted lid to the experiment greatly slowed the reaction mechanisms despite the temperature ramp being held constant. It is very clear that this reaction was not complete at the conclusion of this experiment, and one would be hard pressed to draw conclusions as to the fluorination potential of ammonium bifluoride against molybdenum trioxide. Compared to XeF₂ where total mass loss was observed, the two experiments with NH₄HF₂ did not display

the same results. Additional experimentation should be conducted with ammonium bifluoride as a potential fluorinating agent to hopefully better portray the expected reactions with these surrogate oxides of the used nuclear fuel matrix.

4.5 Niobium Pentoxide (Nb_2O_5)

Niobium pentoxide, Nb_2O_5 is a colorless solid with a molar mass of 265.81 g/mol and a density of 4.60 g/cc. The melting point of the oxide itself is 1512 °C which makes the oxide non-volatile in nature. The fluorination of Nb_2O_5 , however, should result in the formation of a volatile compound, Niobium (V) Fluoride (NbF_5) at a heat of formation of $\Delta H_f = -1812.59$ kJ/mol. The respective melting and boiling points for NbF_5 are 72.0°C and 236.0°C, much higher relative to MoF_6 studied earlier; however, it is still considered volatile at low temperatures.

A baseline experiment was conducted with just the oxide itself to prove its non-volatility. Approximately 8 mg of Nb_2O_5 was placed in a platinum sample pan and heated from ambient to a temperature of 600 °C at a rate of 10 °C/min under 40 sccm argon gas. Results from this experiment are shown in Figure 4.13. As expected, both the TGA and DTA curves are uneventful throughout the duration of the experiment, proving that the surrogate oxide is non-volatile in nature when heated to temperatures below 600 °C.

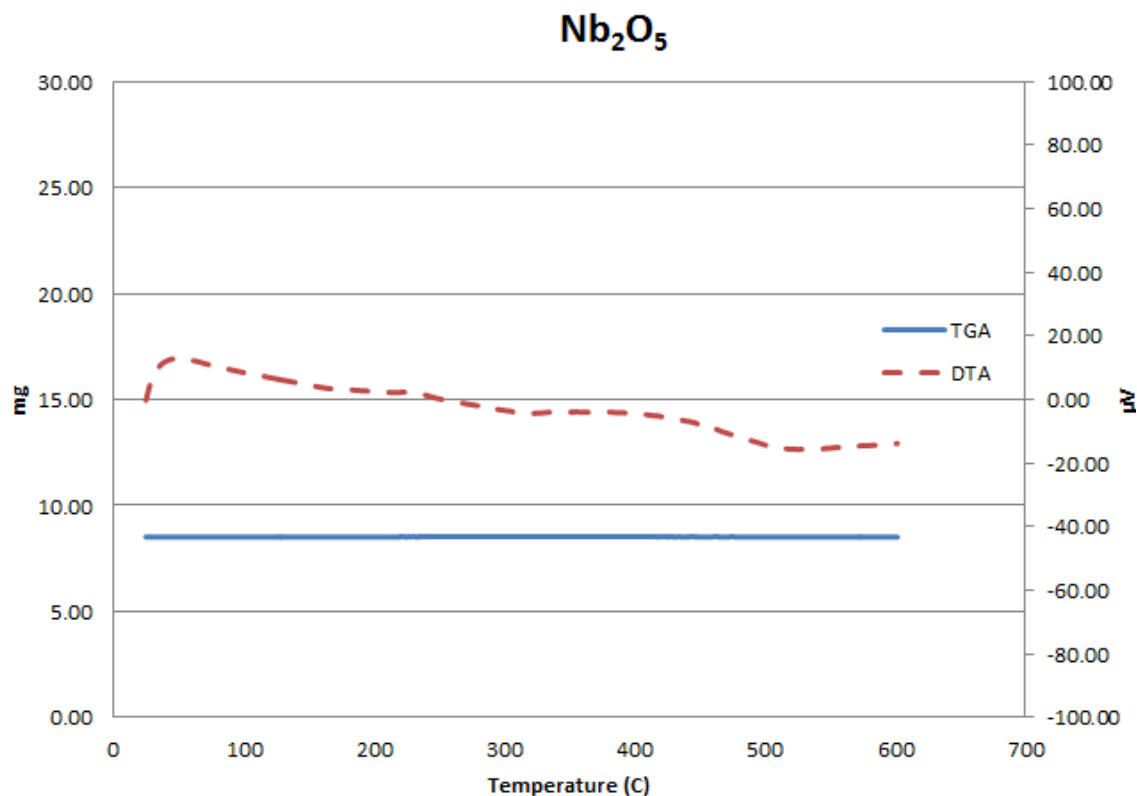


Figure 4.13. TG/DTA Data for Nb_2O_5

After the baseline experiment was completed, niobium pentoxide was tested against XeF_2 as the potential fluorinating agent. A 33.06 mg sample was prepared at roughly a 2:1 ratio of XeF_2 to Nb_2O_5 and inserted into the TG/DTA for data acquisition. The sample was heated at a rate of 10 °C/min until a temperature of 400 °C was reached, and the results from this experiment are shown in Figure 4.14. Of all experiments, the reaction of XeF_2 with Nb_2O_5 produced by far the most intriguing results for a multitude of reasons. First, the largest exothermic peak of all binary experiments was observed with this pairing resulting in a DTA signal slightly above 800.00 μV at the peak of the reaction. Secondly, it is interesting to note that the product of this exothermic reaction appeared volatile at temperatures much below the expected boiling point of 236.0 °C

when graphed as a function of furnace temperature. Again, it cannot be directly proven that NbF_5 was indeed formed, but the TG/DTA curve can still give reasonable assurance despite the apparent disagreement on volatilization temperature. Reasons for the disagreement lie in the fact that the local sample temperature should have reached temperatures much higher than the furnace due to the release of large amounts of heat from the fluorination reaction. This would allow for the fluoride to volatilize and be off-gassed much sooner than expected.

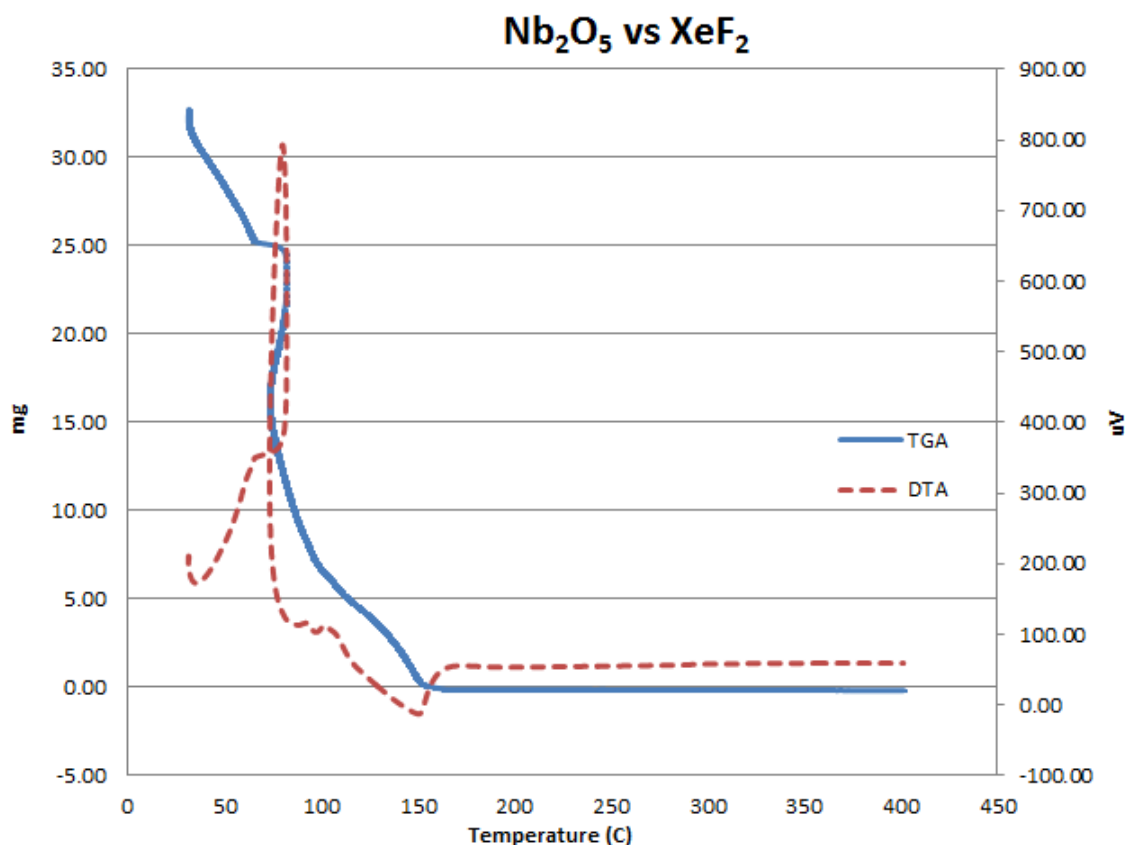


Figure 4.14. TG/DTA Data for $\text{Nb}_2\text{O}_5/\text{XeF}_2$

The results from Figure 4.14 suggest the fluorination and complete volatilization of a roughly 10 mg sample of Nb_2O_5 using XeF_2 as the fluorinating agent. This reaction

appeared complete just after 150 °C as shown by the graphed, bulk furnace temperature. In order for this to be true, a large thermal shock had to occur as a result of the fluorination reaction, giving the necessary temperature for the expected fluoride to become mobile and exit the furnace. Overall, it definitely appears that XeF₂ is a capable fluorinating agent for Nb₂O₅, even at low temperatures.

4.6 Rhodium (III) Oxide (Rh₂O₃)

Rhodium (III) Oxide is a dark grey, odorless powder with a molar mass of 253.81 g/mol and a density of 8.20 g/cc. This oxide has a melting point of 1100 °C making it non-volatile in nature. The fluorination of this oxide could result in the formation of RhF₃, RhF₅, or RhF₆, all of which display largely negative heats of formation and are easily volatilized fluorides at temperature ranges 600 °C and below.

A baseline experiment was conducted with just the oxide itself to prove its non-volatility. Approximately 14 mg of Rh₂O₃ was placed in a platinum sample pan and heated from ambient to a temperature of 600 °C at a rate of 10 °C/min under 40 sccm argon gas. Results from this experiment are shown in Figure 4.15. The TGA curve shows an extremely small mass loss which is not suggestive of any significant reaction occurring. To accompany the mass loss, the DTA signal does show a slight thermal difference between the sample and reference Al₂O₃ material. The endothermic trend on the curve is suggestive of a slight decomposition in the sample, possibly explained by a slight loss in moisture of the sample or various other reasons. Regardless, the oxide does not display any significant volatility alone at temperatures below 600 °C.

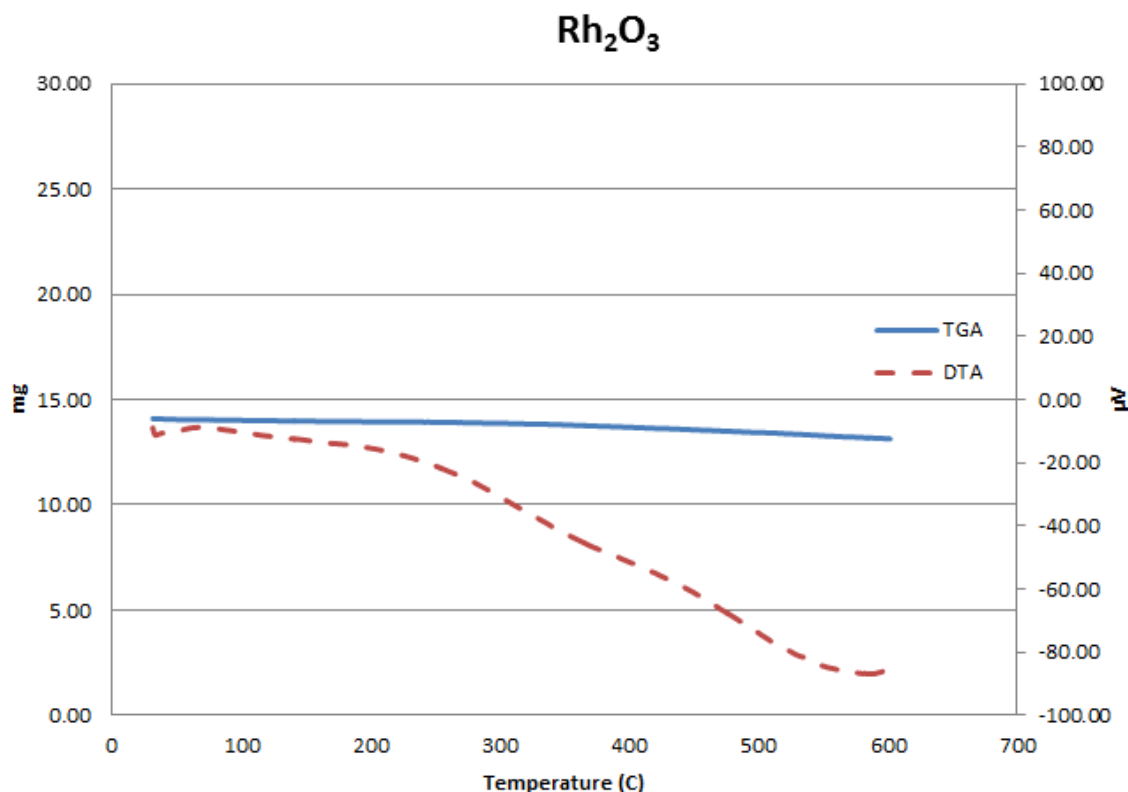


Figure 4.15. TG/DTA Data for Rh_2O_3

After rhodium (III) oxide was confirmed to be non-volatile, the surrogate oxide was tested against XeF_2 as a potential fluorinating agent. Approximately 41 mg of a $\text{XeF}_2/\text{Rh}_2\text{O}_3$ was mixed at a 2:1 ratio of XeF_2 to Rh_2O_3 respectively and inserted into the TG/DTA for data acquisition. The sample was heated at a rate of $10^\circ\text{C}/\text{min}$ until a temperature of 800°C was reached, and the results from this experiment are shown in Figure 4.16. The successful reaction of rhodium (III) oxide with a fluorinating agent should result in the formation of a volatile fluoride, which upon heating to elevated temperatures would eliminate the entire sample from the furnace. It is clear from the results of this experiment that total weight loss was not observed; however, analyzing the two curves does give insight to a possible fluorination and minor volatilization event

happening. Relatively consistent weight loss accompanied by an uneventful DTA curve occurs during the experiment until 600 °C where a large exothermic spike coupled with an increased rate in mass loss is shown. Because this event occurred right when furnace temperature reached 600 °C, one can hypothesize that the volatile fluoride RhF_3 was being formed and subsequently off-gassed out of the system, reducing the sample weight. This reaction appears quick, and the period of increased weight loss only accounts for roughly one-half milligram of the total sample weight. This is a far cry from complete volatilization of the sample, but the characteristic exothermic spike of a fluorination reaction coupled with an increased rate of mass loss is solid evidence that XeF_2 is capable of producing this reaction with Rh_2O_3 .

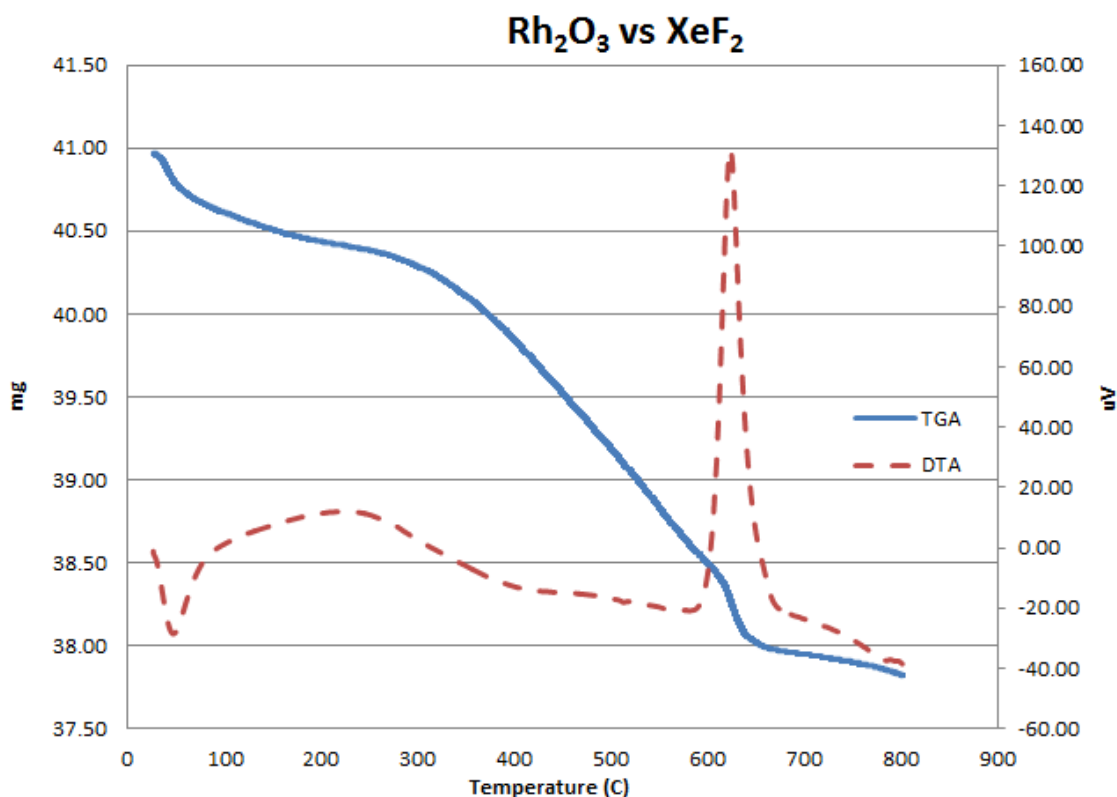


Figure 4.16. TG/DTA Data for $\text{Rh}_2\text{O}_3/\text{XeF}_2$

One interesting note can be made from the experiment in Figure 4.16, and it lies in the fact that XeF_2 remained present in the sample pan for much higher temperatures than in any other experiment conducted in this research. It is known that XeF_2 by itself and at the same $10\text{ }^\circ\text{C}/\text{min}$ heating rate is gone from the sample pan by $120\text{ }^\circ\text{C}$. Even with the reduced kinetics seen when the fluorinator is mixed with a surrogate oxide, all of the other reactions with surrogate oxides appeared complete by $200\text{ }^\circ\text{C}$, as noted by the accompanying TGA and DTA curves. In this experiment, however, most of the sample was still present at the time of the reaction, which at $600\text{ }^\circ\text{C}$ is far higher than in any other experiment. One possible explanation for this occurrence is that the surrogate oxide, Rh_2O_3 , provided a blanket for the XeF_2 , holding it in the sample pan until the appropriate elevated temperature was reached. Another solution is given by the possibility of forming intermediate, non-volatile fluorides; however, one would expect to see greater evidence through an exothermic peak on the DTA curve much sooner in the experiment. Regardless, Figure 4.16 gives reasonable assurance that this reaction is possible, and maybe with better homogeneity of the binary mixture, complete volatilization of the sample may have been observed. Also, off gas analysis would give definite confirmation if indeed RhF_3 was being expelled from the furnace at any point in this experiment.

4.7 Ruthenium (IV) Oxide (RuO_2)

Ruthenium (IV) Oxide is a black powder with a molar mass of 133.07 g/mol and a density of 6.97 g/cc . This oxide has a melting point of $1200\text{ }^\circ\text{C}$ making it non-volatile in nature. The fluorination of this oxide could result in the formation of RuF_5 or RuF_6 , both which display largely negative heats of formation and are easily volatilized fluorides with boiling points of $280\text{ }^\circ\text{C}$ and $70\text{ }^\circ\text{C}$ respectively.

A baseline experiment was conducted with just the oxide itself to prove its non-volatility. Approximately 12 mg of RuO₂ was placed in a platinum sample pan and heated from ambient to a temperature of 600 °C at a rate of 10 °C/min under 40 sccm argon gas. Results from this experiment are shown in Figure 4.17.

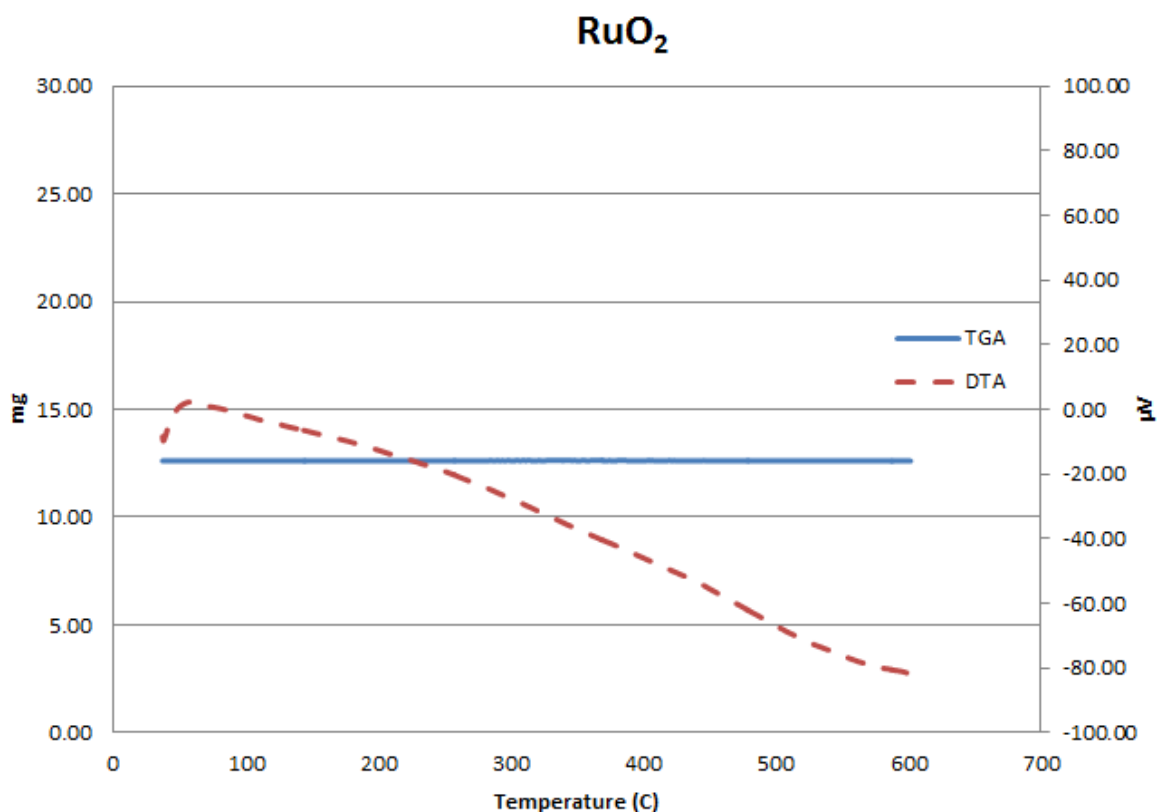


Figure 4.17. TG/DTA Data for RuO₂

After the baseline experiment was completed, ruthenium (IV) oxide was tested against XeF₂ as the potential fluorinating agent. A 41.0 mg sample was prepared using 11.1 mg of RuO₂ and 29.9 mg of XeF₂, mixed, and inserted into the TG/DTA for data acquisition. The sample was heated at a rate of 10 °C/min until a temperature of 600 °C was reached, and the results from this experiment are shown in Figure 4.18. At the onset of data acquisition, an exothermic peak on the DTA line was observed with rather steady

weight loss on the accompanying TGA curve. The exothermic spike on the graph would hint to the reaction between the two compounds to form a fluoride, and in the case of ruthenium (IV) oxide, that fluoride should be volatile. That being said, weight loss plateaued for the better part of the experiment, leaving behind roughly 11 mg of sample residue at the conclusion of the experiment. The visual nature and weight of the residue suggested this material is still unfluorinated RuO_2 , and no appreciable fluorination/volatilization of the sample was observed.

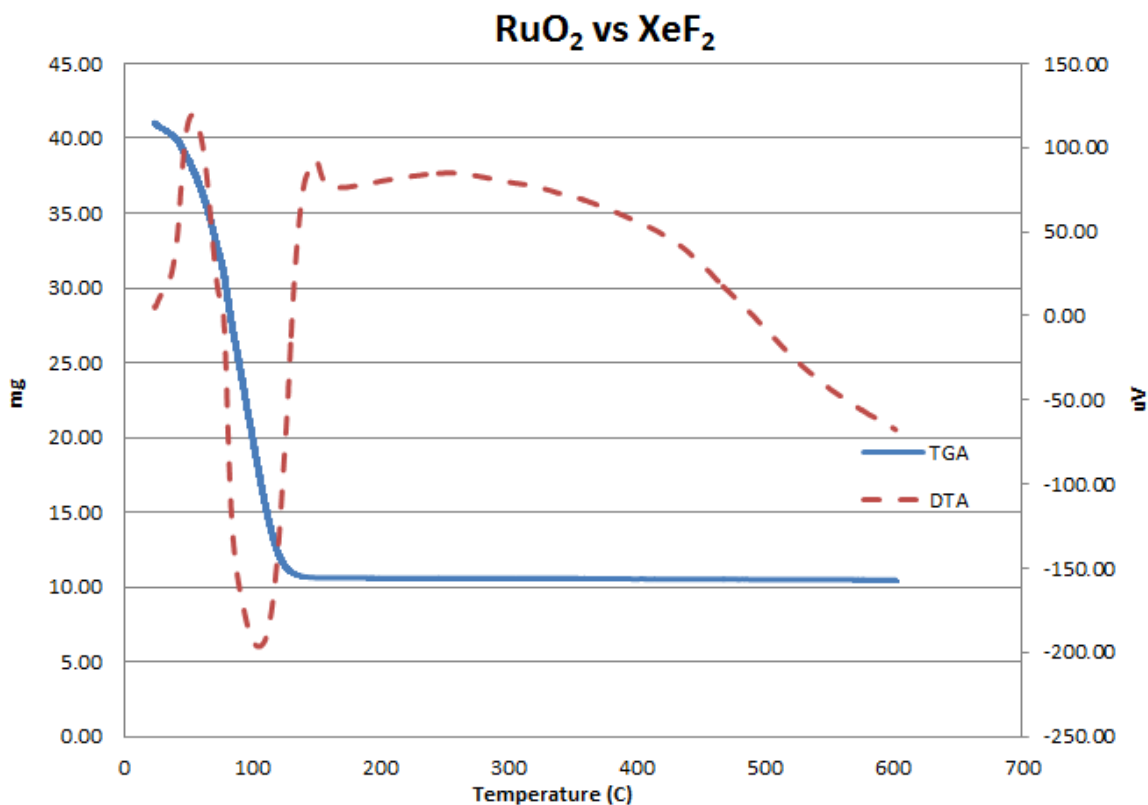


Figure 4.18. TG/DTA Data for RuO₂/XeF₂

With this experimental setup, it appears that XeF₂ is unsuccessful at producing a large fluorination reaction with RuO₂ leading to subsequent volatilization of the sample. Despite the conclusion, this reaction should be investigated further to better explain the

exothermic spike on the DTA curve in Figure 4.18. It may be the case that the reaction kinetics simply were not favorable in this scenario, but XeF_2 may still be a strong enough agent to fluorinate this oxide.

4.8 Zirconium Dioxide (ZrO_2)

Zirconium dioxide is a fine, white powder with a molar mass of 123.218 g/mol and a density of 5.68 g/cc. This oxide has melting and boiling points of 2715 °C and 4300 °C respectively making it extremely non-volatile in nature. The fluorination of this oxide should result in the formation of ZrF_4 , and with melting and boiling points of 912 °C and 918 °C, the expected fluoride is also not volatile at the temperature range for this research.

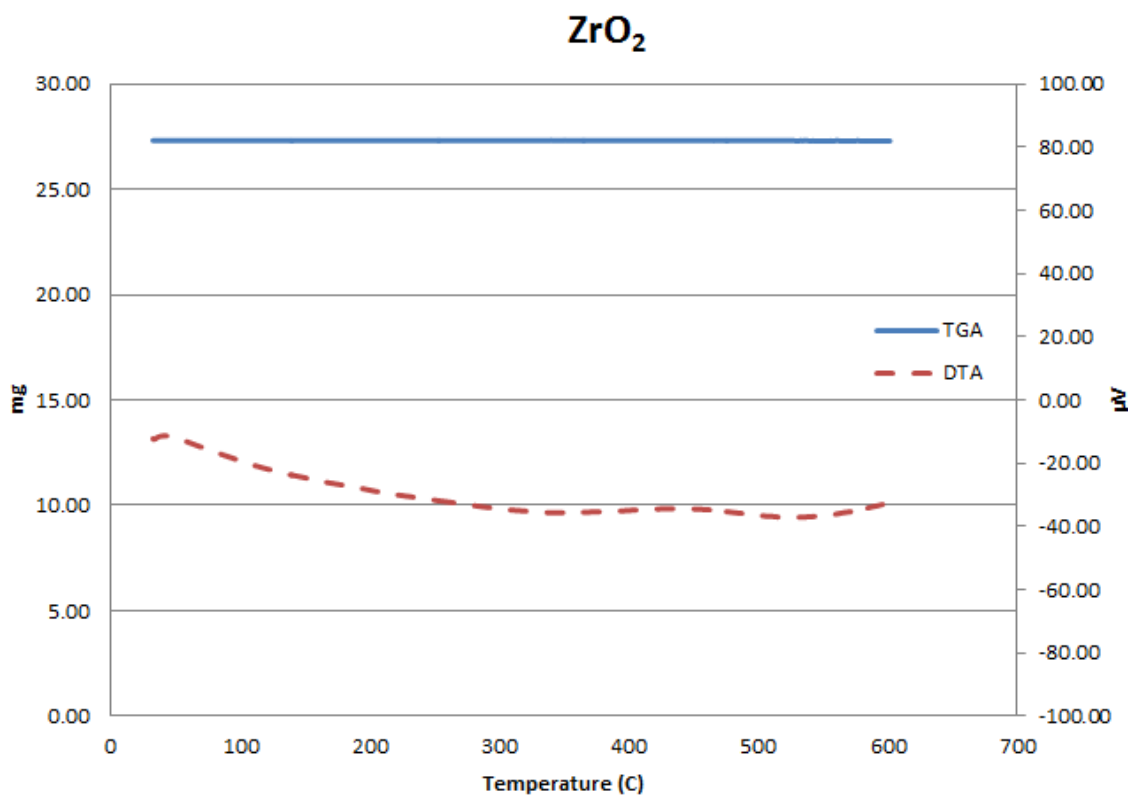


Figure 4.19. TG/DTA Data for ZrO_2

A baseline experiment was conducted with just the oxide itself to further prove its non-volatility. Approximately 27 mg of ZrO_2 was placed in a platinum sample pan and heated from ambient to a temperature of 600 °C at a rate of 10 °C/min under 40 sccm argon gas. Results from this experiment are shown in Figure 4.19. As expected, this experiment was extremely uneventful as the TGA curve was absolutely motionless, and the DTA curve only showed minor, negligible movement throughout the entire temperature range.

After the baseline experiment was completed, zirconium dioxide was tested against XeF_2 as the potential fluorinating agent. A 64.54 mg sample was prepared using 17.8 mg of ZrO_2 and 46.74 mg of XeF_2 , mixed, and inserted into the TG/DTA for data acquisition. The sample was heated at a rate of 10 °C/min and was supposed to continue until a temperature of 600 °C was reached; however, the experiment was halted slightly before this mark was reached. The accompanying TG/DTA results are shown in Figure 4.20.

Unfortunately, the experiment testing XeF_2 against ZrO_2 was as uneventful as the baseline test. Both of the TGA and DTA curves resembled that of the thermal decomposition of XeF_2 , suggesting no interaction with the surrogate oxide. There was no exothermic spike suggesting a fluorination reaction, and the final mass was almost identical to the amount of ZrO_2 that was present at the start of the experiment. It appears that in this setting, XeF_2 does not successfully fluorinate ZrO_2 to the expected fluoride, ZrF_4 .

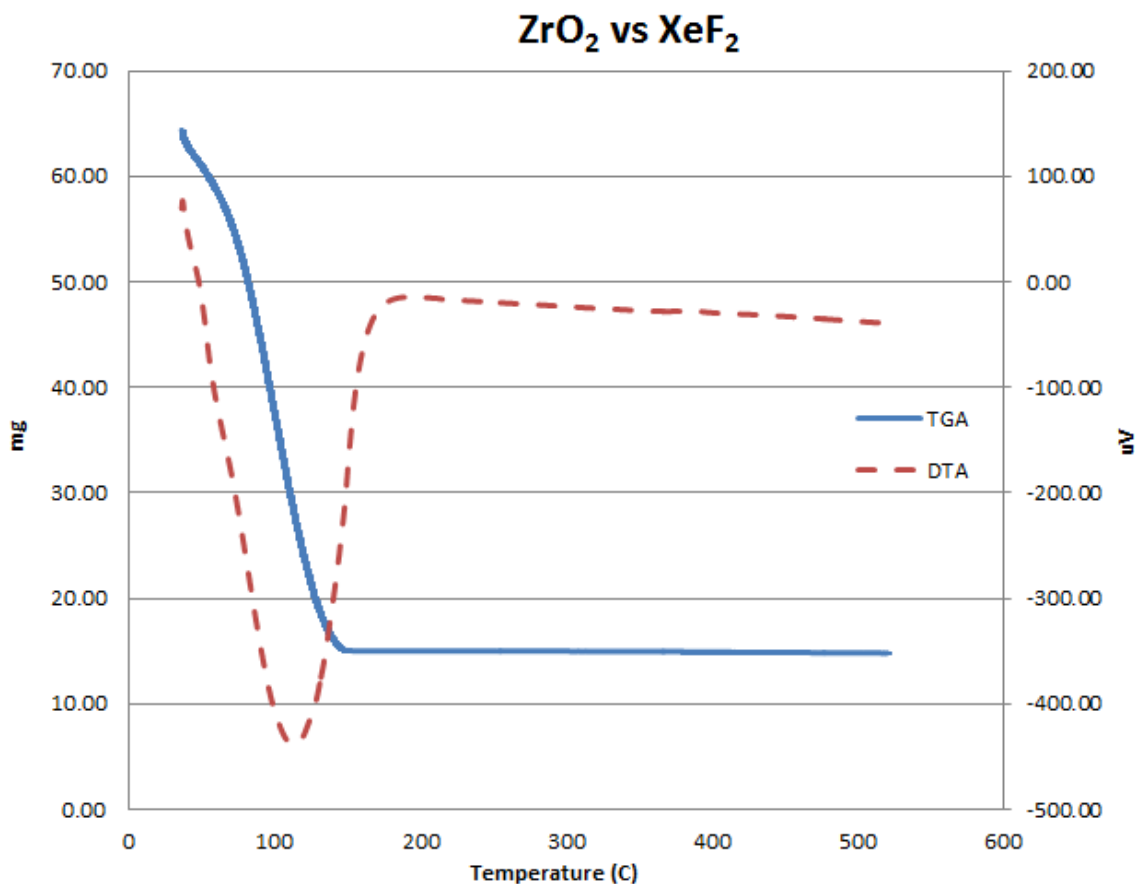


Figure 4.20. TG/DTA Data for $\text{ZrO}_2/\text{XeF}_2$

4.9 Uranium Dioxide (UO_2) – SRNL

Uranium dioxide (UO_2) is a black powder with a molar mass of 270.03 g/mol and a density of 10.97 g/cc. This oxide has a melting point of 2865 °C making it non-volatile in nature. Due to time constraints and availability of the TGA in the RAD labs at SRNL, only binary experiments with the fluorinating agents were conducted with UO_2 , and no confirmation was done for the non-volatility of the oxide itself. This would have only resulted in a redundant test as the thermophysical behavior of the oxide by itself is well understood. The fluorination of this oxide could result in the formation of UF_4 , UF_5 , or UF_6 . Of the three possible fluorides, only UF_6 is easily volatilized with an expected

boiling point of 56.5 °C. The other likely candidate, UF₄, is non-volatile with an expected boiling point of 1450 °C.

First, uranium dioxide was tested against XeF₂ as the potential fluorinating agent. Roughly 76 mg total sample weight was prepared using an excess of XeF₂, lightly mixed, and inserted into the TGA for data acquisition. The sample was heated from ambient at a rate of 10 °C/min until a temperature of 600 °C was reached. The accompanying TG/DTA results are shown in Figure 4.21 below.

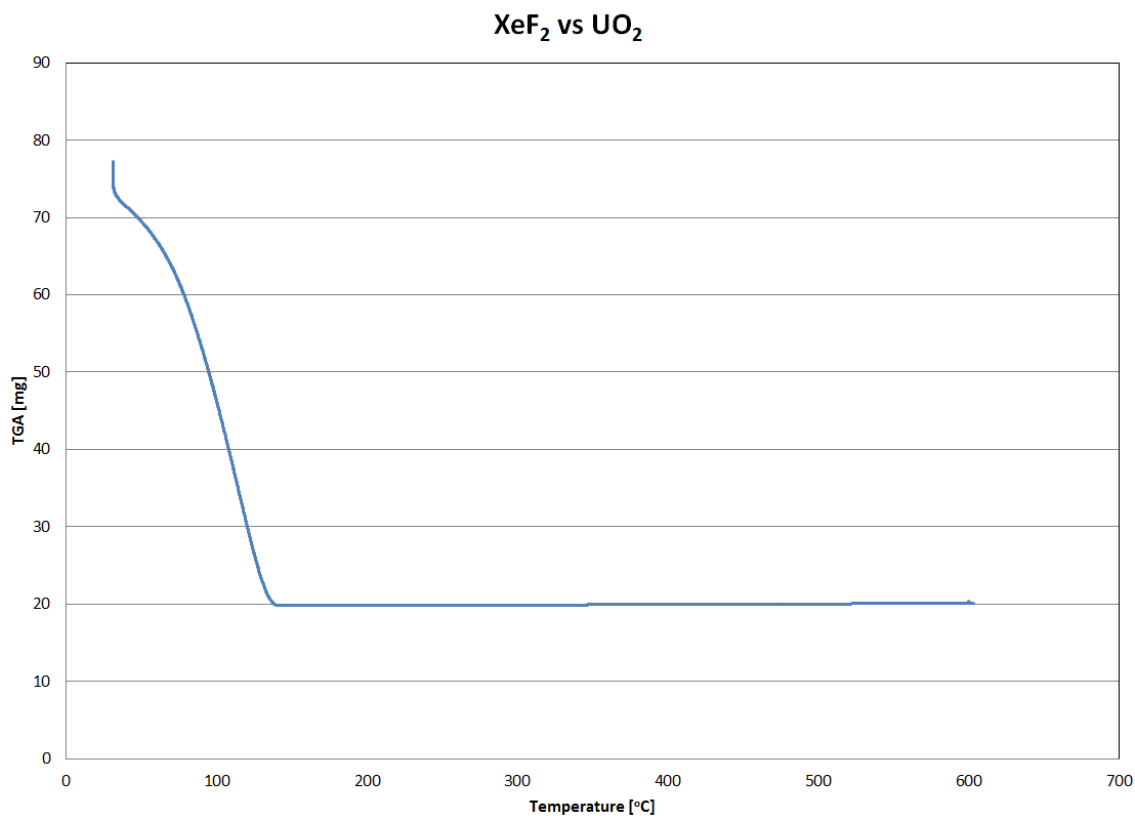


Figure 4.21. TGA Data for UO₂/XeF₂

The results from the binary experiment testing XeF₂ as a potential fluorinating agent for UO₂ were seemingly unsuccessful. It appears that by 150 °C the fluorinator had completely decomposed and left the active volume of the TGA, and at the conclusion of

the experiment, the remaining residue was simply the original UO_2 powder. This was the major pitfall in using the open system design for testing some of these oxides, as uranium oxides require elevated temperatures to promote the fluorination reaction. The nature of XeF_2 is that it decomposes, even more rapidly under increased temperatures, and once this occurs, there is no way within the current experimental setup that additional reactant can be flowed through to come in contact with the oxide. For this reason, the decision was made to redesign the experiments testing uranium oxides against XeF_2 and is the subject of the research done at USC presented later in this report.

For completeness, uranium dioxide was also tested against ammonium bifluoride as a potential fluorinating agent. Using the same experimental parameters, a 27 mg sample of an ammonium bifluoride and uranium dioxide 1:1 mixture was inserted to the TGA for data acquisition. Results from this experiment are shown in Figure 4.22.

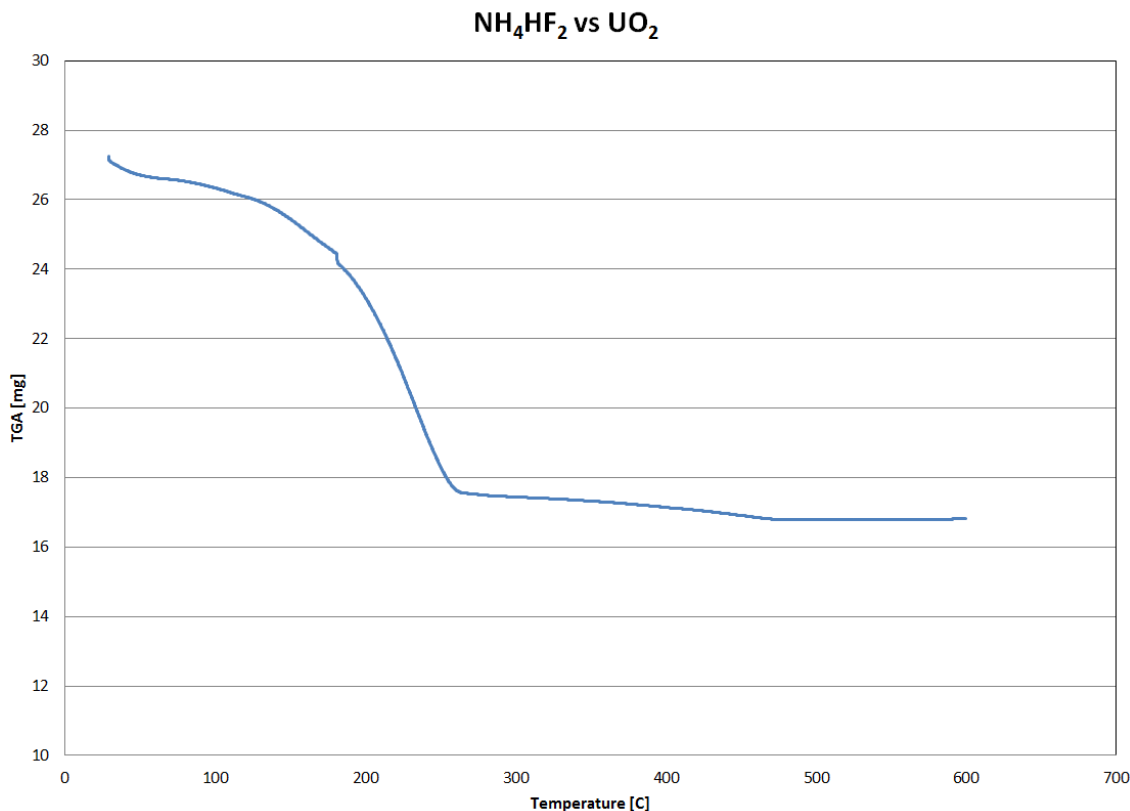


Figure 4.22. TGA Data for UO₂/NH₄HF₂

Like the previous experiment with XeF₂, the testing of NH₄HF₂ as a potential fluorinator for UO₂ seemed unsuccessful as total weight loss was not observed. The ammonium bifluoride seemed to decompose by 250 °C, and although this is a higher temperature than the experiment with XeF₂, it was still not enough to promote the fluorination and subsequent volatilization reaction using an open system.

4.10 Triuranium Octoxide (U₃O₈) – USC

To test the fluorination potential of XeF₂ against U₃O₈ powder, the experimental setup was completely redesigned and conducted at the University of South Carolina. The uranium material that was available for this research was prepared as discussed in

Chapter 3 of this report. The confirmed U_3O_8 sample material appeared as a fine, black powder with a molar mass of 842.1 g/mol and a density of 8.38 g/cc.

Step one of the newly designed, closed system approach was to prepare a mixture of XeF_2 and U_3O_8 in a sealed swagelok volume to be heated in the tube furnace. The first trial used a mixture of 0.388 g of XeF_2 with 0.3487 g of U_3O_8 and was heated in the furnace from ambient at a rate of 10 °C/min to a temperature of 600 °C where it was held for one hour. Two swagelok tubes were prepared in this manner, and both were inserted into the furnace at the same time. Once the experiment was completed and the furnace allowed time for cooling, the molybdenum boat used to transfer the sealed swagelok tube was removed from the active volume of the furnace so that the sample could be extracted. Figures 4.23 and 4.24 show the results of the first set of completed runs in the tube furnace.



Figure 4.23. Sealed Swagelok Volume after Heating in Tube Furnace

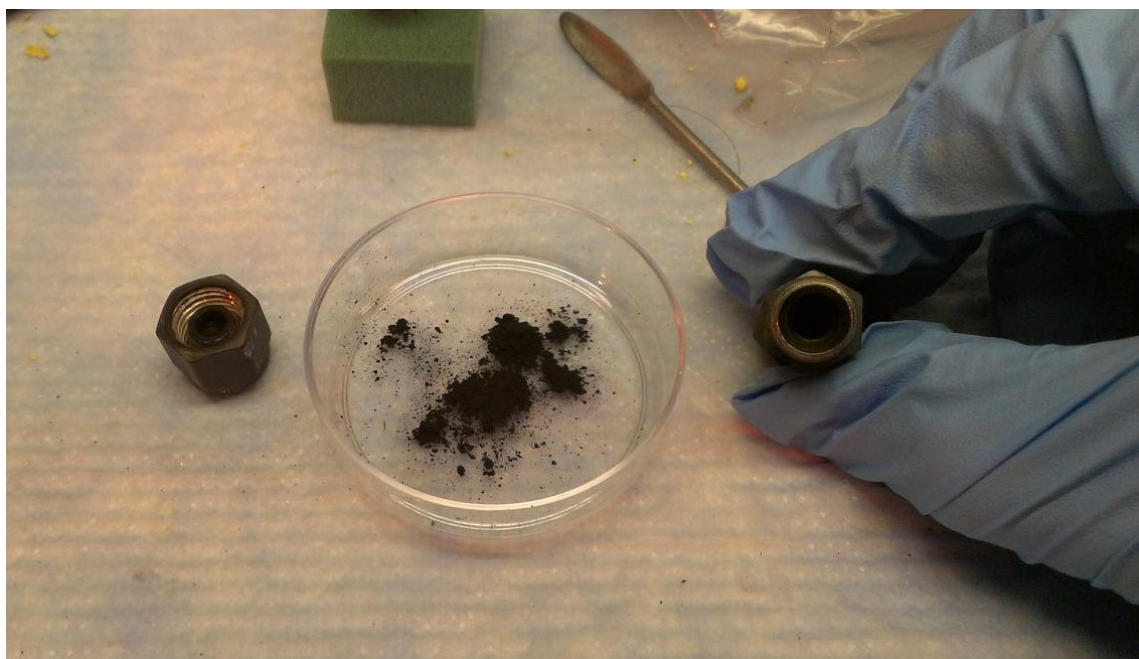


Figure 4.24. Sample as Removed from Swagelok Tube

It was evident just by inspecting the outside of the swagelok tubes that the volume did not remain sealed throughout the duration of the experiment. All of the parts that were used in this research were new, and after the run in the tube furnace, the outsides of both the swagelok tubes and the molybdenum boat showed grey and yellow discoloration. This residue appeared to wipe off with a Kimwipe; however, there was not enough of the residue available for further analysis. Whatever the case, it was clear that the XeF_2 escaping the swagelok tube had effects of both the outside of the stainless steel parts and the molybdenum boat the samples were being transferred in.

When the swagelok tubes were opened, the leftover powder appeared to be the same consistency as the U_3O_8 powder used at the beginning of the experiment. A preliminary hypothesis is that once the XeF_2 escaped from the swagelok tube, it did not have enough further interaction with the U_3O_8 powder to fluorinate the sample. This was later confirmed through TGA analysis when no mass loss was present upon heating to

600 °C. A second effort was made to prepare an additional experiment of the same nature, but this time more emphasis would be placed on ensuring the swagelok tubes were sealed correctly before being inserted into the tube furnace. Using a mixture of 0.3389 g of XeF_2 and 0.2696 g of U_3O_8 , the sample was mixed and placed in the swagelok tube of brand new parts. As stated previously, the parts were made sure of their seals in hopes that the sample material would remain in the volume throughout the entire experiment. Two samples were prepared in this manner, and both were heated in the furnace from ambient to 600 °C at a rate of 10 °C/min and were held at this temperature for one hour. Once the furnace was cooled, the molybdenum boat was removed, and all of the materials were compared to the previous failed run to see if there was any change in the ability of the swagelok tubes to sufficiently seal its contents for the entire temperature range. This comparison is clearly shown in Figure 4.25.

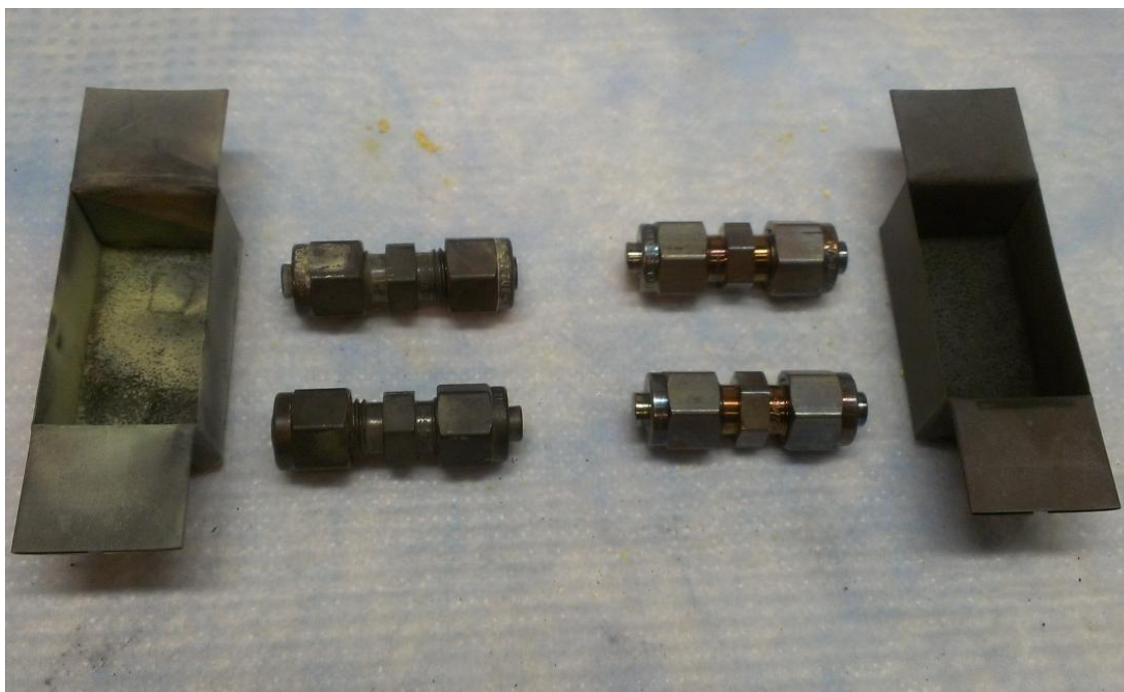


Figure 4.25. Comparison of Materials from Runs 1 and 2 in the Tube Furnace

Right away it is very clear that in the second run, the swagelok tubes appeared to contain the reactants much more effectively than in the previous experiment. There was no yellow or grey discoloration on either the tubes or the molybdenum boat, and the only visual change to the tubes was that the very center volume appeared to have a transitioned from a silver color to bronze. Now that the results of step one of the experiment, heating in a closed system of the tube furnace, appeared sufficient, it was time to transition to the TGA for analysis of the sample residue. The next step was to open one the swagelok tubes and remove the contents. The total weight of the swagelok tube and sample material prior to the tube furnace was 39.0087 g, and once it was removed from the furnace the weight had only been reduced to 39.0022 g. This very slight loss was completely acceptable to determine that the swagelok tube did indeed contain all of the reactants. The contents of the swagelok volume were emptied and are shown in Figure 4.26.

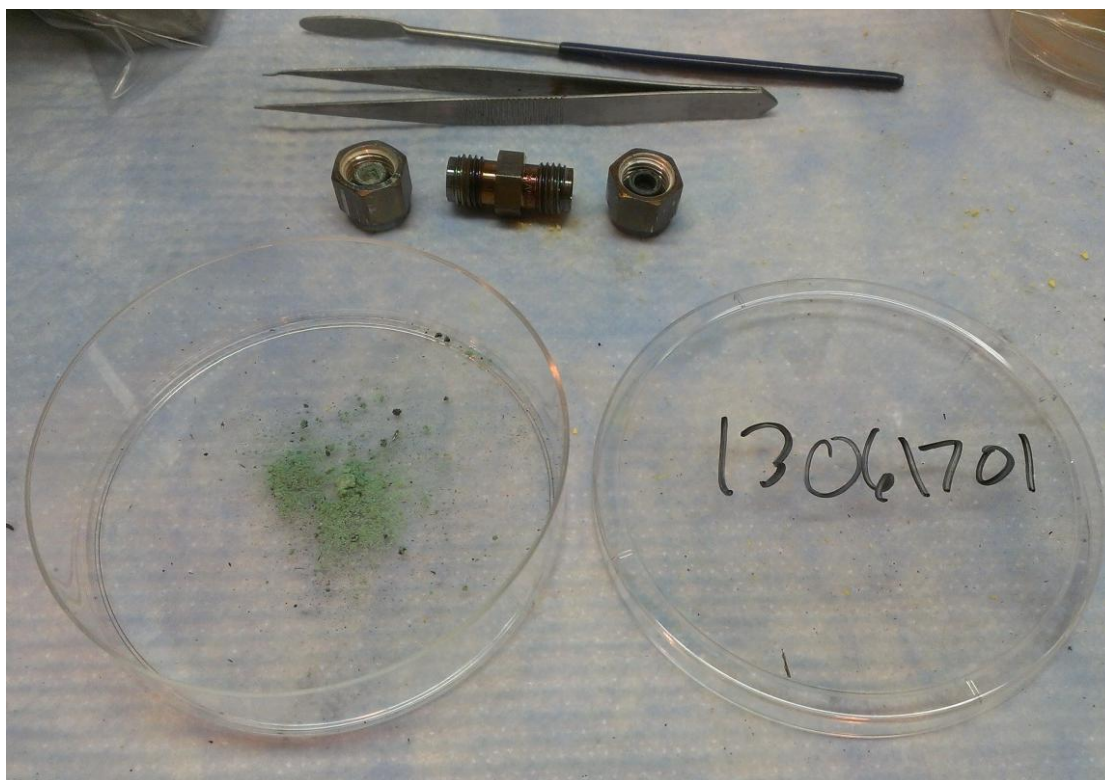


Figure 4.26. Resulting Residue from $\text{XeF}_2/\text{U}_3\text{O}_8$ after Tube Furnace

The sample residue shown in Figure 4.26 is completely different than from the first run, shown in Figure 4.24. It is noted that once the swagelok tube was opened for the first time, a significant volume of gas could be heard escaping. The likely that once the XeF_2 decomposed, the excess stayed in gas form even after being allowed to cool. This gas slightly pressurized the tube, and it was ejected once the seal was broken. The greenish color of the sample is highly characteristic of the formation of the intermediate fluoride, UF_4 . Although this fluoride is non-volatile, it still would suffice as proof that XeF_2 is capable of fluorinating U_3O_8 in some degree. Next, 0.1628 g of the sample residue was placed in the Al_2O_3 crucible to be used in the TGA. The sample was heated at a rate of $10\text{ }^\circ\text{C}/\text{min}$ from ambient to $800\text{ }^\circ\text{C}$ and held for one hour. Results from this experiment are shown in Figure 4.27 below.

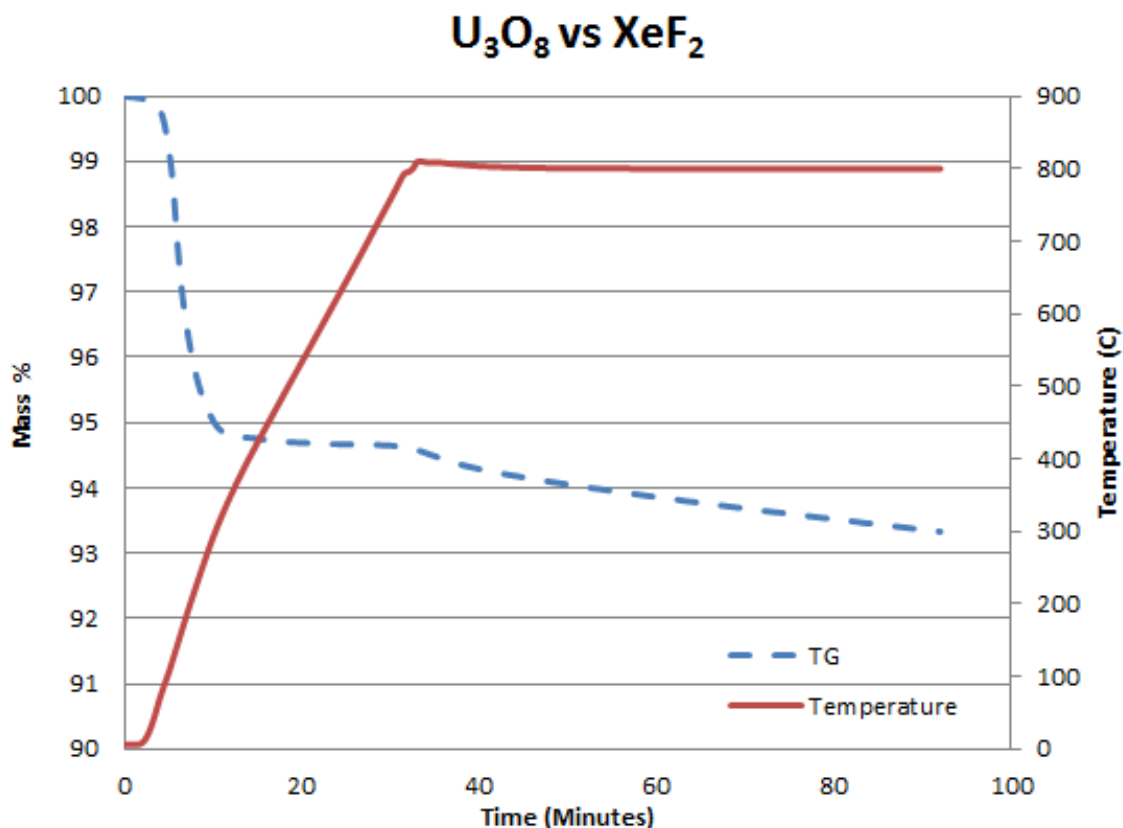


Figure 4.27. TGA analysis of XeF₂/U₃O₈ Sample Residue

At the conclusion of the experiment, the sample experienced almost 7 % weight loss, most of which occurred early on in the temperature ramp. It is quite possible that some UF₆ was formed in addition to the UF₄ which would explain the weight loss in the sample. With a boiling point of 56.6 °C, one would expect UF₆ to volatilize relatively early as seen in the TGA analysis. An additional explanation to the weight loss may have been that residual XeF₂ was still in the sample material and was off-gassed upon heating in an open system. That being said, the Al₂O₃ crucible, Figure 4.28 below, as shown after the TGA run proves that some compound was indeed mobile when it was heated. There was a ring of deposited material roughly halfway up the crucible, much higher than the original sample reached.

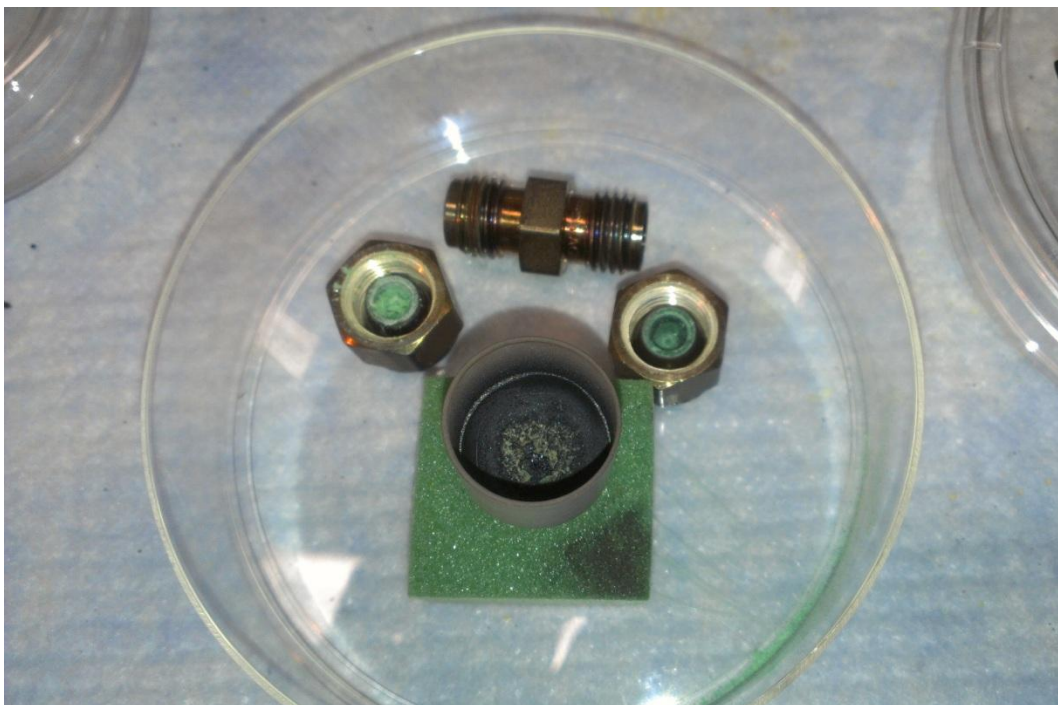


Figure 4.28. Al₂O₃ Crucible after TGA Experiment

The results of the two part, open and closed system approach are proof in the capability of XeF₂ to fluorinate a U₃O₈ sample. Even though it appeared that a majority of the sample tested was the non-volatile UF₄, this would still bode well for marketing the use of XeF₂ as a possible fluorinating agent for a pre-treatment of used nuclear fuel for the use in an additional reprocessing technology.

CHAPTER 5

CONCLUSION AND FUTURE WORK

Experimentation with XeF_2 as a potential alternate, solid-phase fluorinating agent for use in Reactive Gas Recycle was successful for a majority of the non-radioactive, surrogate oxides tested in this research. Employing an open system approach with a TG/DTA system, the fluorination and volatilization profiles were studied at temperatures below 600 °C. Using this experimental setup, the following conclusions can be made:

1. Fluorination and complete volatilization was observed for MoO_3 and Nb_2O_5 .
2. Evidence of fluorination and partial or minor volatilization was observed for Rh_2O_3 and RuO_2 .
3. Confirmed formation of a non-volatile fluoride was observed for SrO .
4. No reactivity was observed when tested against ZrO .

To test the fluorination potential of XeF_2 against radioactive uranium oxides, two experimental approaches were undertaken, an open and closed system approach. Using the modified Dupont 951 TGA in the RAD labs at SRNL, XeF_2 was seemingly unsuccessful at fluorinating a sample of UO_2 powder with an open system approach. When the experimental setup was restructured at USC, positive results did show when XeF_2 formed the intermediate fluoride, UF_4 , when mixed with U_3O_8 powder sample in a closed system. When the sample residue from the latter experiment was tested in the Netzsch STA 409 TGA, some evidence was shown for the possible partial volatilization of the sample suggesting the sample may have contained a small amount of the volatile

UF₆. Overall, it appeared the closed system approach was more effective for the fluorination of uranium samples as the reactants were contained throughout all temperature ranges, enabling a more desired environment for the fluorination reaction.

Future work for the research of XeF₂ as a potential fluorinator for use in RGR may come with yet another redesign of the experimental parameters, meshing the two strategies (open and closed systems) to allow for a constant stream of reactant throughout the entire temperature range of interest. To accomplish this goal, XeF₂ may have to be decomposed outside of the TGA/DTA through whatever means and then flowed through the reactor at controlled levels and onto the surrogate oxide. The constant stream of reactant should also give better insight to the onset of fluorination and reaction kinetics, giving detailed analysis on any possible thermal windows which may also be utilized as an effective separations mechanism. In addition to the redesign, future work may also incorporate the use of a residual gas analyzer to confirm the formation of the volatile fluorides which was previously unavailable as they were off gassed from the system.

Experiments using NH₄HF₂ as a potential fluorinating agent for use in RGR were found to be very inconclusive with this approach. Although mixing the surrogate oxide with the fluorinator had some effect on the respective TGA and DTA curves, no definitive confirmation as to the formation of both non-volatile and volatile fluorides could be made, even with the aid of XRD analysis. Due to the seemingly mild aggressiveness of the fluorinator relative to XeF₂, better homogeneity of the binary mixtures between surrogate oxide and NH₄NF₂ may be necessary to have a favorable environment to promote this reaction. The experimental redesign as just suggested could

also be used to further study the potential of ammonium bifluoride as a fluorinating agent.

Regardless if the United States continues to operate on an open, once through cycle for the foreseeable future, a reprocessing strategy will have to be chosen eventually to further utilize the global uranium resources available as they are not infinite. Because of this limitation, it is only reasonable to research all possible reprocessing methods so that when the time comes to implement a closed fuel cycle, the absolute best method can be chosen in terms of economics, non-proliferation, safety, etc. For now, the elephant in the room in terms of the future of the nuclear power industry still begs to question, “How will the US solve the issue of what to do with used nuclear fuel?”

REFERENCES

- [1] Silva, G., et al. "Fluoride-Conversion Synthesis of Homogeneous Actinide Oxide Solid Solutions". *Inorganic Chemistry*, 50, 11004-11010. (2011)
- [2] Ladd-Lively, J., Spencer, B., Counce, R. "Separation of Cesium and Strontium from Residues Arising from Fluoride Volatility Processing of Spent Nuclear Fuel". *Separation Science and Technology*, 40(1), 17-29. (2005)
- [3] Kamoshida, M., et al. "A New Concept for the Nuclear Fuel Recycle System: Application of the Fluoride Volatility Reprocessing". *Process in Nuclear Energy*, 3(1-4), 145-150. (2000)
- [4] Chandler, J., Hertel, N. "Choosing a Reprocessing Technology Required Focusing on What We Value". *Process in Nuclear Energy*, 51, 701-708. (2009)
- [5] Gray, J.; Korinko, P.; Garcia-Diaz, B.; Visser, A.; Adams, T. "Reactive Gas Recycle for Used Nuclear Fuel." *FCRD Annual Report, FCRD-SEPA-2010-000177*. (2010)
- [6] Torres, R.; Gray, J.; Korinko, P.; Martinez-Rodriguez, M.; Garcia-Diaz, B.; Morgan, G.; Visser, A.; Adams, T. "Reactive Gas Recycle Separation Technology for Used Nuclear Fuel." *FCRD Annual Report, FCRD-SEPA-2011-00096*. (2011)
- [7] Rometsch, R. "Management and Disposal of used nuclear Fuel and Reprocessing Wastes". *The London Institute*, 177-183. (1983)
- [8] Hylko, James M. "How to Solve the Used Nuclear Fuel Storage Problem". *Power*, Vol. 152 Issue 8, 58-66. (2008)
- [9] Barrett, L. "United States Used Nuclear Fuel Policy Options". *IHLRWMC*, 548-553. (2011)
- [10] Del Cul, G., et al. "Comprehensive Recycling of Used Nuclear Fuel – A Practical Alternate". *New Developments in Advanced Fuel Cycles*, 102, 135-136. (2010)
- [11] Thorne, M. "Is Yucca Mountain a Long-Term Solution for Disposing of US Spent Nuclear Fuel and High-Level Radioac". *Journal of radiological Protection*, 32(2), 175-180. (2012)
- [12] Peltier, R., Hylko, J., "The U.S. Spent Nuclear Fuel Policy, Part 2: Playing Hardball". *Power*, Vol. 155 Issue 11, 76-69. (2011)
- [13] "Analyzing the Blue Ribbon Commission Report". *Radwaste Solutions*, 19(2), 55-58. (2012)

- [14] Sowder, A., et al. "What Now for Permanent Disposal of Used Nuclear Fuel and HLW in the United States". *Radwaste Solutions*, 20(1), 26-39. (2013)
- [15] Karraker, D. "The PUREX Process at Savannah River". Unpublished.
- [16] Kolarik, Z., et al. "Separation of Fission Products from U and Pu in the Highly Radioactive Cycle of the Purex Process". Institut für Heisse Chemie, Kernforschungszentrum Karlsruhe, 333-344.
- [17] Von, H. "The PUREX Process For The Reprocessing of Nuclear Fuels with High Pu Content and High Burn-Up". *The Journal for Nuclear Engineers And Scientists*, 18(6), 245-5. (1976)
- [18] Gibson, M. "Pretreatment of Hanford PUREX Plant First-Cycle Waste". *The Symposium on Waste Management at Tucson*, 603-608. (1987)
- [19] Chrusasik, A., et al. "Process for the Treatment of Spent TBP/kerosene (PUREX) Solvents". *International Conference of Nuclear Fuel Reprocessing and Waste Management*, 773-776. (1987)
- [20] "Super-high-temperature Treatment of High-Level Liquid Wastes". *Transactions of the American Nuclear Society*, 62, 111-112. (1990)
- [21] Pereira, C., et al. "Simulation of Head-End Processing of Used Nuclear Fuel". *Transaction of the American Nuclear Society*, 104, 167-167. (2011)
- [22] Jonke, A., et al. "Development of Fluoride Volatility Reprocessing Methods for Plutonium-Containing Fuels". *Chemical Engineering Process Symposium Series*, 63(80), 137-141. (1967)
- [23] Uhlir, J., Marecek, M. "Fluoride volatility method for reprocessing of LWR and FR fuels". *Journal of Fluorine Chemistry*, 130, 89-93. (2009)
- [24] Komura, M., et al. "Thermogravimetric Study of the Reaction of Uranium Oxides with Fluorine". *Journal of Alloys and Compounds*, 451, 673-675. (2008)
- [25] Amano, O., et al. "Development of New Reprocessing Technology, FLUOREX, for LWR Fuel Cycle Hybrid Process of Fluoride Volatility and Solvent Extraction". *NUCEF2001*, 217-224. (2002)
- [26] Lucas, M., et al. "Ruthenium in Fuel Reprocessing by Fluoride Volatility Process. Fluorination in Flame Reactor". *Journal of Nuclear Science and Technology*, 16(8), 574-576. (1979)
- [27] Žagar, T., Buršič, A., Špiler, J., Kim, D., Chiguer, M., David, G., et al. "Recycling as an Option of Used Nuclear Fuel Management Strategy". *Nuclear Engineering and Design*, 10, 1238-1242. (2010)
- [28] Scheele, R., et al. "On the Use of Thermal NF₃ as the Fluorination and Oxidation Agent in Treatment of Used Nuclear Fuels". *Journal of Nuclear Materials*, 424, 224-236. (2012)
- [29] McNamara, B., et al. "Thermal Reactions of Uranium Metal, UO₂, U₃O₈, UF₄, and UO₂F₂ with NF₃ to Produce UF₆". *Journal of Nuclear Materials*, 394, 166-173. (2009)

- [30] Yeamans, C., et al. "Oxidative Ammonolysis of Uranium(IV) Fluorides to Uranium(VI) Nitride". *Journal of Nuclear Materials*, 374, 75-78. (2008)
- [31] Mukherjee, A., et al. "Studies on fluorination of Y_2O_3 by NH_4HF_2 ". *Thermochimica Acta*, 520, 145-152. (2011)
- [32] Mayhew, P.A., Boyle, L.D. "The fluorination of uranium and zirconium oxides with xenon difluoride initiated by the addition of water". *Journal of Fluorine Chemistry*, 87, 97-99. (1998)
- [33] Smit, J.J., Els, E.R. "A pilot plant for the fluorination of UO_3 to UF_6 using XeF_2 ". *South African Journal of Science*, 84, 456-457. (1988)
- [34] 60 Series Thermal Analysis Instruments. <http://www.shimadzu.com>. Shimadzu Corporation, Tokyo, Japan.
- [35] Chatterjee, P. "Application of Thermogravimetric Techniques to Reaction Kinetics". *Journal of Polymer Science: Part A*, 3, 4253-4262. (1965)
- [36] 1700 Series Rapid Temp Lab Furnaces. www.cmfurnaces.com. CM Furnaces Inc. Bloomfield, NJ.
- [37] Netzsch STA 409 Product Brochure. www.ngb.netzsch.com. NETZSCH-Gerätebau GmbH.
- [38] Thein, S., Bereolos, P. "Thermal Stabilization of $^{233}UO_2$, $^{233}UO_3$, and $^{233}U_3O_8$ ". Oak Ridge National Laboratory Report. (2000)